

REPORT OF INVESTIGATIONS NO. 113

**Depositional Framework,
Hydrostratigraphy,
and Uranium Mineralization
of the Oakville Sandstone (Miocene),
Texas Coastal Plain**

**William E. Galloway
Christopher D. Henry
Gary E. Smith**

**BUREAU OF ECONOMIC GEOLOGY • W. L. FISHER, DIRECTOR
THE UNIVERSITY OF TEXAS AT AUSTIN • AUSTIN, TEXAS 78712**

1982



QAe4014

REPORT OF INVESTIGATIONS NO. 113

**Depositional Framework,
Hydrostratigraphy,
and Uranium Mineralization
of the Oakville Sandstone (Miocene),
Texas Coastal Plain**

**William E. Galloway
Christopher D. Henry
Gary E. Smith**

Assisted by C. S. Childs and P. E. Devine

Study sponsored by the U.S. Environmental Protection Agency,

Grant Nos. R805357010 and R805357020

1982

**BUREAU OF ECONOMIC GEOLOGY • W. L. FISHER, DIRECTOR
THE UNIVERSITY OF TEXAS AT AUSTIN • AUSTIN, TEXAS 78712**



CONTENTS

Abstract	1
Introduction	1
Objectives and methodologies	3
The Gulf Coast artesian basin.....	3
Depositional framework of the Oakville aquifer	4
OAKVILLE DEPOSITIONAL SYSTEM.....	6
Hebbronville and George West fluvial axes	6
Conglomeratic bed-load channel-fill facies	9
Sandy bed-load channel-fill facies	10
Sheet-splay facies	13
Facies associations and distribution	13
New Davy fluvial axis	14
Conglomeratic bed-load channel-fill facies	14
Mixed-load channel-fill facies	15
Crevasse splay and sheet-splay facies	16
Facies associations and distribution	17
Moulton streamplain	17
Channel-fill facies	17
Sheet-splay and crevasse splay facies.....	17
Facies associations and distribution	18
Burton/Penn fluvial axes.....	19
Sinuous channel-fill facies	19
Crevasse splay and sheet-splay facies	19
Facies associations and distribution	20
Floodplain facies	20
Facies summary	20
MINERALOGIC COMPOSITION	21
Mudrock petrofacies	21
Sand petrofacies	23
SUMMARY OF GENETIC STRATIGRAPHY	24
Structural framework	25
FAULT DISTRIBUTION	26
IMPACTS ON HYDROGEOLOGY.....	26
Hydrostratigraphy	27
HYDROGEOLOGIC UNITS.....	27
AQUIFER TRANSMISSIVITY	27
Geology and geochemistry of Oakville uranium deposits	31
RAY POINT DISTRICT	32
Geochemical and mineralogical zonation	34
Ore paragenesis	37
GEORGE WEST DISTRICT	38
Geochemical and mineralogical zonation	40
Ore paragenesis	41
Conclusions	42
Acknowledgments	43
References.....	43
Appendix A.....	46
Appendix B.....	48

Illustrations

Figures

1. Index map showing location of the study area, outcrop of the Oakville Sandstone, sample localities, and distribution of cross sections	2
2. Regional structural features of the Tertiary Gulf Coastal Plain and Edwards Plateau	3
3. Generalized offlapping stratigraphic sequence of the Texas Coastal Plain	4
4. Stratigraphic relationships of the Oakville Sandstone, Live Oak County	5
5. Net-sand isolith map of the Oakville Sandstone	7
6. Sand-percentage map of the Oakville Sandstone	7
7. Regional updip strike section illustrating facies of the Oakville fluvial system	8
8. Depositional elements of the Oakville fluvial system	9
9. Facies architecture of a composite sand belt of the George West fluvial axis	10
10. Line tracing showing a channel fill of the Ray Point fluvial axis	11
11. Line tracing illustrating structures and textures characteristic of the George West bed-load channel facies	12
12. Variation of the sandy bed-load channel-fill facies consisting of interstratified sand and mud-clast conglomerate	13
13. Schematic reconstruction of Oakville fluvial depositional environments	14
14. Sheet-splay deposits of the George West axis exposed in the Smith uranium mine	15
15. Schematic facies architecture of a typical New Davy axis sand belt	16
16. Schematic facies architecture of a sand belt within the Moulton streamplain	18
17. Road cut displaying lateral accretion of a mixed-load channel of the Burton/Penn axes	20
18. Schematic facies architecture of a typical Burton/Penn axes sand belt	21
19. Compositional summary of Oakville sands	23
20. A. Euhedral sparry calcite porefill cement. B. Silica cement	24
21. Summary of genetic components and geometric and compositional characteristics of aquifer units within the Oakville depositional elements	25
22. Generalized distribution of faults and diapiric intrusions within or below the Oakville Sandstone	26
23. Stratigraphic dip sections comparing lithostratigraphic and hydrostratigraphic units	28
24. Geohydrologic data base used for pump test permeability data	29
25. Calculated permeabilities for major permeable facies belts	29
26. Regional transmissivity of the Oakville aquifer system	30
27. Schematic distribution of epigenetic zones within an oxidized aquifer	33
28. Geographic and geologic setting of the Ray Point district, Live Oak County	34
29. Cross section of the Oakville aquifer in the Ray Point district	35
30. Core transect of the Zamzow mineralization front	36
31. Paragenesis of the Zamzow mineralization front and associated geochemical zones	39
32. Cross section through the George West district	39
33. Geographic and geologic setting of the George West district, Live Oak County	40
34. Paragenesis of mineralization and associated zones along the southern alteration front, George West district	42

Tables

1. Clay mineralogy of representative fine-grained Oakville samples	22
2. Geochemical barriers capable of concentrating uranium and associated metals in ground-water flow systems	32
3. Summary of Oakville uranium-producing districts and areas	33
4. Compositional summary of Zamzow core cross section sample suite	38
5. Carbon isotope composition of selected Oakville samples	38
6. Compositional summary of George West district core sample suite	41
B-1. Analytical data for core samples, Zamzow mine site	49
B-2. Analytical data for core samples, George West deposit A	50
B-3. Analytical data for core samples, George West deposit B	51

Abstract

The Oakville Sandstone (Miocene) of the Texas Coastal Plain comprises a major sand-rich fluvial system composed of deposits of several major and minor rivers that originated within Texas and surrounding states. Broad bed-load fluvial axes, including the Hebbbronville, George West, and New Davy trends, lie south of the San Marcos Arch and host significant reserves of uranium. To the north, the Moulton streamplain consists of deposits of numerous small, flashy to ephemeral streams that drained the inland margin of the Coastal Plain. The Burton/Penn mixed-load fluvial axes traverse the Coastal Plain in the area of the modern Colorado and Brazos Rivers.

Each fluvial axis consists of diagnostic facies deposited in channel, crevasse splay, and floodplain environments. Sand percentage, sand-body

dimensions and lateral relationships, and composition vary systematically among the axes. Overall transmissivity of the Oakville Formation, which closely corresponds to the Jasper aquifer system in conventional hydrostratigraphic terminology, correlates directly with mapped facies composition and trend. Uranium deposit size relates directly to associated aquifer transmissivity.

Commercial uranium deposits lie within channel and interbedded sheet-splay sands in or along the margin of major fluvial belts, typically near shallow faults. Mineralization occurs along narrow, elongate fronts separating altered, but commonly resulfidized, host sand from epigenetically sulfidized reduced sand. Deposits show pronounced spatial zoning of trace metals and iron sulfide, carbonate, and locally, clay mineral phases across the mineralization front.

Introduction

The Miocene Oakville Formation is a sedimentologically distinct stratigraphic unit that can be traced at outcrop from the Brazos River on the northeast to south-central Duval County where it is overlapped unconformably by the Pliocene Goliad Formation (fig. 1). Equivalent strata extend into the subsurface downdip of the outcrop belt and below the Goliad veneer. Together, the Oakville and overlying Fleming Formations record a major Miocene depositional episode in the Texas Coastal Plain. The Oakville comprises a generally coarse, sand-rich basal unit; the overlying Fleming (locally called the Lagarto Clay) is a somewhat finer, less sandy unit. The two units are undivided in the *Geologic Atlas of Texas* south of Bee County (Barnes, 1975). North of the Brazos River, the Oakville becomes indistinguishable from the Fleming, although careful mapping shows that a basal Oakville lithic unit can be traced as far as Walker County (Spradlin, 1980).

Following initial discovery and development of uranium deposits in the Whitsett Formation of the Jackson Group, exploration revealed commercial uranium deposits in Oakville sands of the Ray Point area, Live Oak County. A mill was constructed to

process Oakville ore in 1970. The resurgence of exploration and development in the late 1970's demonstrates the geologic and economic significance of uranium deposits of the South Texas Uranium Province in general, and of the Oakville Formation in particular. Of the approximately 5.5 million pounds of yellow cake produced in Texas in 1979, almost 60 percent was extracted from the Oakville Formation.

In addition to being an important uranium host, the Oakville is also a major source of fresh water for municipal, domestic, and agricultural use. Approximately 35 percent of the water used in the nine-county outcrop belt comes from the Oakville aquifer.

Despite the geologic and commercial significance of the Oakville, little work on regional Oakville stratigraphy or economic geology has been published since the summary by Sellards and others (1932). Important stratigraphic studies include those by Renick (1936), Weeks (1945), and Ragsdale (1960). Uranium mineralization was discussed by Klohn and Pickins (1970), Harshman (1974), Goldhaber and others (1979a), and Galloway and others (1979a).

Objectives and Methodologies

The increasing economic importance of the Oakville aquifer, the implications of potentially competing uses, and the suitability of the Oakville as a natural laboratory for examining the interrelationships between the physical geology, hydrodynamics, and hydrochemistry of a metalliferous, coastal plain aquifer prompted a regional study by the Bureau of Economic Geology. This report, the first of a series, describes the genetic stratigraphy, mineralogic composition, hydrostratigraphy, and economic geology of the Oakville Sandstone. Future reports will describe the hydrodynamics and hydrochemistry of the aquifer system.

The study area (fig. 1) extends from the outcrop and adjacent subcrop belt downdip to sufficient depths to include all characteristic Oakville sands and to encompass the downdip extent of fresh to brackish water that forms a part of the modern meteoric flow system. It thus encompasses nearly 46,000 km² (18,000 mi²) of the Central and South Texas Coastal Plain.

Geologic and hydrologic data have been synthesized from numerous sources. Development of the regional stratigraphic framework of the Oakville included generation of 10 regional subsurface dip-oriented cross sections and 2 strike-oriented cross sections (fig. 1) utilizing electric logs available from the Texas Department of Water Resources. Sections

were carefully projected to the outcrop belt as mapped on *Geologic Atlas of Texas* quadrangles (Barnes, 1974a, 1974b, 1975, and 1976). Approximately 450 additional wells were correlated into the sections and used to construct primary lithofacies maps, including net-sand and sand-percent maps, for the Oakville Formation. Similar maps for the underlying Catahoula Formation were previously compiled (Galloway, 1977). Regional facies maps, augmented by outcrop and mine sedimentologic investigations, depicted the principal depositional elements comprising the Oakville aquifer. Quantitative facies maps provided the basis for a total aquifer transmissivity map. Regional mineralogic composition of the Oakville Formation was determined by conventional petrographic and X-ray diffraction analysis of samples collected from outcrop exposures, open-pit mines, and subsurface cores. Sample localities are shown in figure 1 and tabulated in appendix A. Within the limits of availability, samples were distributed to represent the vertical and areal extent of principal Oakville depositional elements.

Published data were synthesized to map principal structural features possibly affecting the Oakville aquifer system. Mining permit applications on file at the Texas Railroad Commission and the Texas Department of Water Resources provided additional data on mining districts.

The Gulf Coast Artesian Basin

The Oakville aquifer is a significant component of the Gulf Coast artesian basin. In Texas, the basin is bounded along its updip margin by the Balcones Fault Zone, a major structural discontinuity that separates the gently gulfward-dipping Coastal Plain from the more elevated, marginally dissected Edwards Plateau (fig. 2). The downdip limit of the meteoric groundwater circulation system approximates the present coastline. During low stands of sea level (Pleistocene), the subaerial Coastal Plain and associated meteoric groundwater flow system extended farther basinward as much as 100 km (60 mi) or more.

Quaternary and Tertiary sands of fluvial, deltaic, and marginal marine origin compose the principal aquifers within the artesian basin. These units, which together form the Gulf Coast (post-Eocene) and Carrizo-Wilcox (Eocene) aquifers, are recharged from the surface and by leakage from underlying Cretaceous terrigenous clastic and carbonate aquifers. The meteoric flow system incorporates only a limited upper part of a sedimentary sequence that is several thousand meters thick in most of the basin.

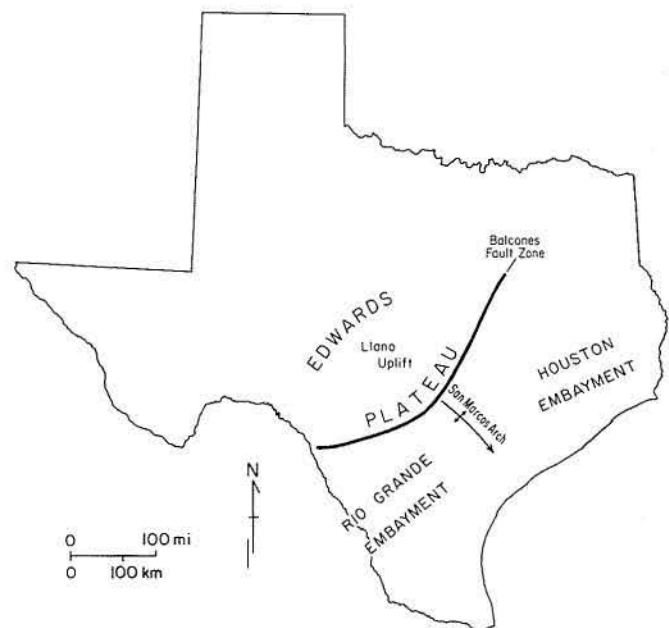


Figure 2. Regional structural features of the Tertiary Gulf Coastal Plain and Edwards Plateau.

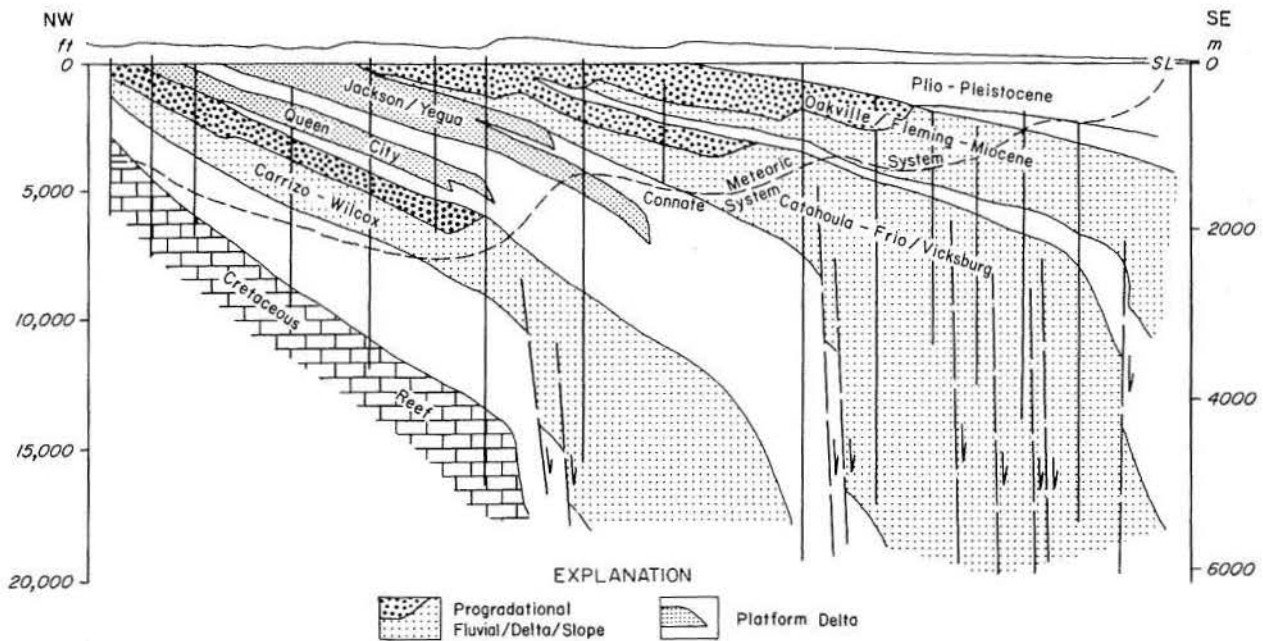


Figure 3. Generalized offlapping stratigraphic sequence of the Texas Coastal Plain. The major progradational wedges, including the Carrizo-Wilcox, Catahoula-Frio, and Oakville-Fleming cycles, consist of extensive fluvial facies that serve as major aquifers in the meteoric ground-water system.

Principal water-bearing stratigraphic units consist of gently gulfward-dipping and gulfward-thickening sand-rich fluvial and deltaic beds. Downdip, these units thicken abruptly across a series of major syndepositional fault zones, forming an offlapping sedimentary wedge (fig. 3). Sand-rich fluvial and deltaic aquifers consequently overlie a thick foundation of undercompacted, abnormally pressured prodeltaic and marine mud and clay. Connate waters driven from this mud substrate by pressure head move vertically into shallow, normally compacted aquifers and then toward the basin margin (Galloway and others, 1979b). Regional flow of meteoric ground water is downdip in response to the regional gulfward topographic slope. The Gulf Coast artesian basin is, therefore, a dynamic cauldron within which interact

two first-order flow systems, the meteoric flow system driven by gravitational head and the connate flow system driven by compactional loading or pressure head. The Oakville Formation is influenced by both flow systems, and the contained uranium deposits result from their interaction.

Tertiary depositional patterns were influenced regionally by three long-lived structural elements (fig. 2). The Rio Grande Embayment and the Houston Embayment are broad depocenters that are separated by the San Marcos Arch, a more stable platform area. The history of these passive structural elements extends back into the Mesozoic. Major rivers entered the Coastal Plain through both of the embayments during deposition of most Tertiary stratigraphic units, as they do today.

Depositional Framework of the Oakville Aquifer

The Miocene Oakville Sandstone is a distinctive sand-rich lithostratigraphic unit whose average thickness ranges between 100 m (300 ft) and 200 m (700 ft) at outcrop. Stratigraphic setting, typical subsurface expression, and nomenclature of the Oakville Sandstone and bounding units are illustrated by dip section F-F' (fig. 4), which intersects the outcrop belt in Live Oak County near the type section (Sellards and others, 1932). The Oakville is underlain by the argillaceous, tuffaceous Catahoula Formation

of fluvial origin (Galloway, 1977), and is the lower part of a major fluvial depositional cycle that includes the Fleming Formation. The Fleming is commonly called "Largarto" in other studies of the South Texas Uranium Province. The entire cycle is correlated simply as Miocene in the deeper subsurface. The Oakville-Fleming cycle is in turn overlain with local, low-angle truncation by the Goliad Formation, the coarse basal unit of a succeeding Pliocene fluvial cycle.

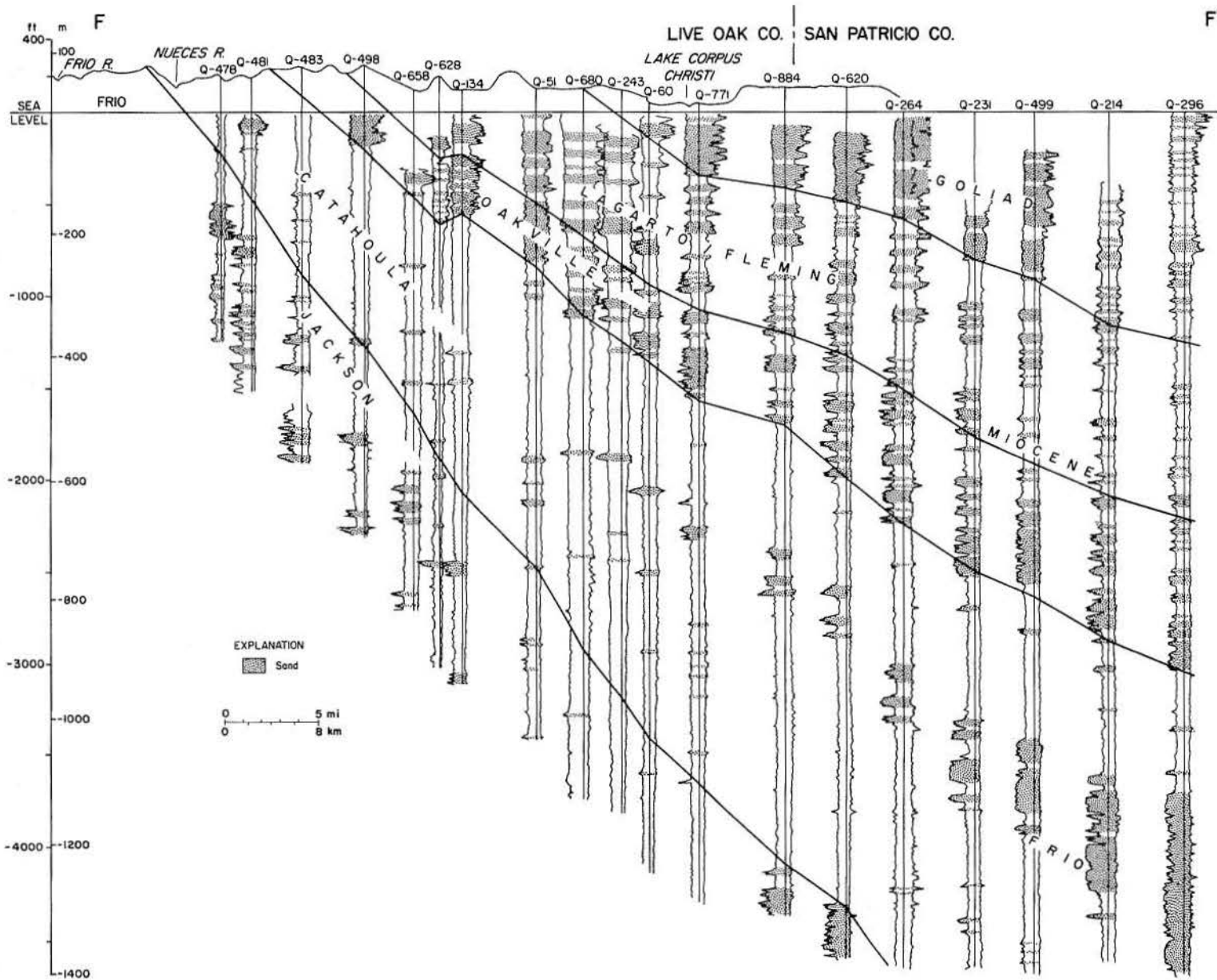


Figure 4. Stratigraphic relationships of the Oakville Sandstone in its type area near the town of Oakville, Live Oak County. For location of section, see figure 1.

Although boundaries between the Oakville and surrounding units locally are easily recognized at outcrop and in the subsurface, development of an internally consistent regional correlation framework is difficult. Correlation within the regional grid of sections relied upon careful projection of updip wells to the outcrop and downdip wells to underlying, laterally continuous, marginal marine facies of the Frio Formation. On many sections, the top of the Oakville must be arbitrarily defined within the overall Miocene fluvial cycle. The base of the Oakville, although generally distinct and the best correlation marker, incorporates a thick transition zone in Karnes and Gonzales Counties; correlations here are necessarily somewhat arbitrary. The produced correlation grid represents an attempt to delineate regionally a physical stratigraphic unit which, in turn, becomes the framework for further sampling and description.

OAKVILLE DEPOSITIONAL SYSTEM

Bulk lithologic composition, geometry and trend of sand bodies, internal sedimentary structures, external facies relationships with bounding fine-grained facies, and position within the reconstructed Miocene Gulf Coast Basin combine to show that the Oakville Sandstone of the outcrop and shallow subsurface constitutes a major bed-load fluvial system (terminology of Galloway, 1977; after Schumm, 1977) that was deposited by several large rivers and smaller Coastal Plain streams. The Oakville system grades laterally into relatively fine-grained lower Fleming mixed-load fluvial and Coastal Plain deposits, and grades downdip into equivalent lower Coastal Plain facies of Miocene deltaic and barrier systems (Doyle, 1979).

The concept of natural systems and its implications for stratigraphic and geohydrologic analysis was thoroughly reviewed by Chorley and Kennedy (1971) and discussed by Galloway and others (1979b). A depositional system is a three-dimensional, genetically defined, physical stratigraphic unit that consists of contiguous, process-related sedimentary facies. As such, ancient depositional systems are the building blocks of a basin fill and provide logical operational units for description and analysis of basin hydrostratigraphy.

Facies maps synthesized from outcrop and log data, including net-sand isolith (fig. 5) and sand-percentage (fig. 6) maps, display the areal distribution of porous and permeable framework depositional elements that compose the bed-load fluvial system. Regional interpretive subsurface cross sections (fig. 7) show that individual sand bodies tend to cluster or stack vertically within the system. Thus, facies maps,

although combining several individual genetic sand bodies, accurately depict depositional patterns.

The maps and sections reveal five principal depositional elements within the study area. The elements include four broad fluvial axes, which define the loci of major river systems on the Miocene Coastal Plain, and a broad interaxial area characterized by small, dominantly ephemeral streams of local origin (fig. 8). From north to south, these elements are informally named the Burton/Penn axes, Moulton streamplain, New Davy axis, George West axis, and Hebbroville axis (fig. 8). The dip-oriented fluvial belts merge in the deeper subsurface with strike-parallel sand isolith trends of coastal deltaic and strandline systems (fig. 8).

Each component depositional element of the Oakville fluvial system exhibits a characteristic textural and mineralogical composition, sand-body geometry, and facies architecture. In turn, each has different hydrologic characteristics and differing potential for, and styles of, uranium mineralization. Principal permeable framework sand facies of each element include one or more types of channel-fill and splay facies. Framework sands, which commonly occur as composite assemblages with lateral and vertical dimensions characteristic of each element, are bounded by less permeable floodplain facies deposited in interchannel environments.

Hebbroville and George West Fluvial Axes

The Hebbroville and George West axes are interpreted to be two principal loci of a single major river on the Miocene Coastal Plain. This river, most likely the Miocene descendant of the large paleo-Rio Grande system identified in the underlying Catahoula-Gueydan fluvial system (Galloway, 1977), first crossed the Coastal Plain along a broad axis in Live Oak County (fig. 8), then shifted nearly 140 km (90 mi) southward and traversed the Coastal Plain through Jim Hogg County, south of the study area. Regional strike sections indicate that the thickest sands of the Hebbroville axis are stratigraphically higher than most sand of the George West axis (fig. 7). Compositional data, discussed below, as well as the southwesterly trend of most proximal preserved sands of the George West axis (fig. 5) support the inference of a single, large, extrabasinal river system that shifted its location on the South Texas Coastal Plain through geologic time.

Only northernmost subsurface parts of the Hebbroville axis extend into the study area; consequently, it was not sampled. Results of scattered drilling indicate that the Oakville Sandstone along this axis is typically coarse grained and conglomeratic. Characteristics of component facies of the George

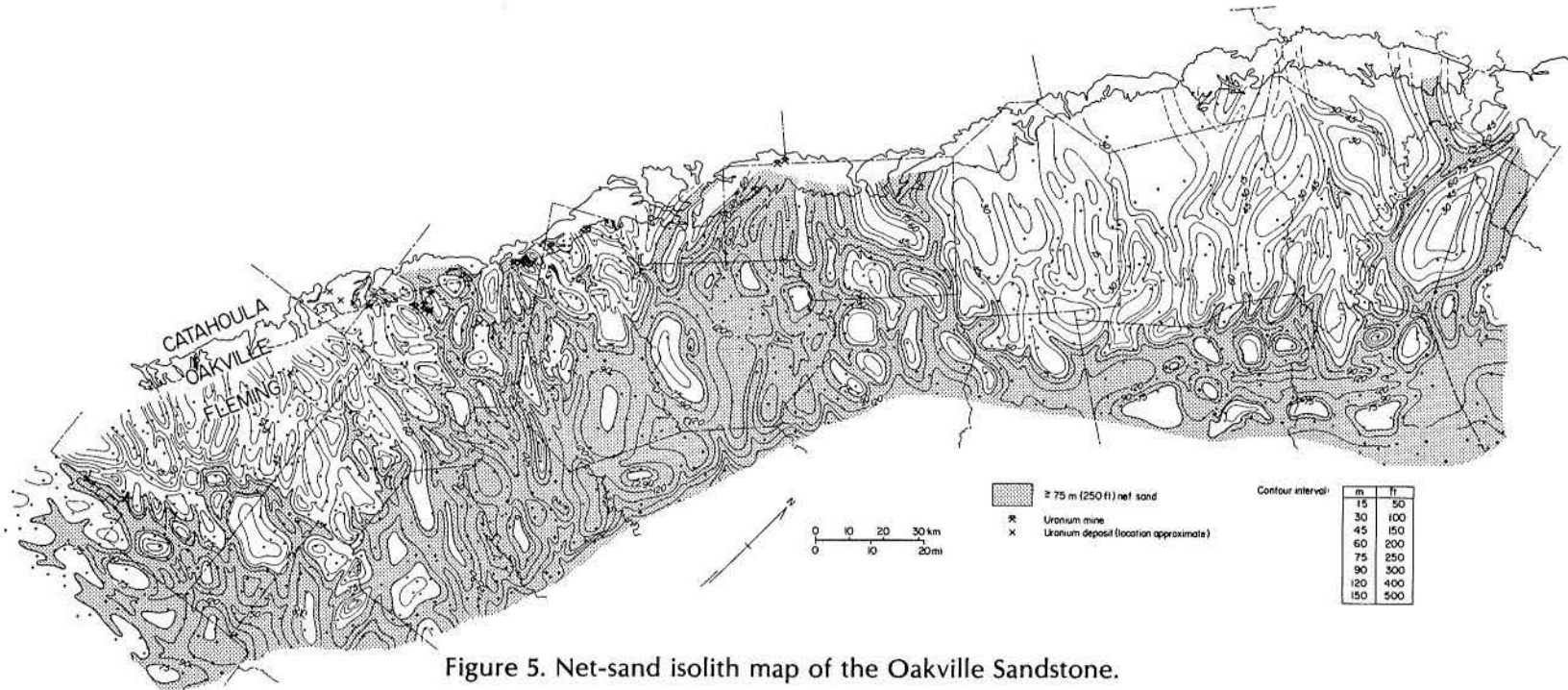


Figure 5. Net-sand isolith map of the Oakville Sandstone.

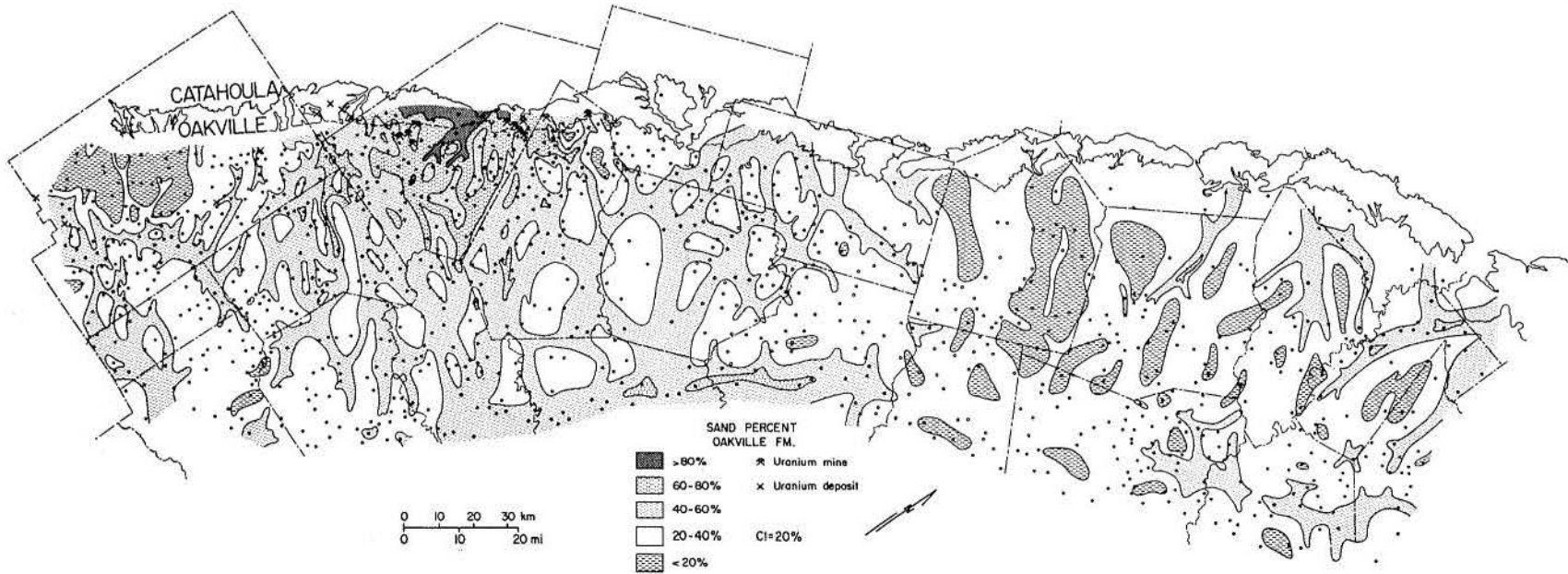
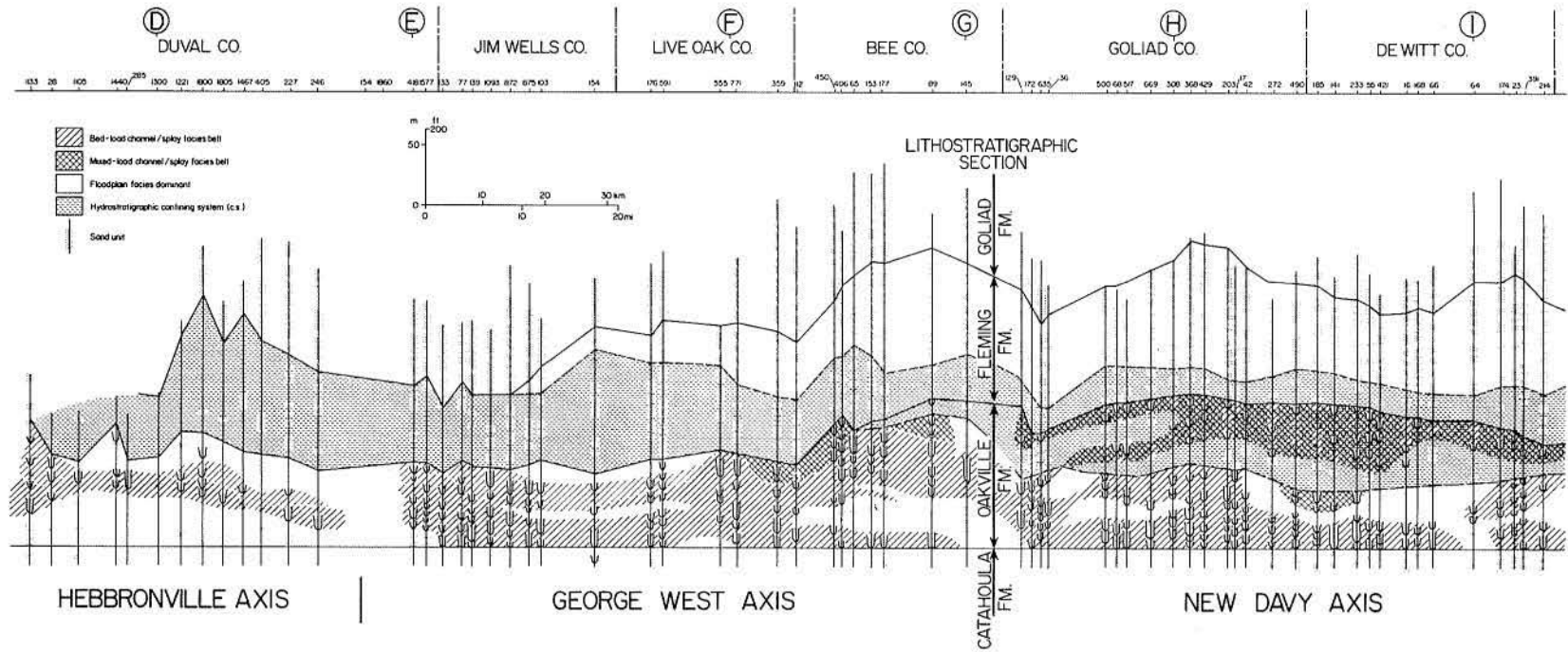


Figure 6. Sand-percent map of the Oakville Sandstone.



8

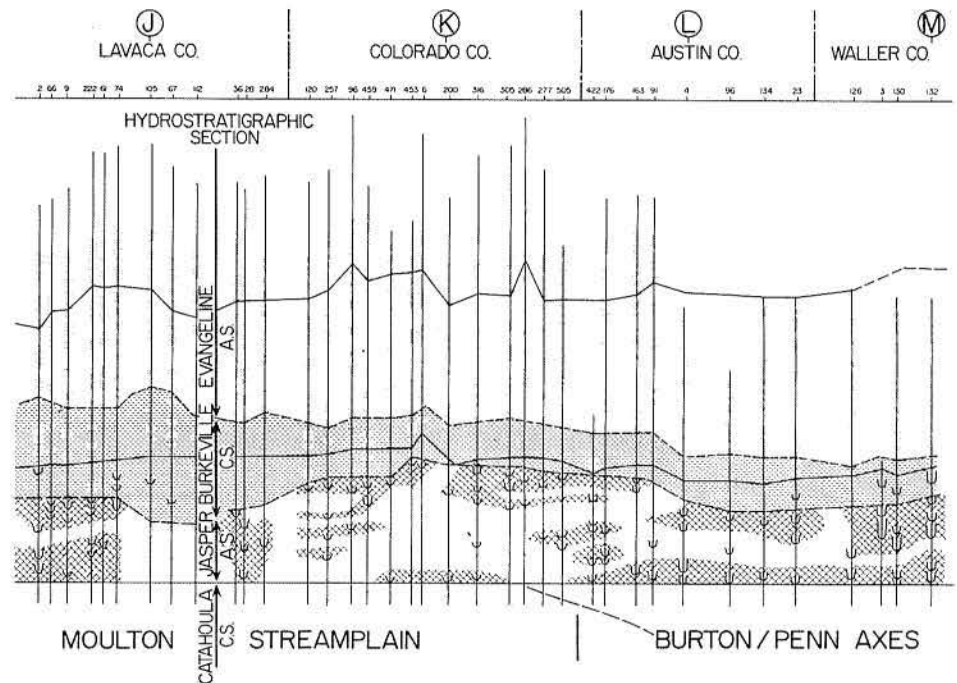


Figure 7. Regional updip strike section (USO) illustrating the lateral and vertical distribution of component facies of the Oakville fluvial system. Channel fills are classified as bed load or mixed load on the basis of log pattern and facies associations discussed in the text. Sand bodies cluster into distinct sand-rich packages defining the principal depositional axes. The Oakville closely approximates the Jasper aquifer system (A.S.) of regional hydrostratigraphic usage.

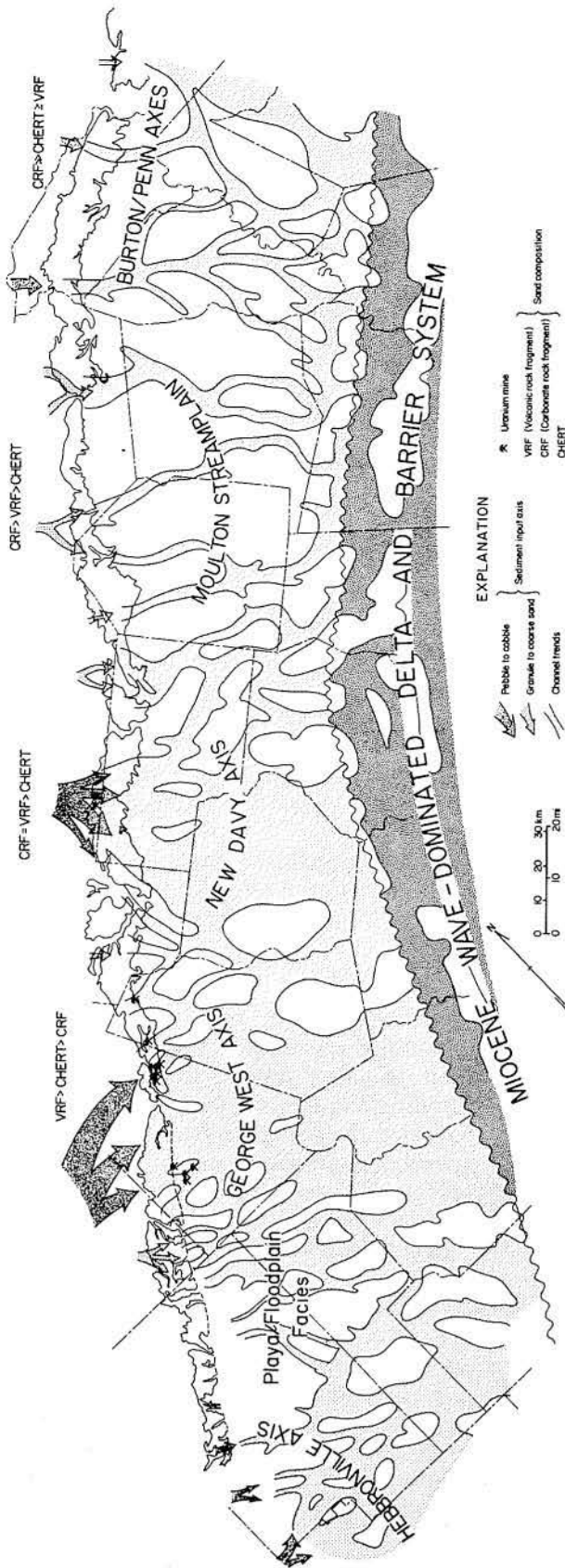


Figure 8. Depositional elements of the Oakville fluvial system. Major rivers are recorded by the Hebronville, George West, New Davy, and Burton/Penn fluvial axes.

West axis may, however, be applicable to the Hebronville axis, particularly if the interpretation of a single major river is correct.

The George West axis hosts the major known uranium reserves of the Oakville fluvial system (fig. 5). Total sand content of the Oakville commonly exceeds 75 m (250 ft) and is almost uniformly greater than 45 m (150 ft). Sand percentage is also high, averaging almost 60 percent and ranging as high as 89 percent in updip parts of the aquifer (fig. 6). As the Oakville thickens downdip, the net sand content increases along individual isolith thicks (fig. 5); however, the proportion of sand to mud decreases (fig. 6).

Along the axis, sand distribution is characterized by multiple dip-oriented, slightly sinuous, anastomosing or basinward bifurcating isolith thicks that form a broad belt nearly 110 km (70 mi) wide (figs. 5 and 6). Individual isolith thicks are generally less than 5 km (3 mi) wide. The high sand percent, complexly intersecting sand-body trends, and broad areal dimensions of the belt suggest a uniformly highly transmissive sand framework characteristic of a major bed-load fluvial system (Schumm, 1977; Galloway and others, 1979b). Outcrop and mine exposures show that framework sands include three principal genetic facies: conglomeratic bed-load channel fill, sandy bed-load channel fill, and sheet splay.

Conglomeratic Bed-Load Channel-Fill Facies

Although volumetrically minor along the George West axis, conglomeratic channel-fill deposits may be significant in the Hebronville axis. The facies consists of interlensed medium to coarse sand and pebbly sand, sandy conglomerate, and clast-supported conglomerate with subordinate amounts of fine sand and silt. Grain size and texture vary randomly both vertically and laterally within sand bodies and within individual depositional units. Individual lenses of sand and gravel range from 1 to 5 m (3 to 15 ft) thick (fig. 9, section A). Internal structures include large-scale, low- to moderate-angle accretionary bed sets containing multiple reactivation surfaces, parallel and planar stratification, scour-and-fill structures, and medium- to small-scale trough cross-stratification (fig. 10). Pebble sizes range up to 7 cm (3 inches) in diameter; common constituents include jasper, chalcedony, silicified wood, volcanic rock fragments, chert, quartzite, and limestone. Clasts exhibit poor to fair imbrication. Intraformational clasts, including sandstone and mudstone grains, pebbles, and large blocks, are common to abundant. Sedimentary

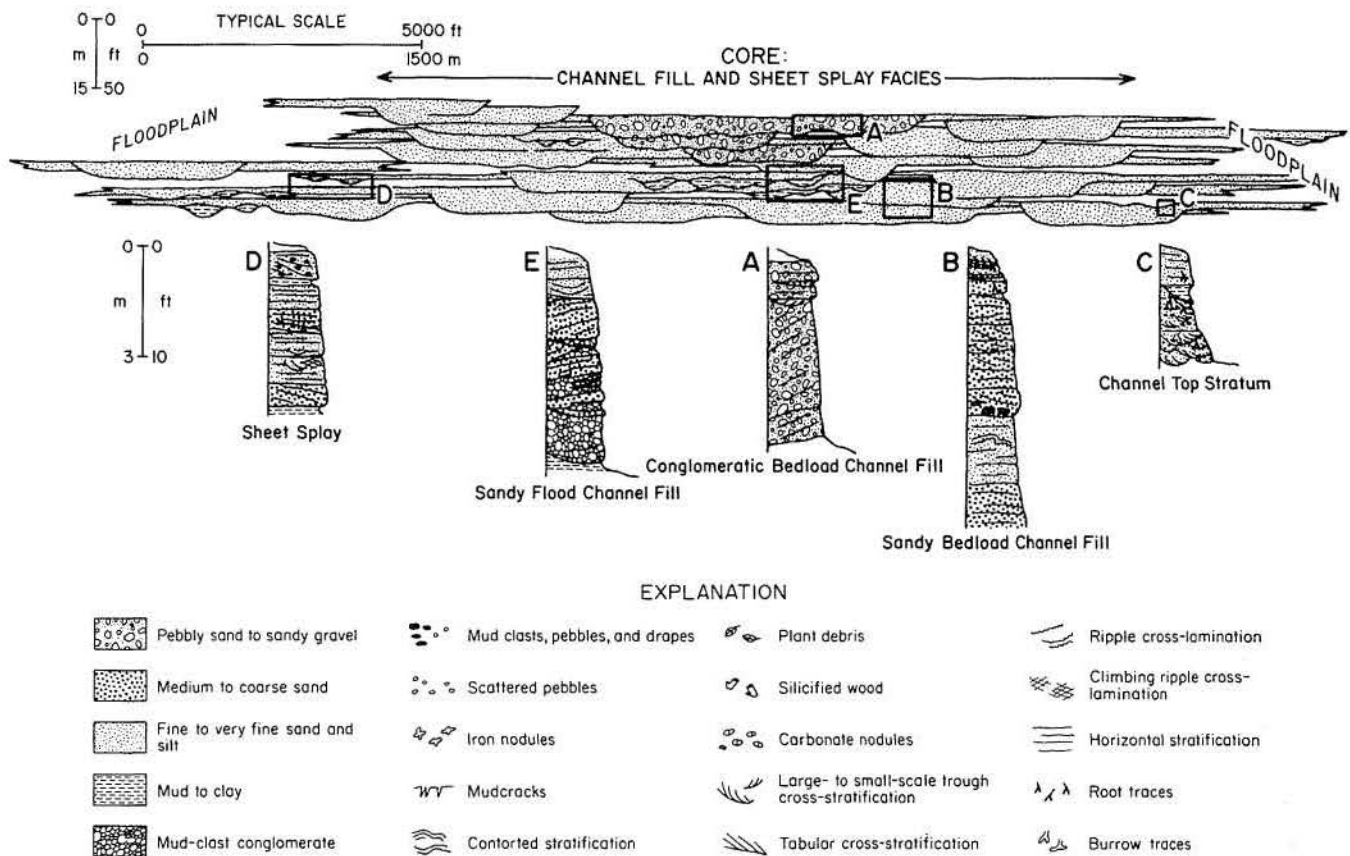


Figure 9. Schematic facies architecture of a composite sand belt typical of the George West fluvial axis. The sand body consists of amalgamated sandy and conglomeratic channel-fill and sheet-splay units interfingering laterally with floodplain deposits. Measured sections illustrate internal features of principal component sand bodies.

features indicate that various types of in-channel bars (most likely including longitudinal, transverse, and marginal) interspersed with small, braided channel lenses and flood channel bars were the primary depositional units (Galloway and others, 1979a).

Sandy Bed-Load Channel-Fill Facies

The principal sediments of the George West fluvial axis are coarse to fine, locally conglomeratic, moderately sorted sand facies deposited in broad, tabular units separated by thin, laterally continuous beds of mud and clay. They contain interspersed, discontinuous lenses and beds of mud-clast conglomerate, silt, and very fine sand. Individual channel-fill sequences average between 3 and 6 m (10 and 20 ft) thick, have sharp, erosional bases, and may be capped by a thin transition zone consisting of finely laminated to massive, root-disturbed, fine sand, silt, and mud (fig. 9, section C). Internal structures consist of abundant planar and low-angle cross-stratified sand and broad lenses of trough and tabular cross-stratified sand (fig. 9, section B; fig. 11).

Common features include local scour-and-fill structures, laterally extensive, internal erosion surfaces, small to large mud clasts and blocks, deformed bedding (in finer sands), and probable antidune cross-stratification (fig. 11). No consistent vertical sequence of grain size or internal structures is present. Local lenses of waxy, sparsely burrowed and finely rippled, laminated claystone indicate local, temporary ponds within abandoned channel segments.

A variation of this facies consists of complexly interlensed, chaotically mixed mud-clast conglomerate and moderately to poorly sorted sand. Structures are dominated by large accretionary, moderate-angle foreset stratification and horizontal stratification (fig. 9, section E; fig. 12). Medium- to small-scale trough and tabular cross-stratification occurs locally within the sand bodies. Reactivation surfaces are abundant.

Interpreted paleochannel geometry, internal structures, and coarse overall texture indicate deposition in flashy, sandy braided bed-load fluvial channels dominated by high-velocity shallow to

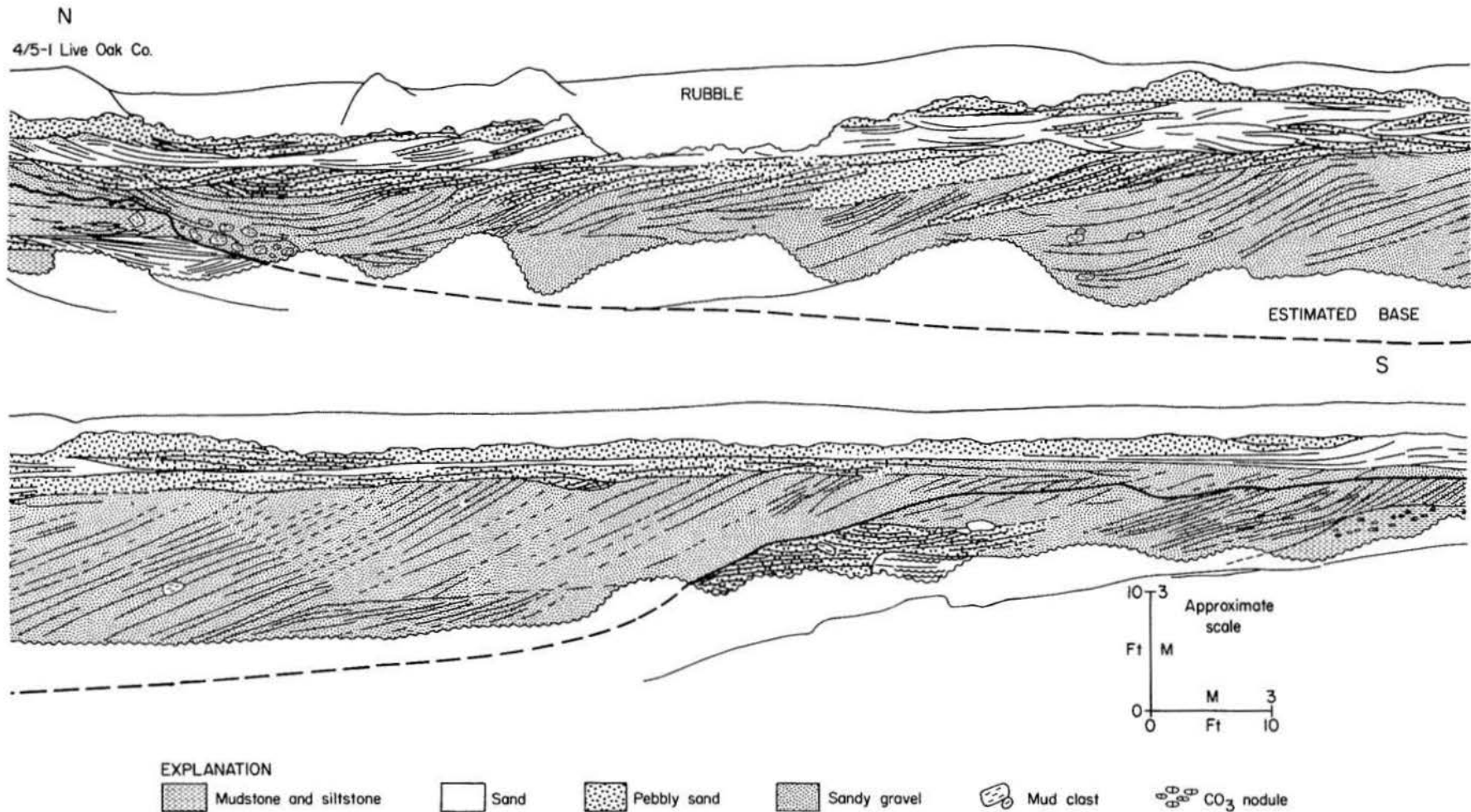


Figure 10. Line tracing of a photomosaic (locality 4/5-1, Live Oak County) showing the internal structure and composition of a well-exposed, conglomeratic braided channel fill of the Ray Point fluvial axis. Internal structure is dominated by large-scale gravel-bar

accretionary bedding. Note abundance of reactivation surfaces. Unit was deposited on irregular scour surface lying directly on fine-grained overbank fine sand and floodplain mud, indicating deposition during major flooding. From Galloway and others (1979a).

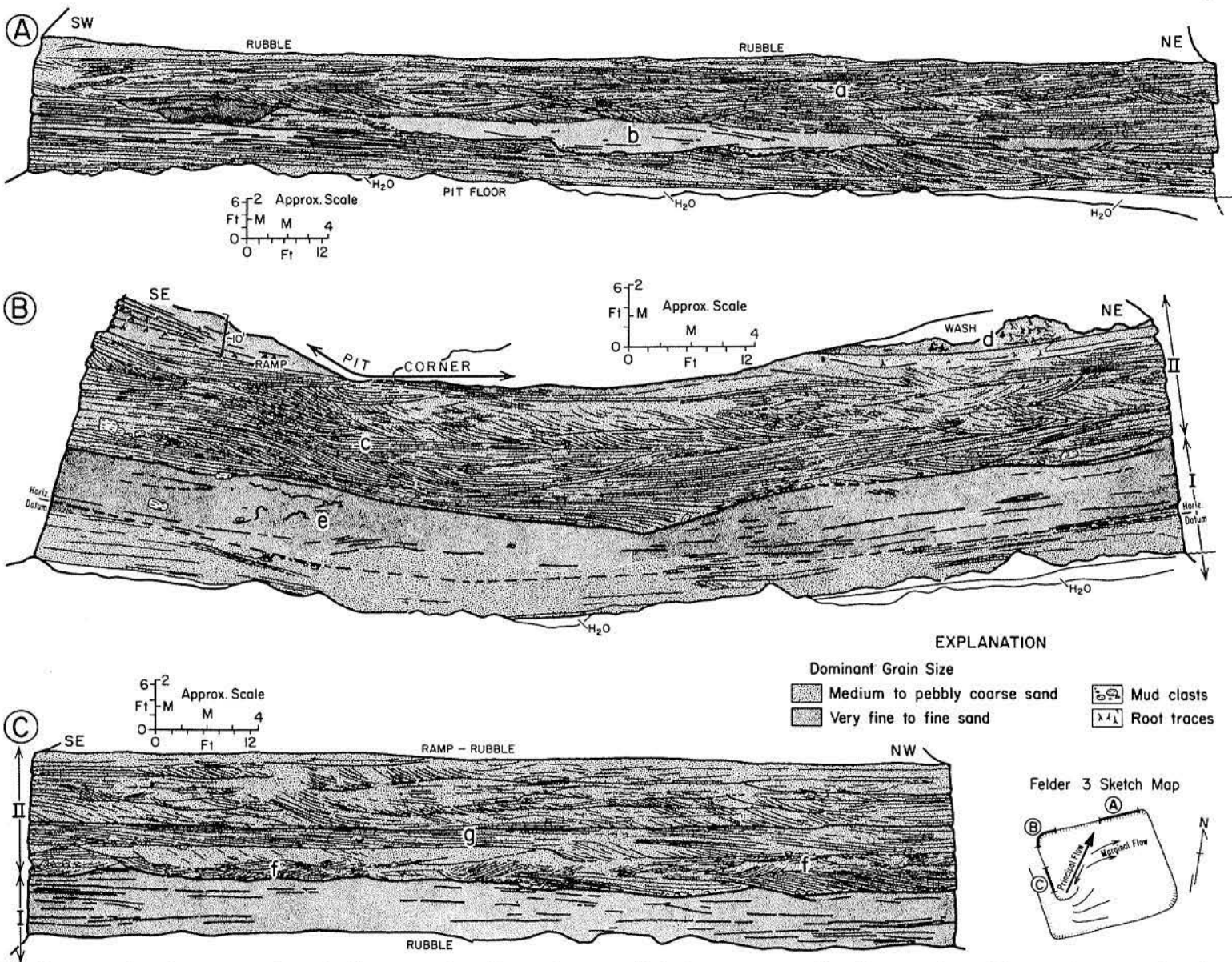


Figure 11. Line tracing from a series of photomosaics illustrating internal structures and textures characteristic of the George West sandy bed-load channel facies. Mosaics A and C provide right-angle views oblique to the interpreted NNE paleocurrent direction; B is a pit corner. Approximately 6 m (20 ft) of additional sand lies below the pit floor. Two channel sequences (indicated by I and II) are separated by an extensive scour surface that can be traced across all sections. (a)

Tabular cross-stratification produced by sand waves migrating up the channel margin during waning flow. (b) Small scour channels. (c) Well-developed tabular cross-stratification with multiple reactivation surfaces. (d) Root-disturbed channel top stratum. (e) Contorted bedding produced by sediment liquefaction. (f) Up-flow dipping trough cross-stratification possibly generated by antidune migration. (g) Planar stratification. From Galloway and others (1979a).

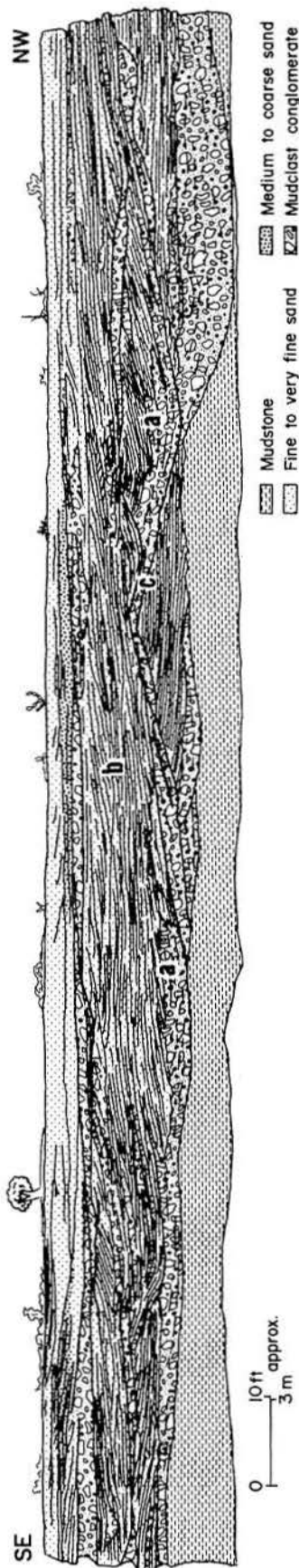


Figure 12. Variation of the sandy bed-load channel-fill facies consisting of complexly interstratified sand and mudclast conglomerate. Many large, lenticular depositional units show crude inverse grading with mud clasts and other unsorted coarse debris deposited at the toe of the large, low-angle accretionary foresets (a).

Multiple reactivation surfaces (b) and cross-cutting scour and fill features (c) are also characteristic, as is horizontal stratification. Features indicate chaotic deposition during short periods of peak discharge. Felder uranium pit, Live Oak County.

intermediate depths (fig. 13). Principal depositional units include linguoid bars and various larger bar forms generated in and marginal to the low water channel during major floods. Similar braided stream deposits of modern fluvial systems, including the Cimarron, Platte, and Saskatchewan Rivers, are reviewed by Shelton and Noble (1974), Miall (1978), and Rust (1978).

Sheet-Splay Facies

Thin to thick sequences of moderately sorted, coarse to fine sand and subordinate interbedded silt and sandy mud occur marginal to and interbedded with channel-fill facies. Sheet-splay units form laterally continuous sheetlike sand bodies; individual depositional units range from less than 1 to over 5 m (3 to 15 ft) thick. Internal structures are dominated by planar stratification (fig. 9, section D; fig. 14). Less common structures include shallow, symmetrically and asymmetrically filled scour channels and troughs, mud drapes, medium- to small-scale tabular cross-stratification, and ripple lamination. Mud clasts and blocks are common accessory features.

The abundant planar and small-scale stratification, sheet geometry, and small-scale vertical variability of grain size and structures indicate pulsatory transitional and upper flow regime conditions in a shallow, unconfined setting. Spatial association of the facies with channel-fill units further suggests deposition of sheet-splay units during periods of intense overbank flooding (fig. 13). Analogous flood sediments were described by McKee and others (1967).

Facies Associations and Distribution

Sandy channel-fill and sheet-splay units occur as intimately interbedded components of broad, tabular sand belts that are commonly several kilometers wide and 5 to 30 m (15 to 100 ft) thick. Sand-rich cores of thicker belts contain vertically stacked, amalgamated sequences of several channel fills (fig. 9). Very little mud or clay is preserved except in lenses or lags of mud-clast conglomerate. Conglomeratic channel-fill deposits occur only in limited areas of the George West fluvial axis. Where present, however, they occur within the core of major sand belts (fig. 9) and represent the most proximal fluvial facies preserved in the Oakville system. Conglomeratic deposits are believed to be more abundant along the

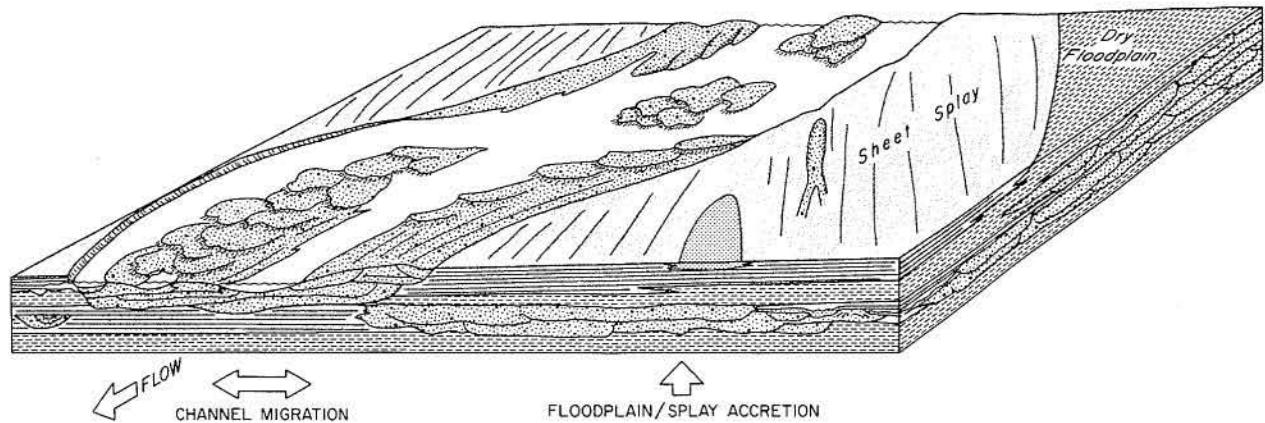


Figure 13. Schematic reconstruction of Oakville fluvial depositional environments. Braided bed-load channels were flanked by extensive sheetflood-dominated crevasse splays, which grade laterally into interchannel floodplain deposits. From Galloway and others (1979a).

Hebbronville axis and probably display facies relationships similar to sandy channel-fill and splay facies.

Composite fluvial belts grade laterally into interbedded sheet splay and pedogenically modified floodplain facies, punctuated locally by isolated channel fills (fig. 9). Sheet-splay sands do not extend far beyond associated channel fills. The amalgamated bundles of sandy and conglomeratic channel fills and marginal sheet splays compose the fundamental high-permeability conduits in the southerly axes of the Oakville bed-load fluvial system. Several such bundles are vertically stacked in areas of thickest sand (fig. 7) and are less abundant in interaxial areas of lower sand percent and abundant, better preserved, and less permeable floodplain deposits.

New Davy Fluvial Axis

The New Davy axis marks the locus of a major river on the Miocene central Texas Coastal Plain. It is particularly well developed in northeastern Karnes County and De Witt County, where total sand content locally exceeds 100 m (300 ft) (fig. 5). The total Oakville section, as defined in this study, is unusually thick, averaging over 200 m (700 ft) (fig. 7). Consequently, sand percentage rarely exceeds 50 percent (fig. 6).

The base of the Oakville Sandstone is difficult to define. Fluvial sedimentation along the New Davy axis occurred during deposition of both the Catahoula and the Oakville Formations; thus, the boundary between the two units is transitional. The hydrostratigraphy of the area indicates that the boundary may be most logically placed at the base of the zone of laterally continuous, massive sand. However, the lowest sands thus included within the

Oakville fluvial system are stratigraphically below basal Oakville sands of the George West axis (fig. 7), and they closely resemble some mineralized fluvial sands within the underlying Catahoula Formation.

Uranium production is concentrated in the Nopal area (fig. 5), where it has been mined exclusively by open-pit methods. Ore occurs at the base of the Oakville in a massive sand host. Much of the uranium is in the form of uranyl minerals concentrated near the zone of modern surface oxidation.

The New Davy axis fans out basinward and consists of a series of bifurcating sand belts that range from 2 to 8 km (1 to 5 mi) wide (fig. 5). Modal thickness of individual sand bodies is 6 to 12 m (20 to 40 ft); about 10 percent of the sand bodies exceed 18 m (60 ft) thick. The somewhat reticulate sand isolith pattern that is particularly obvious in the northeastern half of the axis (fig. 5) probably indicates syndepositional modification of drainage patterns by deep-seated Wilcox fault zones (see Galloway, 1977, p. 26-28). Outcrop and mine exposures and electric log characteristics define three principal framework sand facies within the New Davy axis: conglomeratic bed-load channel fill, mixed-load channel fill, and crevasse and sheet splay.

Conglomeratic Bed-Load Channel-Fill Facies

This facies consists of grain sizes ranging from fine sand to granule conglomerate and sandy conglomerate. Clasts rarely exceed 5 cm (2 inches) in diameter; unlike generally analogous conglomeratic channel fills of the George West axis, open framework gravels have not been observed. Clasts include silicified wood, structureless opal and

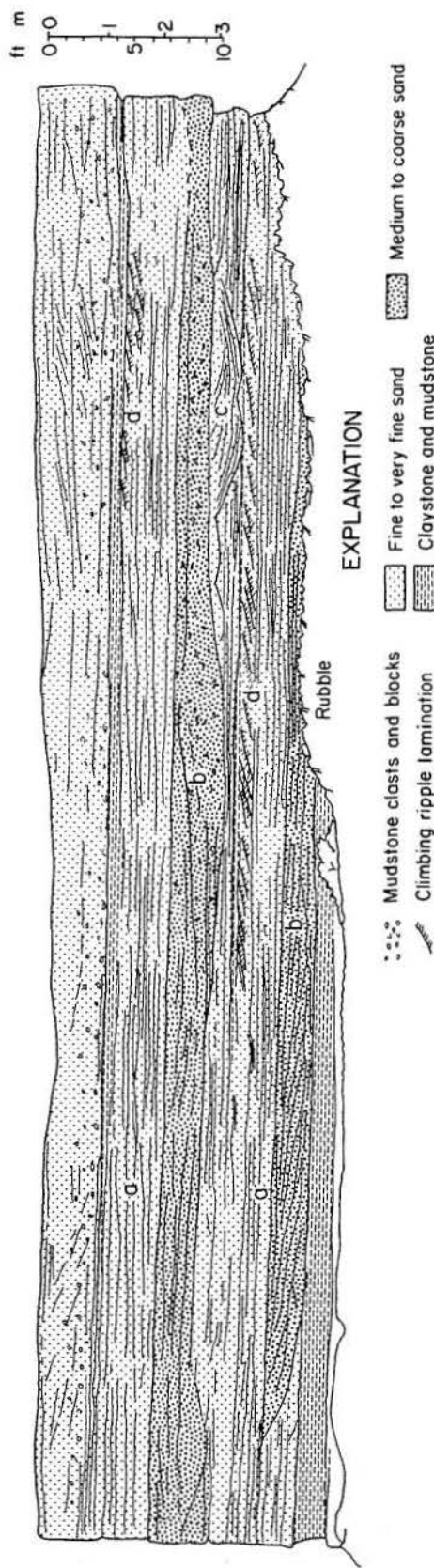


Figure 14. Sheet-splay deposits interbedded with channel fills of the George West axis exposed in the Smith uranium mine (Live Oak County). Principal sedimentary features include (a) well-developed horizontal bedding as well as internal planar stratification, (b) local

small scour channels commonly filled with coarser sand and mud clasts, (c) small scour fills, and (d) waning-flow sequences capped by climbing ripple lamination.

chalcedony, and reworked Cretaceous fossils and limestone fragments. Individual depositional units composing sand bodies consist of texturally distinct beds and lenses ranging from 1 to 5 m (3 to 15 ft) thick. Individual bedded sequences commonly contain coarsest sediment at or above basal scour surfaces. Interlensed units may contain highly diverse sediments. Thick sand bodies consist of many such vertically and laterally amalgamated depositional lenses, producing an internally heterogeneous, but highly permeable, aquifer. Thick, multi-unit sand bodies tend to fine upward, but very irregularly (fig. 15, section B).

Primary structures include abundant planar and low-angle tabular or accretionary stratification, medium- to large-scale trough cross-stratification, scour-and-fill structures, multiple reactivation surfaces, and local internal erosion surfaces (fig. 15, section A). Less common structures, typically limited to finer grained units, include ripple cross-lamination, deformed stratification, and sparse root or burrow traces. Large blocks (up to a meter in diameter), pebbles, and chips of reworked mud and silt are abundant. Sedimentary structures, heterogeneous internal composition, scale of depositional units, and tabular sand-body geometry all indicate deposition in large, braided, flashy (flood-dominated) bed-load stream channels (Miall, 1977; Galloway and others, 1979b; Rust, 1978).

Mixed-Load Channel-Fill Facies

Channel-fill sand units that consist of coarse- to fine-grained sand and subordinate silt and mud are smaller than bed-load channel fills. Mixed-load channel-fill sand units are finer grained, typically fine upward from sharp, scoured basal surfaces, and are capped by interbedded fine sand and mud. Poorly developed, lateral accretionary bedding typical of sinuous mixed-load channels is preserved in some units. Locally, channel fills are capped by lenses of coarse sand or pebbly coarse sand, suggesting possible chute channel and bar deposition on the upper point-bar surface (Galloway and others, 1979b). Primary sedimentary structures include abundant, low-angle, medium- to large-scale, trough cross-stratification, planar stratification, and, in finer grained sediments, subordinate wavy, deformed, and ripple lamination (fig. 15, section C). Mud clasts, grains, and blocks are common accessory constituents; silicified and/or carbonized wood is present.

The relatively orderly vertical sequence of grain size and internal structures produces individual genetic sand bodies 4 to 8 m (12 to 25 ft) thick. Vertical stacking and amalgamation of units occurs but is less

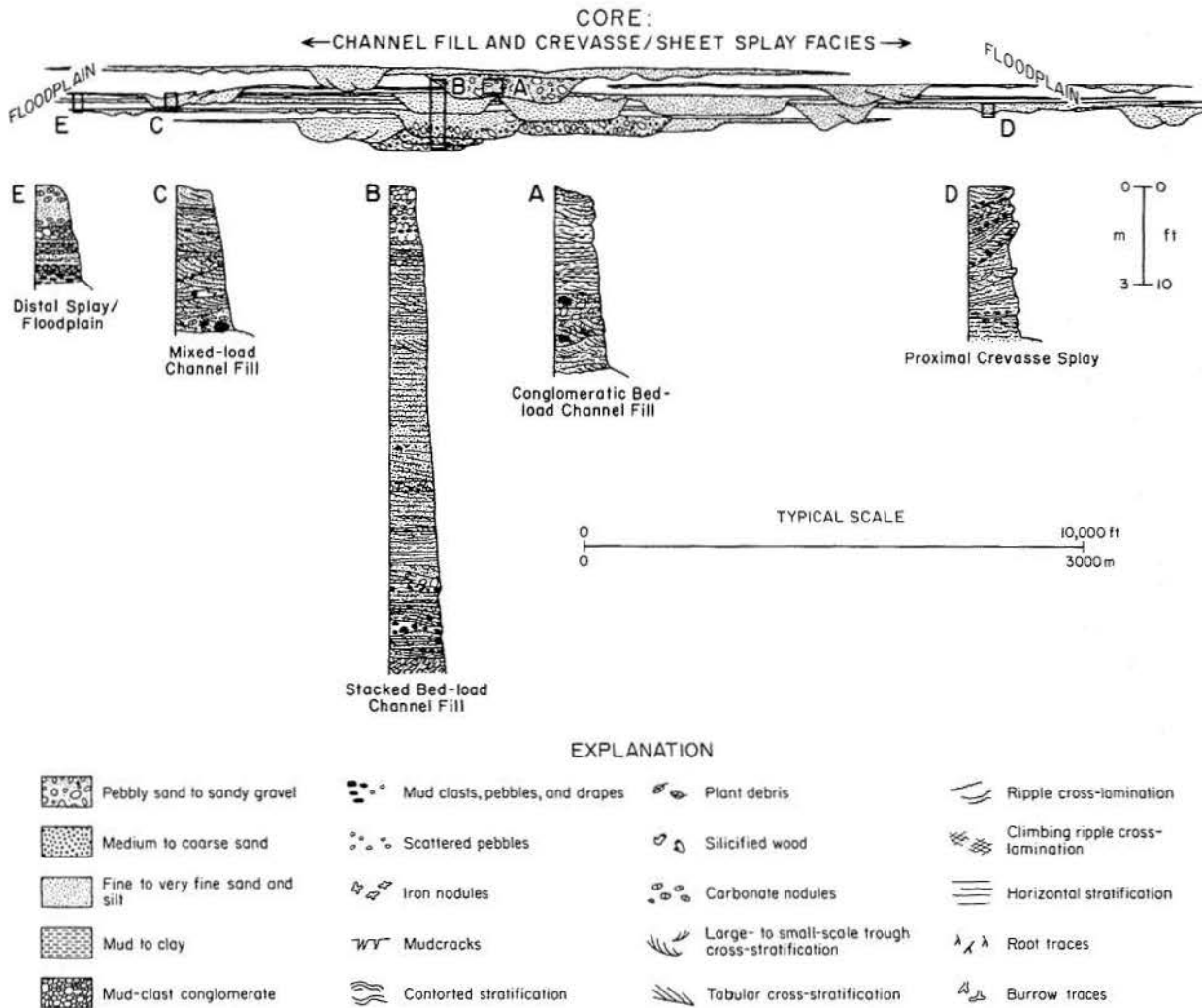


Figure 15. Schematic facies architecture of a typical New Davy axis sand belt. The belt consists of laterally and vertically amalgamated bed-load channel-fill units and associated sheet and crevasse splay sands. Measured sections illustrate typical internal features and composition of permeable facies.

common than in conglomeratic bed-load channel-fill sequences. Net permeability of mixed-load channel-fill sand bodies, although still great, would probably be somewhat lower than in coarser, better interconnected, bed-load fluvial facies.

Crevasse Splay and Sheet-Splay Facies

The New Davy axis contains tabular units composed of fine to coarse, horizontally laminated sand interbedded with channel-fill facies, which are comparable in size, composition, and origin to the sheet-splay facies of the George West axis. In addition, crevasse splay units, which consist of medium to very fine sand and interbedded mud, silt,

and clay, were deposited where flood flow was diverted from main channels onto the surrounding floodplain. Crevasse splay units form repetitive tabular beds deposited during major floods, crosscut by lenticular symmetrically to asymmetrically filled crevasse channel and scour sequences up to several meters thick. Splays are characterized by internal heterogeneity of both textures and sedimentary structures, which include abundant planar, trough, tabular, ripple and climbing ripple stratification, load structures, and root marks (fig. 15, sections D and E). Mud lenses, drapes, and clasts are abundantly interspersed throughout. Dimensions of splay units are variable, but they probably extend no more than a few thousand meters from the associated channel fill.

Facies Associations and Distribution

Although the distribution of the component facies along the New Davy axis is complex, two general patterns emerge. First, in the lower part of the Oakville, principal sand belts consist of broad, irregular cores of conglomeratic bed-load channel fills surrounded laterally and interbedded with mixed-load channel fills. Laterally associated remnants of sheet-splay and crevasse-splay sand units combine with the multiple intersecting channel fills to form a complex mosaic sand body (fig. 15). Relatively little floodplain sediment is preserved within such sand belts, which form well-integrated, highly permeable conduits. Second, in contrast to the lower Oakville, the upper Oakville section lacks bed-load channel facies. Sand units consist of multilateral and multistory sequences of mixed-load channel fills (fig. 7) and abundant interbedded floodplain and crevasse splay deposits. Finer grain size and poorer interconnection of individual genetic sand units produce a less permeable aquifer.

Both types of composite sand belts grade laterally into thick sequences of interchannel floodplain mud and clay, broken locally by more extensive splay beds or isolated channel fills (fig. 15). Complete Oakville sections consist of as many as four such superposed sand belts separated by laterally continuous floodplain mud (for example, fig. 7, well 517, Goliad County).

Moulton Streamplain

Northeast of the New Davy fluvial axis, the Oakville fluvial system grades into a relatively mud-rich section encompassing Lavaca and Fayette Counties, and contains several narrow, localized, dip-oriented sand trends (fig. 8). Within this area, net thickness of Oakville sand rarely exceeds 45 m (150 ft), and sand content commonly ranges between 10 and 40 percent (fig. 6). Net sand thickness increases substantially only at depths below 600 m (2,000 ft).

The narrow, thin sand-rich belts encased in abundant fine-grained sediment indicate that deposition in the central part of the Miocene Coastal Plain was characterized by small, local, primarily mixed-load streams. Small streams with local catchment basins would probably be flood-prone or ephemeral, a supposition supported by sedimentologic evidence. The small size of individual sand bodies of the Moulton streamplain severely limits the potential for large-scale uranium mineralization. However, in several sand bodies, small, potentially commercial uranium deposits are known. Their geology probably resembles that of similar Catahoula deposits found in the same geographic area

(Galloway and Kaiser, 1980). Principal component facies of the Moulton streamplain include framework sands of channel-fill and sheet/crevasse splay facies, as well as finer grained floodplain facies.

Channel-Fill Facies

Moderate- to well-sorted coarse to very fine sand, and sparse granule conglomerate and pebbly sand occur as lenticular channel-fill units ranging from 3 to 7 m (10 to 25 ft) thick. Channel fills exhibit a sharp, irregular erosional base and crudely developed fining-upward textural sequence. Commonly, a lower massive zone of medium- to large-scale, low-angle trough cross-stratified medium to pebbly coarse sand is overlain by several meters of planar-laminated fine to medium sand. This is capped in turn by interbedded very fine sand, silt, and sandy mud containing ripple, climbing ripple, wavy, and planar lamination, medium-scale isolated trough-bed sets, and sparse root traces (fig. 16, sections B, C, D). Lateral accretion bedding occurs in the upper parts of a few channel sequences, particularly in the upper Oakville Formation.

Gravel is a minor component in many channel fills of the Moulton streamplain facies, and consists of granule to fine pebble-sized reworked Cretaceous fossils, carbonate rock fragments, and silicified wood. Mud clasts and chips are locally concentrated within both cross-stratified and planar-stratified units. Reworked, syngenetic micrite nodules are common in zones containing abundant mud clasts.

Both outcrop and well log sections demonstrate vertical superposition of several channel units (for example, fig. 7, wells 257 and 316, Colorado County; fig. 16, section A). However, amalgamation of several channel-fill units is relatively rare; fewer than 10 percent of the shallow sand bodies sampled are more than 12 m (40 ft) thick.

Sheet-Splay and Crevasse Splay Facies

Channel fills are interbedded with a great variety of sand and silt units deposited during flooding of small coastal plain streams. Splay deposits include sheets up to 3 m (10 ft) thick of planar-stratified, well-sorted medium, fine, and coarse sand, and more discontinuous beds and lenses of well to moderately sorted, medium to very fine sand, silt, and mud (fig. 16, sections E and F). Sheet splays were produced by shallow, high-velocity flood waters flowing along active channel margins and onto adjacent floodplain areas during flash floods, which are common to local streams with small drainage basins (McKee and others, 1967). Crevasse splays formed under flood

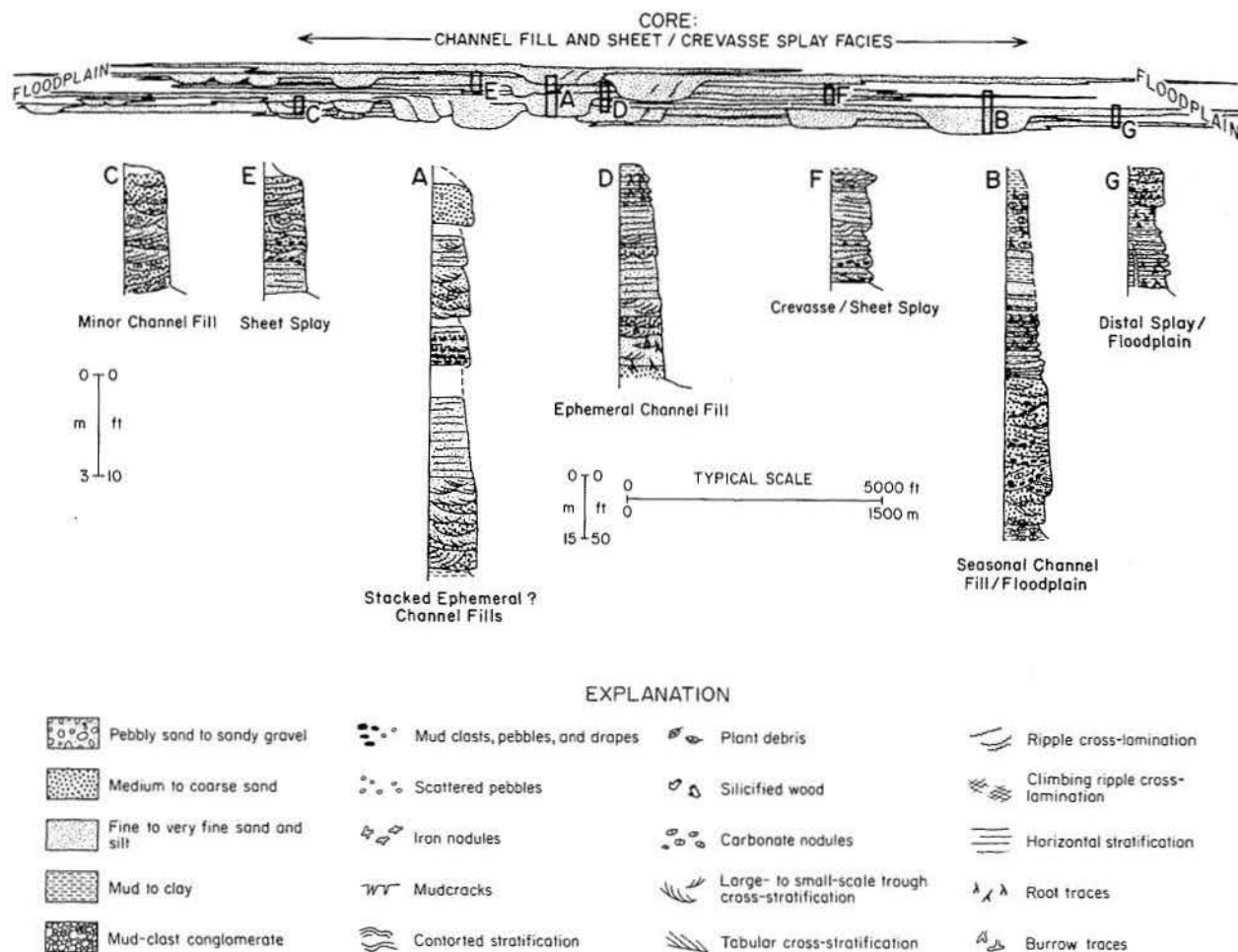


Figure 16. Schematic facies architecture of a composite sand belt within the Moulton streamplain. Numerous laterally and vertically amalgamated small channel-fill and abundant sheet and crevasse splay units produce sand belts that internally are highly heterogeneous. Sedimentary features indicative of flashy or ephemeral flow characterize many channels. Measured sections illustrate internal features of a variety of specific sand facies.

conditions where flow was partly channelized as it topped stream channel margins and spread onto the floodplain. Variable water depths, flow velocities, and sedimentation rates created diverse suites of sedimentary structures. Pulsatory sedimentation is indicated by abundant clay drapes and lenses, reactivation surfaces, internal scours separating individual depositional units, and waning-flow sequences of primary structures. Both types of splay sequences locally contain root traces and other evidence of subaerial exposure. Mud clasts and chips are common.

Splay deposits are similar to those of the New Davy axis. However, within the Moulton streamplain complex, they constitute a large proportion of the

total sand volume, which reflects the extremely flashy to ephemeral nature of the associated streams. Deposits can extend far into the interchannel floodplain environment.

Facies Associations and Distribution

Multiple, vertically stacked channel-fill sand units produce several distinct, mappable belts a few kilometers wide. Together with genetically associated crevasse and sheet-splay sands, which provide a permeable interconnecting matrix (fig. 16), such composite channel belts are basinward-trending permeability zones that are laterally isolated within

thick sections of low-permeability floodplain facies. Thickness of composite sand belts rarely exceeds 15 m (50 ft), although several sand belts may occur within a single vertical section (fig. 7).

Burton/Penn Fluvial Axes

In the northeastern part of the Oakville fluvial system, thick, coarse-grained deposits of large rivers again appear in the section. Subsurface data are sparse, but sand distribution patterns and localization of coarsest sediments at outcrop indicate at least two main channel complexes (fig. 8). The first entered the coastal plain near the present Washington/Fayette county line. From this apex, sand trends fan out into a series of downdip diverging belts. A second, less well defined sand belt is centered at outcrop near the modern Brazos River. Although limited exposures indicate that these two fluvial complexes differ in detail, they are similar in composition, sand-body geometry, and geographic location.

Sand belts comprising the Burton/Penn axes are commonly several kilometers wide and are well defined by total sand thicknesses in excess of 45 m (150 ft). As much as 90 m (300 ft) of sand is present locally in the subsurface (fig. 5). Sand percentages range from less than 30 in interchannel areas to more than 50 along isolith thicks (fig. 6). Intermediate sand content, restriction of sands to laterally isolated belts, and internal features of the channel deposits indicate deposition by flashy, coarse mixed-load to distal bed-load rivers (Galloway and others, 1979b).

Uranium exploration in the Burton/Penn axes has been minimal, and no discoveries of commercial deposits have been announced. However, mineralization is known, and the well-developed sand framework has significant potential for hosting small- to medium-sized deposits (fig. 1). Mineralization most likely would be associated with carbonaceous sediments that occur in the section and might resemble the small Catahoula deposits of the central Texas Coastal Plain (Galloway and Kaiser, 1980, p. 49). Constituent facies include a sinuous channel-fill facies and genetically associated crevasse and sheet-splay facies.

Sinuous Channel-Fill Facies

Channel-fill facies consist predominantly of medium to fine sand with common coarse sand, pebbly sand, and very fine sand and silt. Modal grain size typically decreases upward within individual sand bodies, although interbedding of different textures is

common. Large-scale, low-angle, lateral accretionary bedding, a primary indicator of point-bar deposition within a sinuous channel (Galloway and others, 1979b), has been observed at outcrop (fig. 17). Scale of primary sedimentary structures also tends to decrease upward. Medium- to large-scale, broad, low- to moderate-angle trough cross-stratification dominates the lower, massive coarse to medium sand. Overlying finer intervals contain planar or parallel stratification, small- to medium-scale trough and tabular cross-stratification, lenses and beds of ripple and wavy lamination, and laterally continuous, low-relief, uniformly dipping reactivation surfaces (fig. 17; fig. 18, section A). Locally, sand bodies are capped by thick beds or lenses of coarse sediment containing abundant conglomerate, mud clasts, and woody debris (fig. 18, section B). Large-scale crossbedding and coarse lenses occurring at the top of the channel-fill sequence suggest deposition on chute-modified point bars (McGowen and Garner, 1970). In addition, many smaller channel fills, similar to those of the Moulton streamplain, occur within the Burton/Penn axes (fig. 18, section C).

As is typical of sinuous mixed-load streams, several cycles of channel fill commonly occupy the same drainage course, producing vertically amalgamated sand bodies much thicker than actual channel depth. Channel superposition is evident in outcrop and by sand-body thicknesses. Over 25 percent of measured subsurface sand bodies are greater than 18 m (60 ft) thick. Original channel depths were more likely 5 to 10 m (15 to 30 ft).

Mud clasts and blocks, and reworked micrite nodules are less abundant here than in other parts of the Oakville fluvial system. Plant debris, preserved in carbonized or silicified forms, is more common, however.

Crevasse Splay and Sheet-Splay Facies

Rivers of the Burton/Penn axes were subject to flashy discharge and extensive flooding. Bed load was distributed far out onto the floodplain by crevassing and sheet flow. Resultant deposits are concentrated along the margins of channel-fill sequences and, like their counterparts in the New Davy axis and Moulton streamplain, consist of heterogeneous sequences containing a variety of sediment types and structures indicative of pulsatory, shallow flow (fig. 18, sections D and E). Splay sequences of the larger Burton/Penn rivers are relatively thick (up to several meters), but appear to have extended only a few thousand meters beyond associated channel segments. Largest splays are cut by lenticular crevasse and flood-runoff channel deposits up to several meters thick.

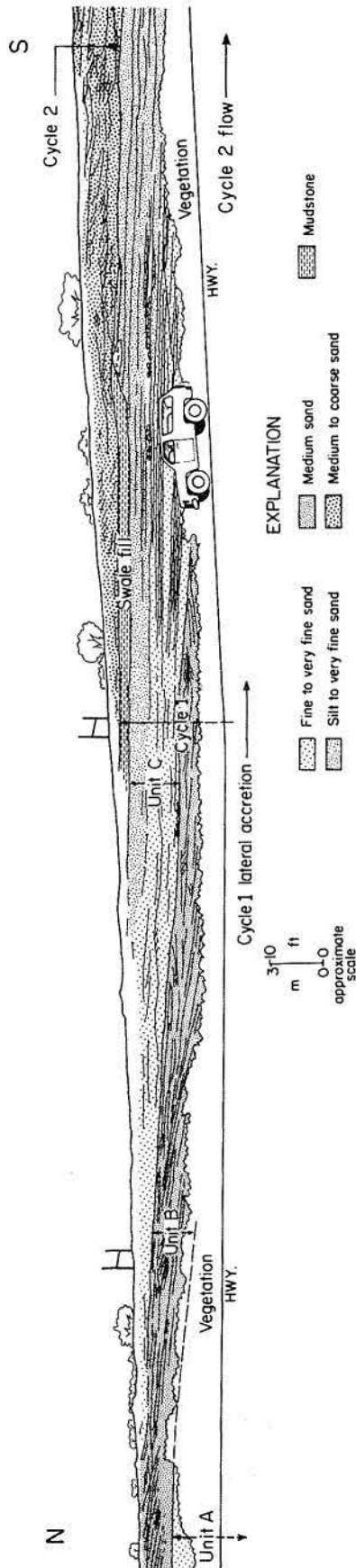


Figure 17. Road cut (locality 5/18-1, Grimes County) displaying lateral accretion bedding typical of upper point-bar deposits (units A, B, and C, cycle I) of a sinuous mixed-load channel of the Burton/Penn axes. A second cycle (II) is stacked on the upper point bar and local swale fill

deposits of cycle I. These lower point-bar and channel-lag deposits consist of medium to coarse sand, in contrast to the fine sand typical of the upper point bar. Internal features include abundant parallel and trough cross-stratification.

Facies Associations and Distribution

Highly transmissive, permeable sand-rich belts consist of several vertically and laterally amalgamated channel-fill sequences, including point-bar and chute-modified point-bar deposits, and laterally associated splay deposits (fig. 18). Conglomeratic and chute-modified point-bar sequences appear to be more common along the Burton axis, which is best developed at the base of the Oakville Formation. Sand-rich belts range from 10 to 60 m (30 to 200 ft) thick, and two or more may be stacked (fig. 7, Waller County wells).

Floodplain Facies

Permeable framework sand facies are bounded laterally and vertically by massive- to thick-bedded, homogeneous mud, sandy mud, clay, muddy silt, and muddy fine sand deposited in interchannel areas. Muds are typically blocky, churned or mottled, moderately to highly calcareous, and break into blocky, slickensided clumps resembling soil clods or peds. Less commonly, fine lamination or discrete root traces are preserved. Diffuse and discrete pedogenic micritic calcium carbonate nodules are abundant, typically clustering along distinct horizons. Manganese stains (mangans of Brewer, 1964) coat many fracture surfaces. Colors range from brown or brick red to olive, gray, or cream, depending on the oxidation state.

In Duval County, Oakville floodplain deposits are highly calichified both at outcrop and in the shallow subsurface (fig. 8). Outcrops are poorly exposed, but sparse exposures of highly calichified and silicified interbedded sand, silt, and mud display mudcracks, rippled bedding surfaces, wavy lamination, mud chip breccias, chaotic fabrics, and clay drapes. The suite of sedimentary and diagenetic features suggests deposition in local interfluvial playa lakes or ponds (Hardie and others, 1978).

Facies Summary

The five fluvial axes consist of the same principal components—sand-rich channel-fill units, flanked by flood-deposited crevasse splay sand units, and interbedded fine-grained deposits of interchannel, dry floodplain origin. These features, however, differ in size and position in each fluvial axis. Mineralogic

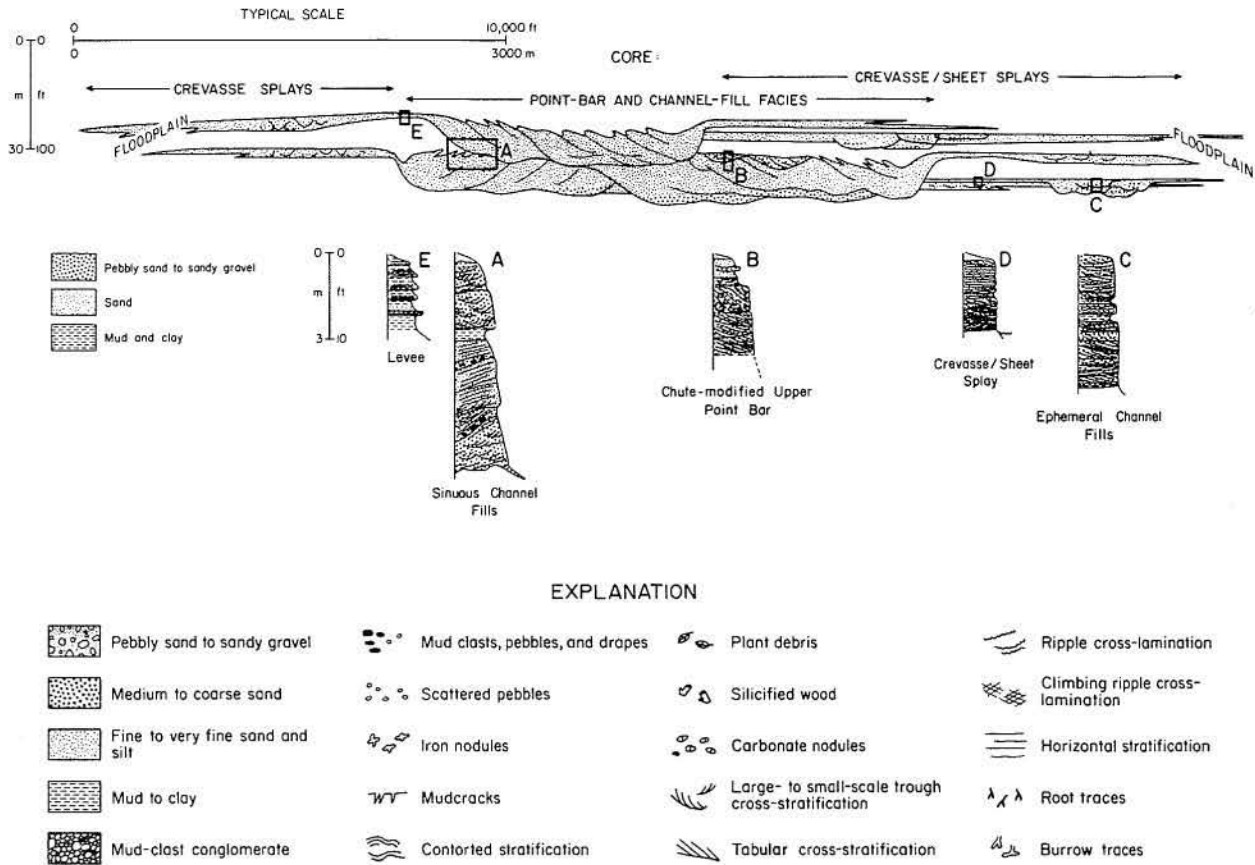


Figure 18. Schematic facies architecture of a sand belt typical of the Burton/Penn axes. The composite sand body consists of vertically stacked channel-fill sequences including both chute-modified and conventional point-bar facies and associated crevasse and sheet-splay units. Measured sections illustrate internal features and composition of component permeable facies.

analysis confirms the individuality of each of the fluvial axes.

water chemistry and cumulative epigenetic modification of aquifer matrix.

MINERALOGIC COMPOSITION

A regional inventory of Oakville mineralogy provides a framework for analysis of important water/rock interactions affecting modern hydro-chemistry and further aids definition of major depositional elements of the aquifer. Mineral phases of an aquifer system provide the matrix through which ground water circulates. Contact time for waters is great, particularly in semiconfined aquifer systems. Consequently, interactions between mineral phases and ambient waters may proceed toward equilibrium, yielding downflow modification of

Mudrock Petrofacies

Conventional X-ray diffraction studies of 47 regionally selected samples of mudrocks show that clay minerals in fine-grained Oakville sediments consist of montmorillonite and kaolinite (table 1). Illite is present in at least trace amounts in all samples from the Hebronville and George West fluvial axes, and is present in trace amounts in about one-third of the samples from the remaining Oakville depositional elements (table 1). Montmorillonite is dominantly of the Ca-Na mixed-layer type. Most samples contain approximately 80 to 90 percent montmorillonite;

Table 1. Clay mineralogy of representative fine-grained Oakville samples.

County	Locality	Lithology	Mont.	Kaol.	Ill.	Comments
Duval	4/4-1b	silicified v.f. sandy to silty mudstone	abs	abs	D	Silicified, possibly Goliad Possibly Goliad
	4/4-1d	calc. mudstone	abs	abs	P	
	4/4-6c	calc. v.f. sandy mudstone	tr	abs	D	
	4/5-11	calc. silty mudstone	D	P	tr	
Live Oak	3/31-1	calc. mudstone	tr	D	P	Fleming
	4/5-1a	calc. med.-f. sandy mudstone	D	P	tr	
	4/5-1b	calc. mudstone	D	P	tr	
	4/5-3b	calc. mudclast conglomerate	D	P	tr	
	4/6-2	calc. mudstone	D	tr	tr	
	Lam-3b	calc. sandy mudstone	D	tr	P	
	3/22-3b	calc. claystone	D	P	tr	
	3/22-3c	calc. mudstone	D	P	tr	
	Feld-2b	calc. silty claystone	D	P	tr	
	Feld-2e	calc. silty claystone	D	P	tr	
	Feld-2k	calc. muddy sandstone	D	P	tr	
	Z-3-151.5	calc. muddy siltstone	A	P	abs	
	GW-7-324	med. sandstone w/clay clasts	A	tr	abs	
	GW-6-441	claystone	D	P	tr	
	GW-6-449	mudstone	D	P	P	
GW-6-463	mudstone	D	P	abs		
GW-6-466	med. sandstone w/clay clasts	P	abs	P	Trace clinoptilolite	
Bee	Paw-1	calc. sandy mudstone	P	P	D	
Karnes	3/22-1b	calc. silty mudstone	D	P	tr	Highly calcareous
	4/6-5	calc. mudstone	tr	abs	I	
	4/6-9b	silty mudstone	D	tr	abs	
	Tms-1a	calc. clay clast conglomerate	D	P	abs	
	Tms-1f	siliceous sandy mudstone	D	P	tr	
Gonzales	3/21-1a	indurated mudstone	D	tr	P	
	4/10-1	calc. f. sandstone and non-calc. silty mudstone	D	P	abs	
De Witt	4/10-6a	muddy siltstone	D	P	abs	
	4/10-6b	mottled claystone	D	P	abs	
	4/10-7a	calc. mudstone	D	P	tr	
	4/10-7b	calc. v.f. sandy mudstone	D	P	tr	
	4/10-11	mottled claystone	D	P	abs	
Lavaca	5/15-1a	calc. sandy mudstone, clay nodules	D	tr	abs	
	5/15-2a	calc. muddy v.f. sandstone	D	tr	abs	
	5/15-6	calc. claystone	D	P	abs	
Fayette	5/16-1c	calc. claystone	D	P	abs	
	5/16-1e	calc. claystone	D	P	abs	
	5/16-2a	calc. mudstone	D	tr	abs	
	5/16-9a	calc. claystone	D	abs	tr	
	5/17-1	calc. claystone	D	tr	tr	
	5/17-5a	muddy v.f. sandstone	D	tr	abs	
	5/17-5b	calc. claystone	D	P	tr	
Washington	5/17-9	calc. mudstone	D	P	P	Highly calcareous
	5/18-3a	calc. muddy siltstone	D	tr	abs	
	5/18-6a	calc. claystone	D	tr	abs	

D = dominant; P = present; tr = trace; abs = absent; and A = abundant.

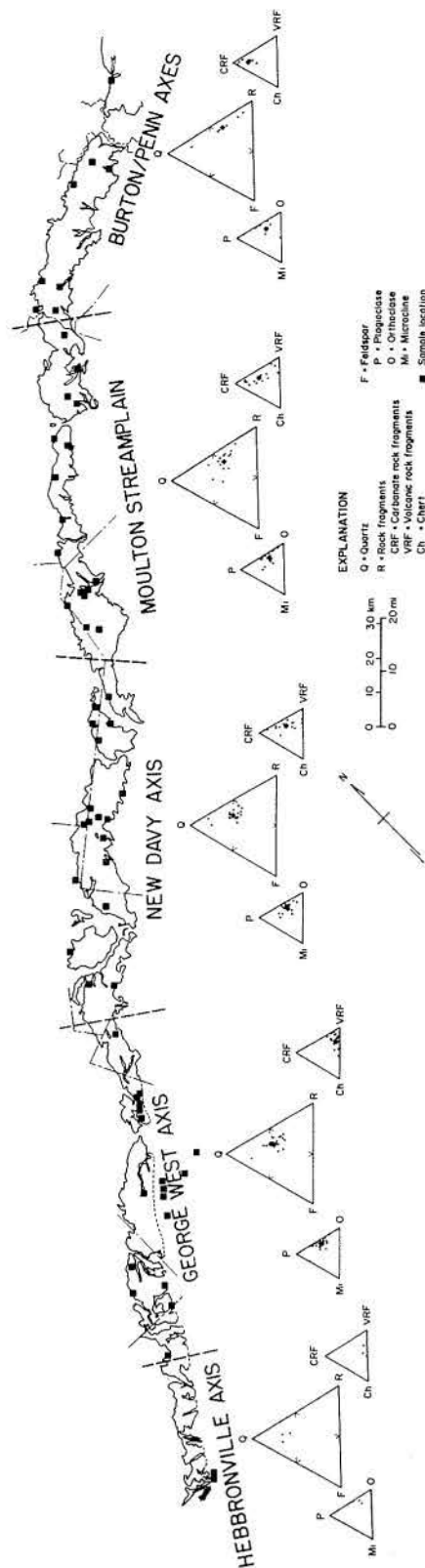


Figure 19. Compositional summary of Oakville sands. Compositional data, based on petrographic point counts, are grouped by each depositional element, illustrating the compositional differences and similarities of each fluvial axis.

however, the X-ray methods used are semiquantitative. Observations agree with more limited work by Thomas (1960) and Ece (1978).

Additional components include a variety of detrital sand and silt-sized grains compositionally similar to those of associated sands, abundant finely crystalline calcite that filled pore spaces and replaced detrital matrix, and rare authigenic opal or chalcedony. Three anomalous illite-rich samples (4/4-1b, 4/4-6c, and 4/6-5, fig. 1) are highly silicified or calcified.

The abundant calcite, which is a diagnostic feature of Oakville mudrocks, is largely a product of early pedogenesis. Additional carbonate precipitation probably occurred in shallowest Oakville sections during Quaternary exposure and outcrop calichification. Kaolinite appears to be best developed in relatively more mature soil horizons characterized by root traces and zones of pedogenic micritic calcite nodules. It is also abundant in root-disturbed, uppermost parts of fluvial channel fills. Silicification and development of thick, colloidal clay segregations (cutans) may be indirect evidence of the initial presence of easily dissolved volcanic glass or other silicate minerals. However, despite common description of the Oakville as tuffaceous, textures and weathering features typical of pedogenically altered, first-cycle, vitric debris are rare. Much of the montmorillonite is likely recycled from older sedimentary strata, particularly Upper Cretaceous mudrocks of the basin margin. Extensive volcanism did, however, persist from Oligocene well into Miocene time across the western and southwestern United States (Shell Oil Company, 1975); thus, continued contribution of fluvially resedimented, air-fall ash into Oakville deposits is likely.

Sand Petrofacies

Petrographic examination of 60 geographically and stratigraphically dispersed samples shows that each of the principal depositional elements possesses a characteristic sand mineralogy inherited from petrologically differing drainage areas of each major stream (fig. 19). Oakville sands are quartz-poor litharenites or feldspathic litharenites (classification of Folk, 1974). Common constituents include felsic siliceous volcanic rock fragments, chert, carbonate rock fragments, including reworked Cretaceous fossils (Ely, 1957), plagioclase, orthoclase, and microcline. Ubiquitous minor components include

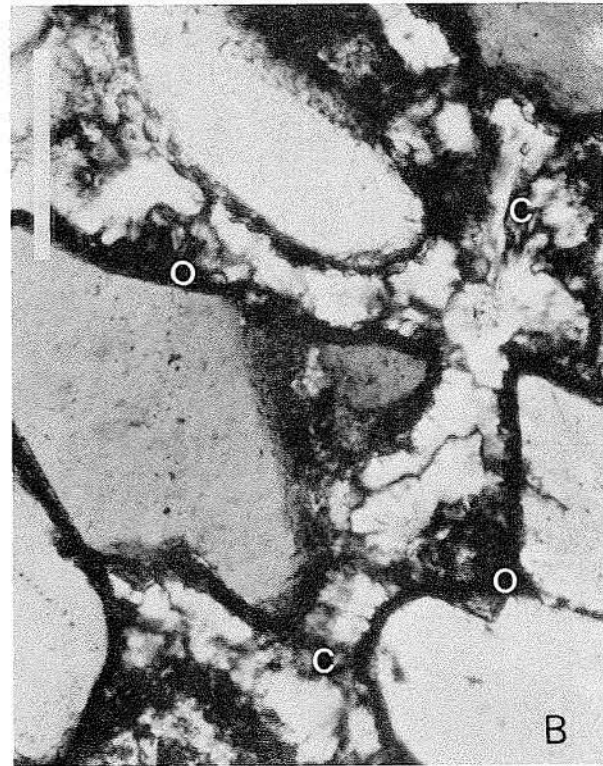
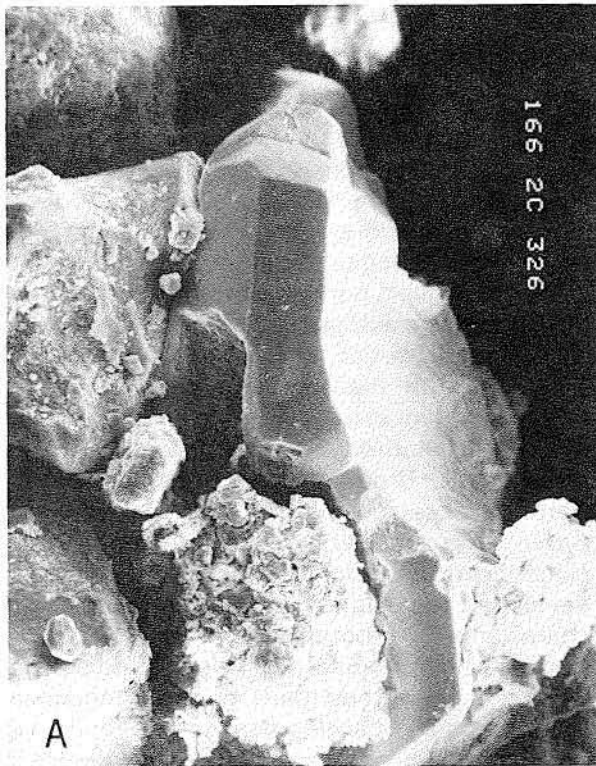


Figure 20. A. Euhedral sparry calcite pore fill(s) cementing several sand grains. Note dusting of detrital and authigenic clay on grains. SEM photomicrograph; length of bar equals 100 microns. B. Silica cementation of medium-grained sand. Both an opal rim (o) and chalcedony pore fill (c) are present. Such cementation is found only at or near outcrop. Crossed-polarizers. Length of bar is 0.25 mm.

iron oxyhydroxides or pyrite, iron-titanium oxides, and mud pellets. These observations agree with earlier reconnaissance analyses by Ragsdale (1960).

Diagenetic features of the sands include (1) calcite spar and microspar pore-filling cements and grain replacement (fig. 20A), (2) leached detrital grains (principally plagioclase), (3) clay coats on detrital grains, (4) opal-chalcedony grain coats and pore-filling cement (fig. 20B), and (5) clinoptilolite rims and dispersed crystals within matrix. Calcite cement is abundant in both surface and subsurface sample suites; its abundance and varying forms indicate the probability of several periods of formation, a supposition borne out by detailed studies of ore-body paragenesis, as discussed herein. Leaching of detrital silicate phases, particularly plagioclase, also appears to be a common attribute of diagenesis of polymictic/fluvial aquifer sands (Walker and others, 1978). Intense cementation of entire sand bodies by opal and chalcedony was noted only in restricted outcrop segments of the George West axis near major underlying fault zones. As in the Catahoula Formation (Galloway, 1977), such pervasive silicification appears to be limited to the outcrop and is most likely a product of Quaternary weathering.

Clinoptilolite occurs dominantly in basal Oakville sand bodies that rest directly on typically tuffaceous Catahoula strata.

Calcite and silica cementation significantly reduces porosity and permeability of the framework sands (fig. 20). Subsurface samples collected in and adjacent to mineralization indicate that approximately one-half of the Oakville sands are somewhat lithified. Porosity of such samples, as determined by thin section examination, averages 11 percent. A few samples exhibit no visible macroporosity. Friable, well-sorted sands are estimated to retain 30 to 35 percent porosity.

SUMMARY OF GENETIC STRATIGRAPHY

Physical stratigraphic analysis shows that the Oakville Sandstone, a lithostratigraphic unit deposited by a major Coastal Plain fluvial system, consists of five mappable depositional elements. Each element is the product of one or more rivers traversing the Miocene Coastal Plain. In turn, each river possessed a unique sediment load, discharge

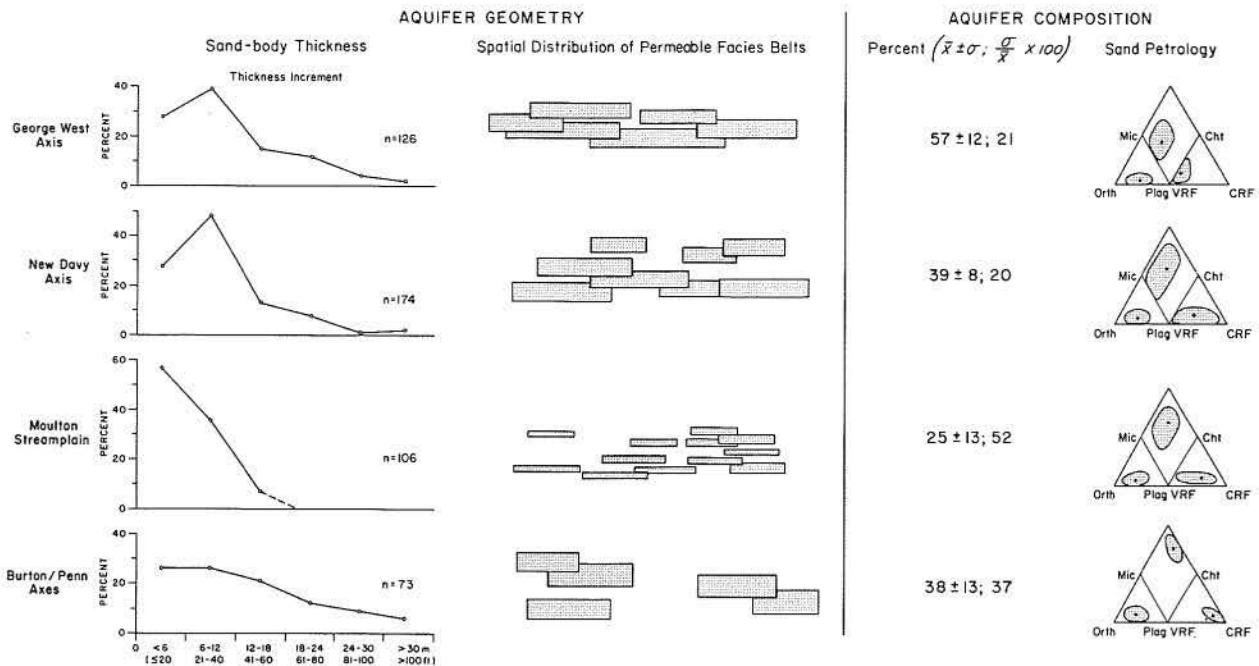


Figure 21. Summary of genetic components and geometric and compositional characteristics of aquifer units within each of the principal Oakville depositional elements.

characteristics, and source terrane. Consequently, each element exhibits distinguishing geometric and compositional parameters that may influence the flux and hydrochemical evolution of contained ground waters. Systematic variations in sand-body thickness, vertical sequence (as indicated by log curve shape), dimensions and interconnectedness, as well as percentage, average grain size and mineral composition of sand (fig. 21), and internal facies architecture and heterogeneity (figs. 9 through 18) are depositional products characteristic of each river.

The early Miocene climate of the central and southern Texas Coastal Plain was subarid to arid, as indicated by (1) the interpreted flashy to ephemeral character of river channels of all of the fluvial axes, (2) the abundance and widespread distribution of pedogenic carbonate, paleo-caliche horizons, and possible playa deposits, (3) the abundance of carbonate rock fragments, including thin-walled pelagic foraminifers reworked from Upper

Cretaceous strata along the basin margin, (4) the pervasive oxidized, hematitic coloration of floodplain and levee deposits, and (5) the absence of bedded organic deposits. Significant eolian sands are notably absent, but some massive caliche units that occur south of the George West axis may represent calichified loess.

A large river, which alternately flowed along the George West and the Hebronville depositional axes, drained West Texas, as indicated by its volcanic rock fragment-rich composition and diagnostic pebble suite, which includes riebeckite rhyolite (S. E. Clabaugh, 1980, personal communication) and fusulinid grainstone. The New Davy axis records drainage basin integration for a major Central Texas basin fringe river that is analogous to the Holocene San Antonio or Guadalupe Rivers. The Burton/Penn axes reflect development of larger basin fringe rivers in the somewhat more humid terrane of East Texas and adjacent areas.

Structural Framework

The Gulf Coast Tertiary Basin is characterized by passive tectonics. Structural elements include major coast-parallel growth and associated relief fault trends, and diapiric intrusions cored by salt or abnormally pressured mud. Both growth faults and diapirs were most active during deposition of thick

oceanic deltaic and slope systems. However, these zones of structural weakness commonly propagated upward through the section as overlying fluvial coastal plain sediments progressively loaded the underlying thick sedimentary wedge. Consequently, units such as the Oakville Sandstone

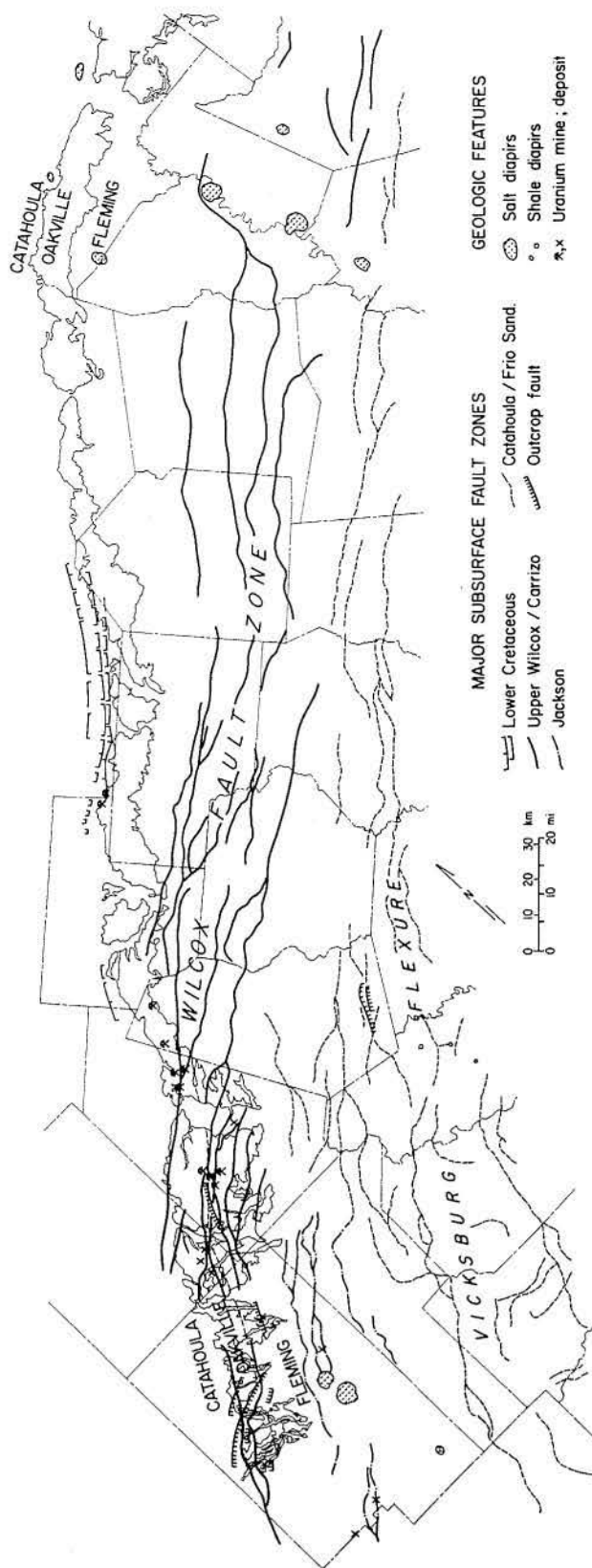


Figure 22. Generalized distribution of faults and diapiric intrusions mapped within or below the Oakville Sandstone. Map horizon of fault zones is indicated by line style.

are locally displaced a few meters to tens of meters along shallow faults that are rooted in growth fault zones having displacements of up to several hundred meters. Growth faults are characteristically arcuate, concave toward the coast, and dip at about 60° in the shallow subsurface. Up-to-the-coast antithetic or relief faults accompany many growth faults (Bruce, 1972).

FAULT DISTRIBUTION

Figure 22 shows the distribution of major known fault and diapiric structures compiled from several sources, including commercial structure maps (Tucker, 1967) and the Austin, Seguin, Beeville - Bay City, and Crystal City - Eagle Pass sheets of the *Geologic Atlas of Texas* (Barnes, 1974a, b; 1975; 1976). Fault patterns were mapped at several different horizons ranging from a few hundred to several thousand meters below the base of the Oakville because fault recognition is best where throws are large and map horizons are more continuous. The map therefore provides a general guide to distribution of deep structures that *might* influence Oakville geohydrology.

Two broad Tertiary growth fault zones underlie the Oakville fluvial system. The Wilcox fault zone trends slightly oblique to strike, intersecting the southerly outcrop belt of the Oakville Sandstone. Faults rooted in this trend are directly associated with many major uranium deposits, including those of the Ray Point and George West districts (fig. 22). The Vicksburg flexure, a relatively narrow belt of major Oligocene growth faults, extends across the downdip part of the study area and commonly displaces Oakville sands. In addition, a deep-seated Cretaceous fault zone locally intersects the outcrop belt in Karnes and Gonzales Counties (fig. 22). Although it has no apparent effect on the structure of middle Tertiary units, the Nopal uranium area and associated, unusually ferruginous sands are coincident with this fault zone. Salt diapirs are present only at the margins of the study area (fig. 22), but they locally affect Oakville structure and hydrogeology.

IMPACTS ON HYDROGEOLOGY

Shallow extensions of growth faults exhibit several manifestations in the Oakville fluvial system that potentially affect its hydrogeology:

1. Displacement on some faults is locally adequate to separate physically the individual sand bodies.
2. Subtle topographic gradients induced by syndepositional deformation in and around faults

have been shown to modify Coastal Plain paleodrainage patterns (Kreitler, 1976; Galloway, 1977). Right-angle deviation of dip-oriented channel-fill sand bodies at fault zones causes major changes in directional transmissivity within the aquifer units.

3. Diagenetic modification of the aquifer matrix is commonly concentrated near fault zones. Opal/chert cementation of outcropping Oakville

sand has been noted primarily near faults. Intense calcite cementation occurs locally near faults. Most obvious is the common localization of ore-forming epigenesis near fault zones (fig. 22). Such associations provide evidence of leakage and mixing of waters along faults, which in turn may have significantly modified intrinsic aquifer permeability.

Hydrostratigraphy

The Oakville Formation (and fluvial system) constitutes a major fresh-water resource of the Texas Coastal Plain. Furthermore, emplacement of uranium is a product of ground-water flow. Consequently, the hydrogeology of the Oakville is as important as its conventional genetic stratigraphy. The capacity of the Oakville aquifer to transmit ground water, its transmissivity, and the nature of flow boundaries, including structural discontinuities and confining units, determine present water chemistry and resource value as well as probable history and location of large-scale mineralization.

A hydrogeologic unit, as defined by Tóth (1978, p. 807), is a "single stratum or a combination of strata that function in bulk as either a water-bearing or a water-retarding rock complex relative to adjacent strata." In the Gulf Coast basin, hydrogeologic units are conventionally called aquifer systems or confining systems. Neither term denotes absolute transmissivity; rather, *relative* water-bearing capacity of major lithostratigraphic complexes is the basis for subdivision of the section.

HYDROGEOLOGIC UNITS

The Oakville Sandstone, as a mapped lithostratigraphic unit in the study area, corresponds closely to the Jasper aquifer system, an equally well-defined Gulf Coastal Plain hydrogeologic unit (Baker, 1978). Principal surrounding hydrogeologic units include the underlying Catahoula confining system and the overlying Burkeville confining system (fig. 7). The Evangeline aquifer system includes much of the Fleming Formation (fig. 7).

Stratigraphic relationships between each of the principal Oakville depositional elements and the regional hydrogeologic units synthesized by Baker (1978) are illustrated in figures 7 and 23. Most significantly, the Jasper aquifer system is everywhere bounded above and below by relatively less transmissive, finer grained confining systems,

although absolute transmissivity varies greatly within both the Jasper and the confining units. Lithostratigraphic and hydrogeologic boundaries coincide within the Hebronville fluvial axis (fig. 23, section D). The Oakville Sandstone comprises the Jasper aquifer; overlying Fleming muds comprise the Burkeville confining system. Correspondence of stratigraphic and hydrogeologic boundaries is also good within the George West axis; however, the top of the Burkeville drops into the upper Fleming section where it becomes increasingly sandy (fig. 23, section F). Within the New Davy axis, hydrogeologic and conventional stratigraphic boundaries diverge, particularly at intermediate depths (fig. 23, section H). The upper part of the Oakville, which contains primarily mixed-load fluvial facies (fig. 7), and the lower part of the Fleming Formation form the Burkeville confining system. Only the lower half of the Oakville is included in the Jasper aquifer system. Within the area of the Moulton streamplain, the Burkeville confining system still includes the upper Oakville and lower Fleming at depth. In shallowest parts of the aquifer, however, the Jasper expands to incorporate fluvial sands of the upper Catahoula Formation and all the Oakville Sandstone (fig. 23, section J). Farther to the northeast, the base of the Jasper aquifer occurs progressively lower in the Catahoula section until, along the Burton/Penn axes, the close correlation between hydrogeologic and stratigraphic units completely breaks down (fig. 7). At the northeast end of the study area, the Jasper aquifer includes the lower Oakville and most of the Catahoula; the Burkeville confining system thins and generally spans the Oakville-Fleming boundary (fig. 23, section L).

AQUIFER TRANSMISSIVITY

Water-bearing capacity of an aquifer is expressed in terms of transmissivity, which is measured by conventional pump tests. However, few pump test

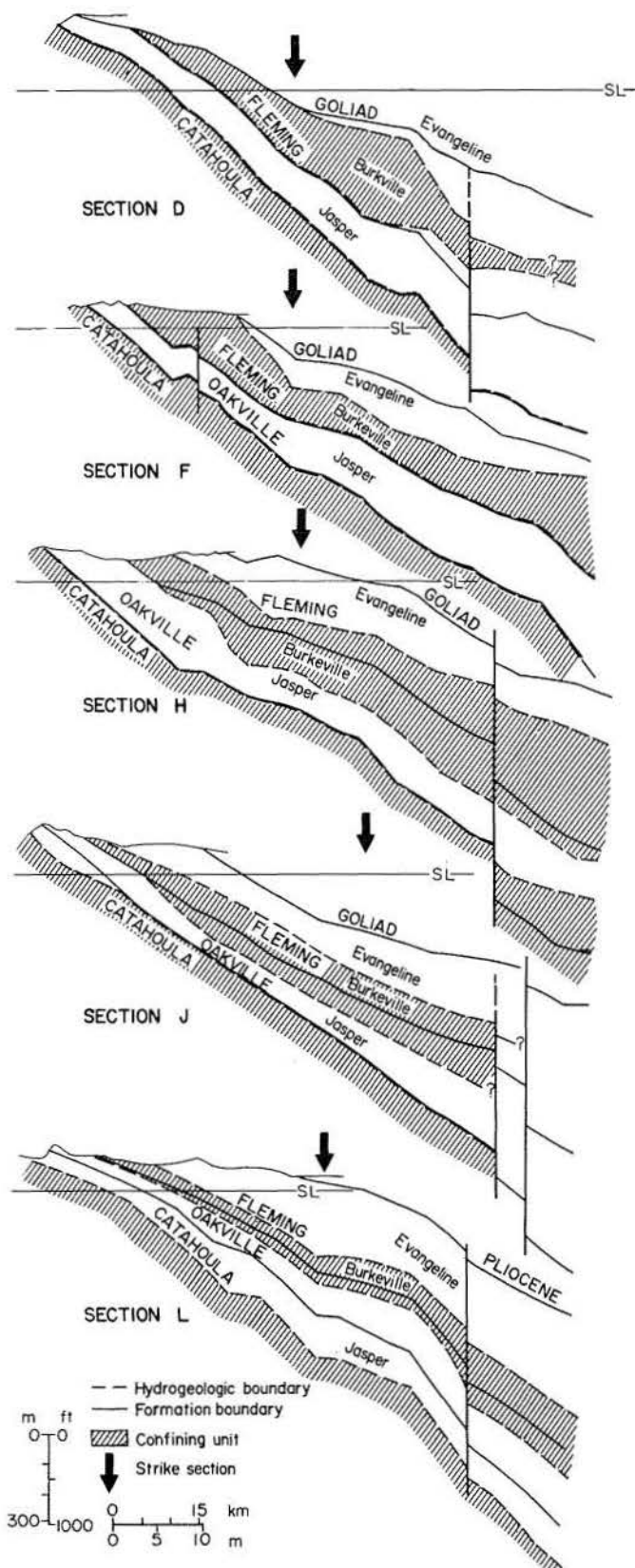


Figure 23. Representative stratigraphic dip sections comparing lithostratigraphic and hydrostratigraphic units. The Oakville fluvial depositional system (1) corresponds directly to the Jasper aquifer in the South Texas Coastal Plain, (2) includes both the Jasper aquifer system and part of the Burkeville confining unit in the middle Texas Coastal Plain, and (3) includes the upper part of the Jasper aquifer in the upper Texas Coastal Plain. For location of sections, see figure 1.

data on Oakville sands have been published. Additional transmissivity values of the ore-bearing sands are included in leach mining permit applications. Twenty-three usable pump test analyses were compiled from all sources (fig. 24). In each, the tested interval included only a part of the Oakville section, and the measured transmissivity is, at best, only that of the screened sand body. Because transmissivity is the product of aquifer permeability and total thickness, all tests measured only a fractional transmissivity for the Oakville Sandstone or Jasper aquifer system. The available data are thus both geographically and stratigraphically inadequate for direct preparation of a transmissivity map of the entire Oakville.

Variations in sand content, average grain size, and geometry of framework sand facies inherent in each of the depositional elements indicate that transmissivity of the Oakville fluvial system should vary widely. Further, if different framework sand facies possess consistent permeability ranges, interpreted facies distribution as well as the net-sand isolith map should provide a basis for constructing a derivative, semiquantitative transmissivity map of the total Oakville unit. Pump test results are used for calibration; the procedure includes six steps:

1. For each pump test site, thickness of the screened sand unit(s) was determined on an available log of a well closely adjacent to the test well site.
2. Average permeability was calculated by dividing measured transmissivity (conventionally reported in ft^2/d) by the total thickness of screened sand unit(s). Overlap of the screened interval into bounding silt or mud facies contributed little to the measured transmissivity and thus was ignored. Calculated permeabilities given in a few reports verified previous calculations or were used directly if nearby logs were unavailable.
3. The electric log pattern and regional or local facies maps were used to interpret the specific sand facies assemblage screened within each test well.
4. Geologic considerations suggested initial separation of data from bed-load channel and mixed-load channel facies belts (fig. 25). Mixed-load channel belts of the Moulton streamplain, Burton/Penn axes, and upper part of the New Davy axis have average permeabilities consistently below 5 meters per day (m/d). Bed-load channel belts exhibit a much broader range of average permeabilities, with a maximum reported value of 13 m/d. However,

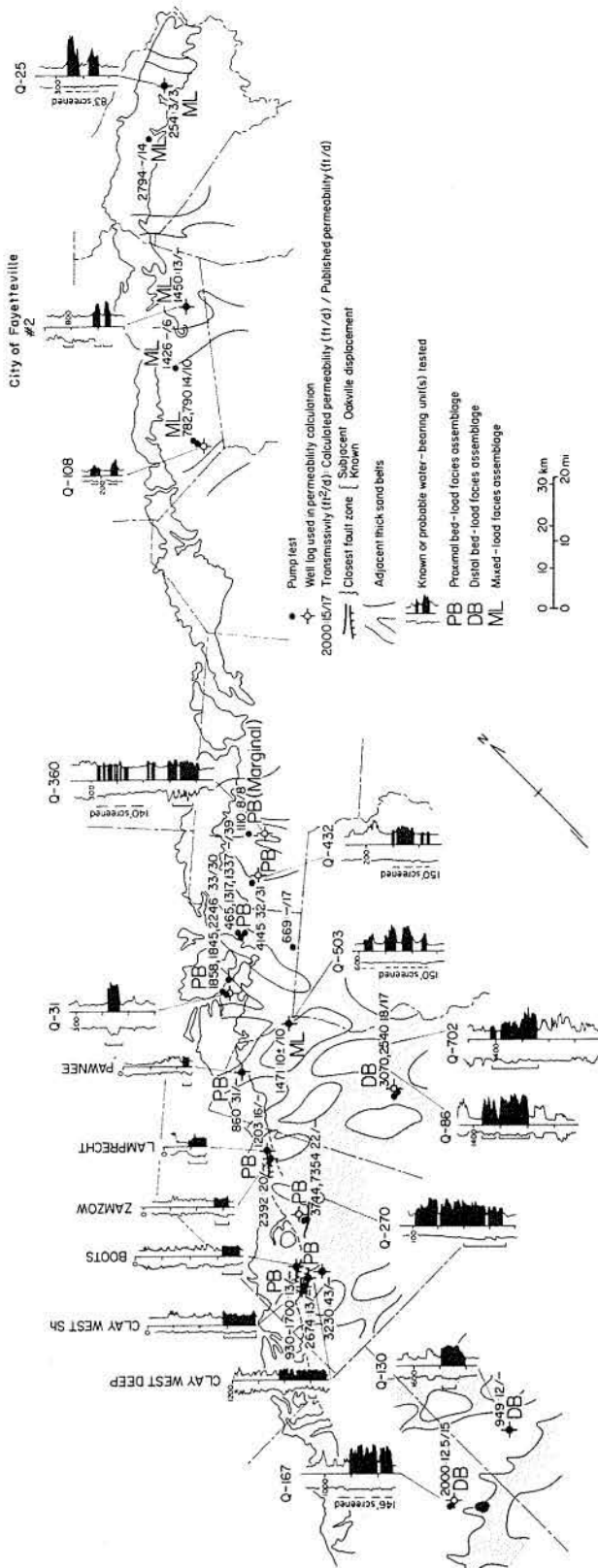


Figure 24. Geologic data base used for compilation and interpretation of pump test permeability data. Major aquifer units are classed as (1) updip or proximal bed-load, (2) downdip or distal bed-load, and (3) mixed-load facies belts. Original data were recorded in English units and are reproduced accordingly.

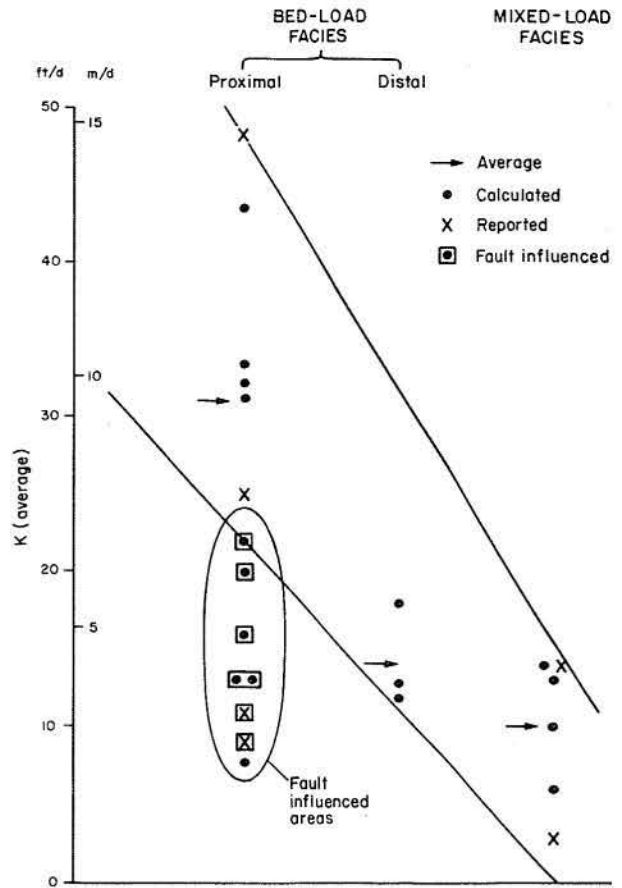


Figure 25. Calculated permeabilities for major permeable facies belts. Both maximum and average values decrease from proximal bed-load to distal bed-load to mixed-load facies. Proximity to faults substantially decreases calculated permeability of bed-load facies; averages exclude these data points.

several test wells lie close to known or projected fault zones (fig. 24). Average permeability values calculated for these wells are consistently low, ranging from about 2.5 to 7 m/d (fig. 25), a result consistent with the observation of enhanced cementation of Oakville sands adjacent to fault zones. Only a single proximal bed-load aquifer, from an area unaffected by faulting, tested below 7 m/d. This well, Q-360, was screened largely in interbedded overbank and splay facies marginal to a major channel complex. Three test wells, which lie significantly downdip of the others (fig. 24), tested aquifer sands that are relatively deeply buried and lie farther downflow or marginal to the George West and Hebronville axes. These distal bed-load units are probably somewhat finer in average grain size and have experienced greater physical compaction than more proximal, updip and upflow counterparts along the same sediment dispersal axis; they form a second,

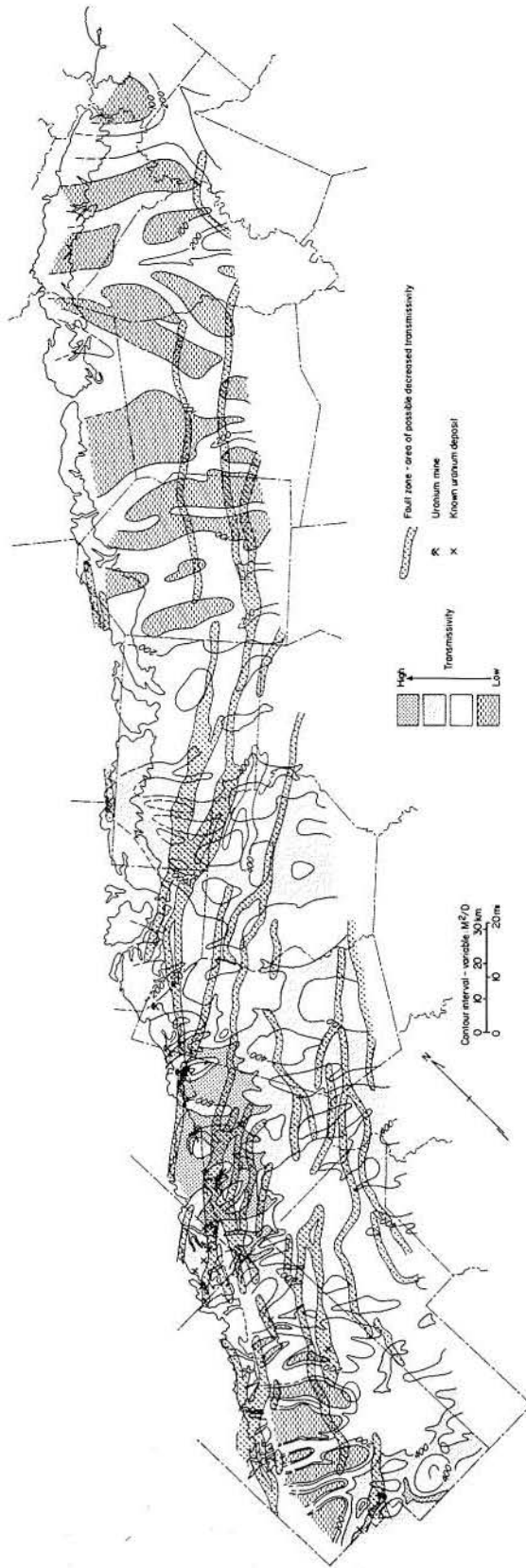


Figure 26. Regional transmissivity of the Oakville aquifer system. Transmissivity was calculated by multiplying average sand-body permeability for the appropriate facies components of each depositional element by total sand thickness (fig. 5). Map compilation

was done graphically, and, given the limited available permeability data, should be considered semiquantitative. Fault zones are areas of possible decreased transmissivity due to local cementation or facies changes.

relatively low permeability population (fig. 25). In summary, three facies-related suites of permeability values were distinguished: proximal bed-load sand complexes are most permeable, averaging about 9.5 m/d; distal bed-load sand complexes average slightly over 4 m/d; and mixed-load sand complexes average 3 m/d (fig. 25).

5. An average regional transmissivity map for the total Oakville Sandstone (fig. 26) was constructed by combining sand isolith and percentage maps with electric log patterns to project fluvial facies and their thicknesses into the subsurface (using criteria described in Galloway and others, 1979b). A crossplot of isolith thickness versus equivalent transmissivity for each of the three framework facies assemblages was used to convert sand thickness contours in each depositional element into transmissivity form lines. Form lines were arbitrarily graded across facies boundaries to create transition zones several kilometers wide.

6. Known fault zones were broadly outlined to indicate areas of possible anomalously low transmissivity. Within the proximal bed-load facies, the observed decrease averages nearly 5 m/d in the sample suite; however, inconsistent handling by different authors of problems introduced by the presence of a fault-produced flow boundary makes this number suspect. Data are adequate, however, to document the association of anomalously low transmissivities with fault zones. However, the magnitude and consistent occurrence of this decrease remains somewhat speculative.

The transmissivity map of the Oakville Formation (fig. 26) displays the areal variation of hydraulic conductivity. Iso-transmissivity contours are primarily form lines and should be considered semiquantitative. Nevertheless, the map illustrates that each of the principal depositional elements of the Oakville is characterized by distinct regional and local transmissivity patterns, which, in turn, are products of the genetic stratigraphic and structural framework. Salient observations include:

1. The Hebbroville and George West proximal bed-load fluvial axes have the highest transmissivities. Transmissivities decrease downdip because of increasing compaction and down-channel decreasing average grain size.
2. The New Davy axis displays intermediate transmissivity values because it includes both bed- and mixed-load facies.
3. The Burton/Penn mixed-load axes produce moderate to low transmissivity.
4. Lowest transmissivities occur in inter-axis floodplain mud facies and in the sand-poor Moulton streamplain.

5. Transmissivity anisotropy is produced by the generally dip-oriented fluvial framework facies belts and strike-parallel fault zones. Fault zones produce direct offset of individual sand bodies, local strike-parallel deflection of paleodrainage trends, and diagenetic modification of aquifer permeability.

6. Most known large uranium deposits lie within or along the margin of relatively highly transmissive parts of the Oakville fluvial system and in zones of potential or known fault influence (fig. 26). Major ore districts, including Ray Point and George West, that are estimated to contain between 5 and 10 million pounds (2.2 to 5×10^3 m.t.) of U_3O_8 are each closely

associated with the highest transmissivities recorded within the formation. Moderate-sized deposits occur along the intermediate transmissivity axis of the New Davy fluvial trend. Small deposits occur scattered along minor transmissivity trends. The good correlation between district/deposit size and host transmissivity confirms the inferred importance of ground-water transport in the uranium mineralization model proposed by Galloway (in Galloway and others, 1979b, p. 248). The appropriate transmissivity map may well be the single most powerful stratigraphic map that can be constructed for epigenetic sandstone uranium exploration.

Geology and Geochemistry of Oakville Uranium Deposits

Uranium ores of the Oakville and other South Texas Coastal Plain aquifer systems are variously described as roll front, roll-type, and alteration front deposits (Harshman, 1974; Eargle and others, 1975; Galloway, 1977; Reynolds and Goldhaber, 1978). Ore bodies occur along laterally continuous mineralization fronts up to several kilometers long and may lie individually within a sand body or stacked within thicker sand sections. Ore-grade mineralization occurs in sinuous ribbons that rarely exceed 100 m (300 ft) in width. A C-shaped cross-sectional geometry, referred to as the ore roll, is exhibited by many deposits, but modifications of this ideal geometry are the rule. The uranium ore is lean; ore grade of volumetrically important reserves ranges from a few tenths to a few hundredths of a percent of U_3O_8 . Isolated pods or zones of ore may contain several percent of U_3O_8 . Common accessory materials include marcasite, pyrite, clay minerals, calcite, and, in some districts, organic matter and clinoptilolite.

Results of this and other studies, notably those of Harshman (1974), Goldhaber and others (1978), and Galloway and Kaiser (1980), show that South Texas mineralization fronts are highly structured assemblages of uranium and several associated major and minor elements that are concentrated along an epigenetic alteration interface developed during the hydrologic and hydrochemical evolution of the host aquifer. The general formation and evolution of supergene epigenetic sandstone deposits has been summarized by Galloway (1978) and Galloway and others (1979b):

1. Uranium and commonly associated metals, including selenium and molybdenum, were leached from volcanic ash by vadose or shallow ground waters.

2. Oxidizing, uranium-enriched waters entered semiconfined aquifers in zones of regional recharge.

3. Uranium was transported down regional hydrodynamic gradient through the aquifer system.

4. Uranium was stripped from the ground water as flow crossed aqueous geochemical barriers present within the aquifer. Concentration of trace metals during the mineralization phase was closely associated with extant iron oxidation-reduction boundaries within the aquifer.

5. Post-mineralization changes in ground-water flux and chemistry have resulted in local redistribution and/or diagenetic modification of primary mineralization fronts.

Concentration of uranium and associated trace metals from ground water requires the presence of a physiochemical or geochemical barrier within the flow system. Perel'man (1972, p. 24-25) identified four idealized geochemical barriers capable of forming epigenetic uranium deposits (table 2). Reducing barriers of both the sulfide and the gley (sulfide deficient) types are capable of reducing uranium from the U^{6+} to the less soluble U^{4+} valence state. Sulfide must be present for contemporaneous concentration of some additional metals, however. The acid barrier, involving a decrease in pH, can also concentrate uranium and is considered particularly effective at concentrating molybdenum. Detailed analytical and theoretical studies of processes active at the mineralization front show that the decrease in Eh occurring as oxidizing ground waters react with a reducing aquifer matrix is accompanied by a decrease in pH (Huang, 1977; Reynolds and Goldhaber, 1979; Galloway and Kaiser, 1980). Adsorption of uranium and other metals by clay minerals, zeolite, iron and manganese oxyhydroxides, and organic matter can

Table 2. Geochemical barriers capable of concentrating uranium and associated metals in ground-water flow systems. After Perel'man (1972).

Class of the barrier	Geochemical environment		Concentrations of elements	Examples of concentration
	before the barrier	beyond the barrier		
Reducing hydrogen sulfide	Oxidizing or gley	Reducing hydrogen sulfide	Fe, V, Zn, Ni, Co, Cu, Pb, U, As, Cd, Hg, Ag, Se	Epigenetic uranium deposits, cupriferous sandstones
Reducing gley	Oxidizing	Gley	U, Se, Cu?	Epigenetic uranium deposits, native copper in bogs
Acid	Neutral, acid, basic	More acid	SiO ₂ , Mo, Se, U	Uranium-selenium-molybdenum ores of epigenetic deposits, secondary aureoles, silicified wood
Adsorption	Waters of low activity	Waters of low activity	P, S, V, Cr, Zn, Ni, Co, Cu, U, As, Mo, Hg, Ra	Secondary aureoles of many metals in peats and clays

produce significant matrix enrichment and may be a primary control of dissolved metal content. Consequently, in pyritic, argillaceous, sulfide-bearing aquifers typical of South Texas, the potential for concentration of a large suite of metals exists at uranium mineralization fronts.

Two additional features are well displayed by Oakville uranium deposits. The first, *geochemical zonality*, is an inherent characteristic of epigenetic processes that arises from the tendency for many physiochemical barriers within ground-water flow systems to be locally abrupt gradients separating major geochemical environments or plateaus (Perel'man, 1972, p. 26). As a result, a succession of distinct geochemical or mineralogical zones records the present or former position of geochemical barriers within the aquifer. Spatial relationships of zones define the direction, or polarity, of the barrier gradient. For example, the consistent Eh-dependent zonation of trace metals across epigenetic uranium deposits has been well described (Vasil'eva, 1972; Harshman, 1974). Second, *multiple epigenetic events*, each characterized by different barriers and zonal impositions within the aquifer, may develop sequentially as directions and sources of ground-water flux change with time. Shmariovich (1973) described zonal patterns produced by intrusions of oxidizing meteoric and sulfide-bearing reducing waters into an aquifer. Sequential sulfidizing reduction epigenesis followed by oxidation ideally produces the complex but distinctive suite of geochemical zones illustrated in figure 27. Analogous zonal patterns have been described in mineralized

parts of the Catahoula Formation in South Texas (Goldhaber and others, 1978; Galloway and Kaiser, 1980), and sequential epigenetic events are recorded in the paragenetic history of Oakville deposits of the Ray Point district (Galloway and others, 1979a; Goldhaber and others, 1979a).

Uranium production from the Oakville Sandstone dates from 1967 (table 3). Known, potentially commercial deposits currently extend from southernmost Duval County northward to southernmost Gonzales County (fig. 1). Most exploitation of large deposits has occurred in the Ray Point and George West districts, which are described as representative examples of Oakville mineralization.

RAY POINT DISTRICT

The Ray Point mining district currently covers approximately 24 km² (9 mi²) in east-central Live Oak County. As first pointed out by Klohn and Pickins (1970), the district lies at the north margin of a broad fluvial axis (the George West axis, in this report). Mineralization occurs dominantly within the highly permeable, basal Oakville sand body and along a relatively thin, east-northeast-trending fluvial facies complex that lies marginal to a much thicker basal sand trend (figs. 28 and 29). Pit exposures and subsurface log patterns show that the host sand consists of interbedded sheet splay and sandy bed-load channel-fill deposits (Galloway and others, 1979a). The basal host sand body is separated from an

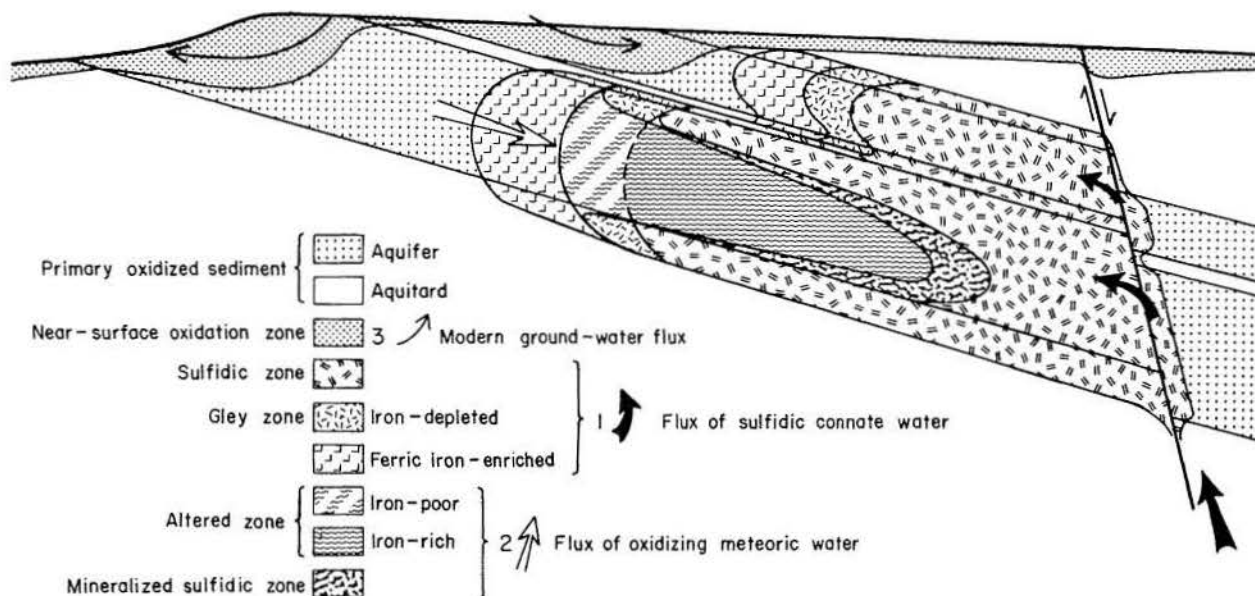


Figure 27. Schematic distribution of principal epigenetic zones produced within an oxidized aquifer, by sequential intrusion of sulfidic, reducing connate waters followed by downdip circulation of oxidizing meteoric ground water. Reducing waters produce successively, (1) a sulfidic, pyritic zone, (2) a reduced, sulfide-poor, iron-depleted zone (commonly referred to as gley in Russian literature), and finally (3) a zone of iron oxidation and concentration. Intruding meteoric waters set up a dynamic alteration interface characterized by both Eh and pH changes causing concentration of dissolved metals, including uranium, molybdenum, and selenium. Near-surface oxidization occurs above the water table or within shallow, rapidly circulating flow cells.

overlying fluvial sand of similar origin by a clay bed that can be traced throughout the mining district (fig. 29). This upper sand contained ore in the Smith Mine (fig. 28). The base of the Oakville Sandstone is displaced as much as 30 m (100 ft) by a down-to-the-coast fault (fig. 29) that veers eastward from its general northeast strike and dies out within the mine area. A second fault occurs 2 to 3 km (1 to 2 mi) north of the main ore trend and continues northeast along strike. Several shallow, mineralogically complex redistributed ore bodies occur along both of the faults (McLean, Martin, and Kopplin Mines). The primary ore trend is a shallow but well-developed mineralization front extending from the Felder lease, where it is being subjected to near-surface oxidation and redistribution, northeast along and slightly updip from the fault through the Hahn lease, and then northward across the depositional grain of the host sand unit into the Lamprecht lease where it apparently dies out (fig. 28). Thus, both depositional and mineralization trends closely parallel the fault and appear to cross the fault zone preferentially where it is discontinuous. Further evidence of early movement along the fault is seen in the apparent thickening of middle Oakville sands on the downthrown side of the fault (fig. 29). However, the mineralization front locally crosses the fault on the Zamzow lease and is displaced along with the host

Table 3. Summary of Oakville uranium-producing districts and areas.

Location	Mining method	Mining begun	Estimated reserves (m.t. U ₃ O ₈)
George West district	In situ	1975	10 ³ - 10 ⁴
Ray Point district	Open pit	1967-72; 1978	10 ³ - 10 ⁴
	In situ	1977	
Pawnee area	In situ	1977	10 ²
Benham area	In situ	1979	?
Nopal area	Open pit	1975	10 ³⁺

sand, an indication that most movement postdated earliest mineralization (Galloway and others, 1979a; fig. 47). Such intermittent activity appears to be common for faults of the deep-seated Wilcox trend.

The mining district lies in an area of Oakville ground-water recharge; according to limited mining permit data, water levels average 3 m (10 ft) higher in the shallower sands than in the basal uranium-

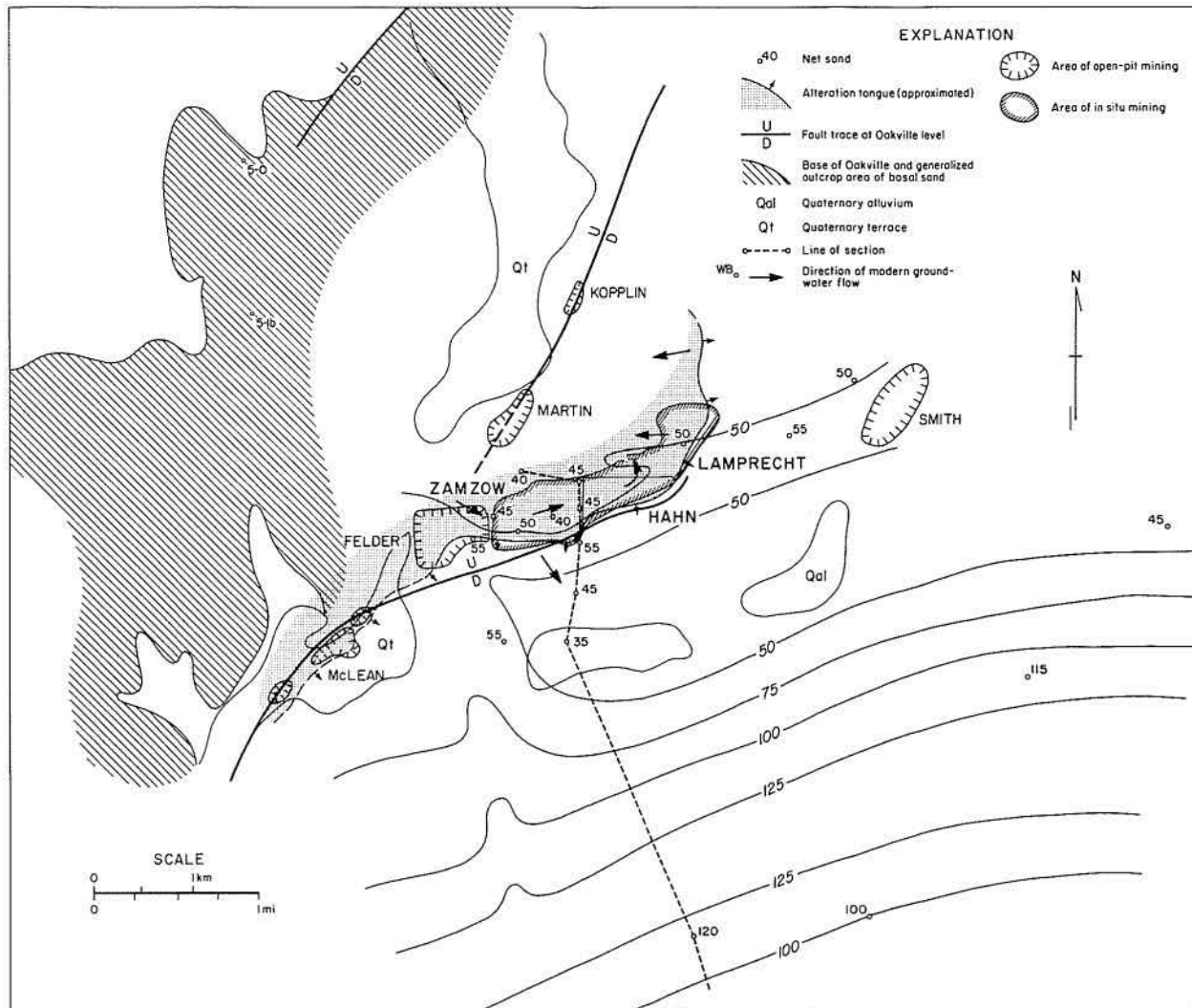


Figure 28. Geographic and geologic setting of the Ray Point district, Live Oak County. The Kopplin, Martin, and McLean mines intercept redistributed ore concentrated along or near the fault plane. The remaining deposits are more typical mineralization fronts that lie dominantly within the sphere of a local flow cell bounded to the southeast by the fault line and to the east by a topographic high outlined by the 300 ft (100 m) contour. The net-sand isolith describes thickness of the basal ore-bearing sand only (see figure 29).

bearing unit. However, the unusually saline water composition, the presence of methane in the mine waters, and the complex hydraulic head surface indicate additional significant recharge of the Oakville sand by waters moving up the fault zone. The fault acts as a flow boundary separating the basal Oakville sand into disconnected segments exhibiting differing head magnitudes and gradients (fig. 28). Ground water generally moves northeastward, parallel to structural and facies trends. In the Lamprecht lease, permit data indicate a gradual north-to-west reorientation of flow lines. Consequently, shallow Oakville water may discharge along the northern arm of the fault zone into Sulfur Creek, which lies to the west of the Martin and Kopplin pits.

Geochemical and Mineralogical Zonation

The basal Oakville sand body exhibits four of eight idealized epigenetic zones in the Ray Point district: (1) an active near-surface phreatic oxidation zone, (2) an altered zone, which has been modified by post-mineralization resulfidization, (3) a mineralized sulfidic zone, and (4) a barren sulfidic zone. Geochemical and mineralogical studies of 60 samples from a core fence that crosses the mineralization front on the Zamzow lease provide the basis for describing parts of the three sulfidic zones. Additional data reported for a core set from the Lamprecht lease by Goldhaber and others (1979a) show similar results.

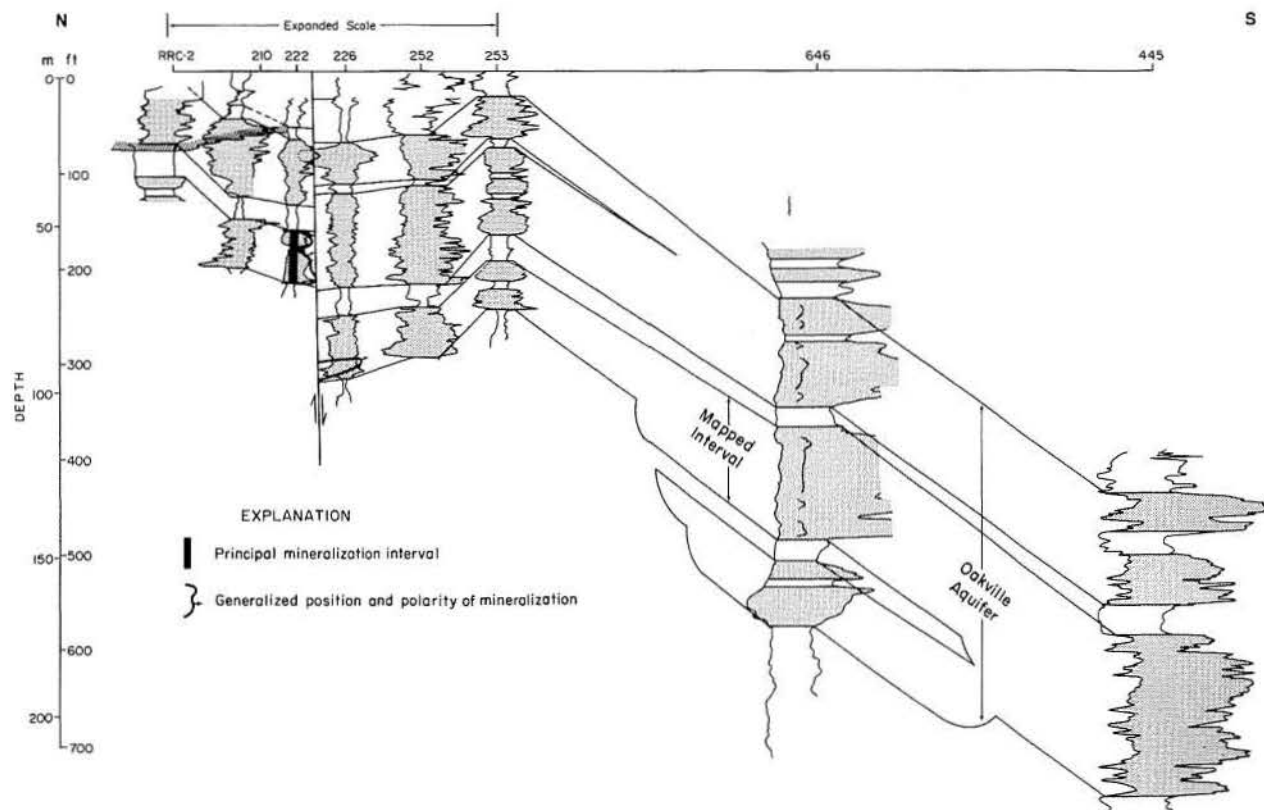


Figure 29. Cross section of the Oakville aquifer in the Ray Point district. For location of section, see figure 28. This section is somewhat atypical in that the nose of the mineralization front extends into the downthrown fault block (well 226). Note that the horizontal scale is expanded in the mine area.

Zonal partitioning of various mineral phases, chemical components, and important trace metals is illustrated in figure 30 and summarized in table 4. All analytical results are tabulated in appendix B, table B-1. Important conclusions are:

(1) Principal trace metals concentrated in the mineralization zone are uranium, selenium, molybdenum, and arsenic. In the sample suite analyzed, the first three metals occur in a distinct spatial zonation (fig. 30B) that establishes the directionality or polarity of the Eh barrier responsible for their concentration (Harshman, 1974). Proportions of U:Mo:Se average 7:2:1 in the core suite; however, the extent of the molybdenum zone into protore is not defined by the core fence. Uranium occurs in part as coffinite, which was identified by X-ray diffraction. Highest selenium content occurs in the distal fringe of the altered zone and extends across the zonal boundary into the mineralized sulfidic zone (fig. 30B). Molybdenum and uranium are concentrated almost exclusively within unaltered sediment along the periphery of the complex lobate alteration tongue. Molybdenum concentration is highest (exceeding 600 ppm) slightly downflow from the zone of maximum uranium (fig.

30B). An apparent inversion of the metals' zonal pattern in the upper part of cores Z-3, Z-4, and Z-6 (fig. 30B) indicates either the projection of a small frontal salient into the plane of section or the development of multiple, imperfectly superimposed episodes of alteration and resulfidization.

(2) Iron is present as both oxidized (limonitic and hematitic) and reduced (pyritic and marcasitic) forms in all samples. Highest iron content occurs within the mineralized sulfidic zone, which commonly contains more than 3 weight percent Fe^3 (expressed as Fe_2O_3) and/or 3.5 percent Fe^2 (as FeS_2) (fig. 30C). Both forms are least abundant in altered samples. Analogy with similar types of uranium deposits suggests that a probable intermediate iron content would be likely in the barren sulfidic zone.

(3) Carbonate, occurring as calcite, is also somewhat more abundant within the mineralized sulfidic zone (averaging 10 percent CO_3), and is depleted within the altered zone (averaging only 8 percent) (table 4, fig. 30D). Paragenetic features observed in thin section indicate an early leaching stage in altered sand near the mineralized zone. Concomitantly, a minor iron-rich calcite phase, identified by staining, precipitated at or immediately

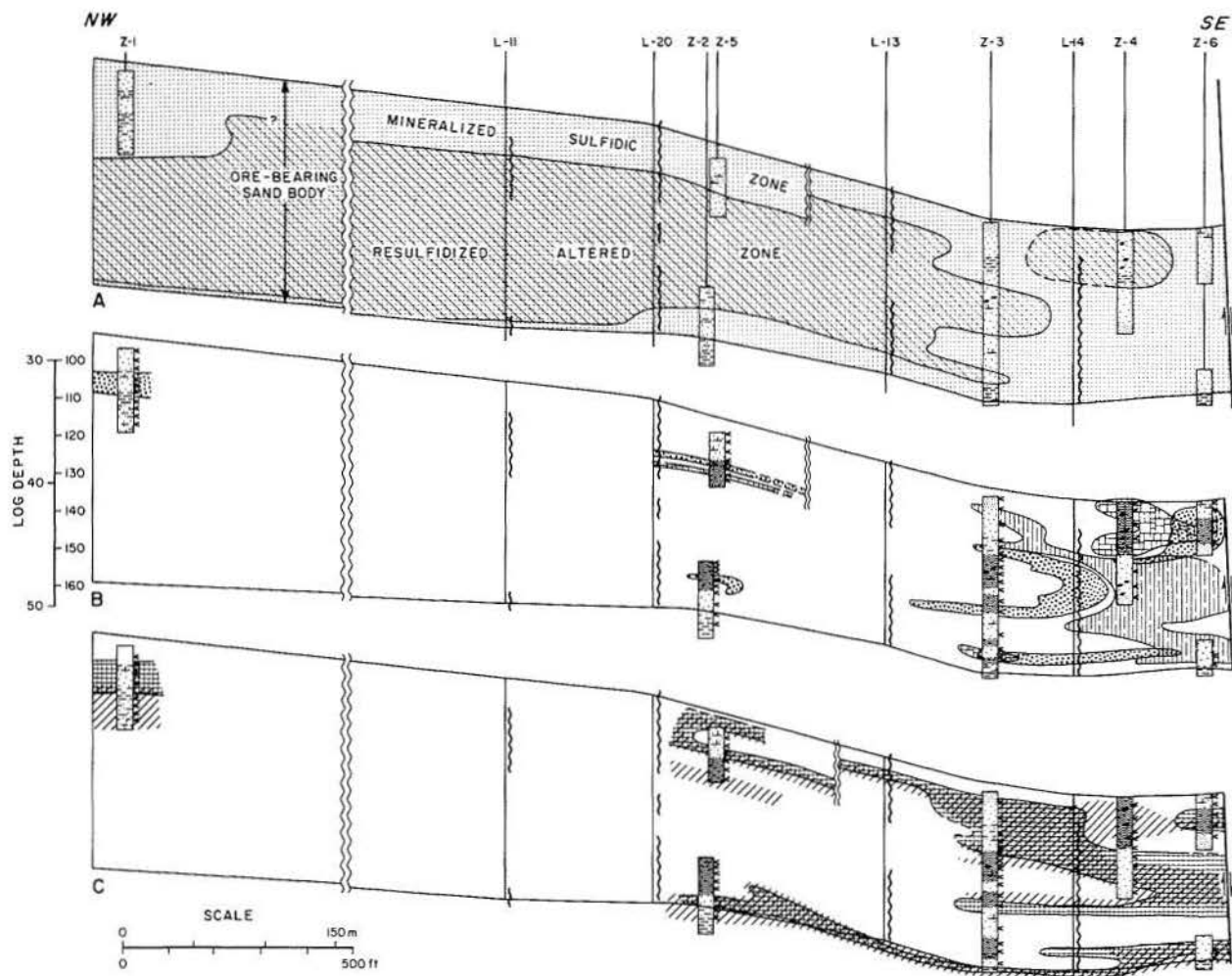


Figure 30. Core transect of the Zamzow mineralization front (basal Oakville sand unit), Ray Point district, illustrating geochemical and mineralogic trends in rock matrix composition. Compositional data are included in table B-1 (Appendix B). Figure is continued on p. 37.

adjacent to the zone of leaching (fig. 30D). Calcite commonly occurs in the mineralized zone in Wyoming Tertiary ores. Pervasive late-stage carbonate cementation and grain replacement occur in lenses and beds, particularly at the top of the ore-bearing sand body and locally along the fault zone as fracture filling within highly cemented sands.

Analysis of carbon isotopes of eight selected Oakville samples from the Ray Point and George West districts (table 5) indicates a combined methane and early meteoric or pedogenic origin for the carbon. One uncemented sample, containing an average amount of early diagenetic and detrital carbonate (10 percent), has a ^{13}C of -9.9 per mil, which falls within the range typical of pedogenic and ground-water carbon. In contrast, nearly pure, coarsely crystalline, vein-filling calcite from the faulted McLean deposit has a value for ^{13}C of -33 per mil, indicating oxidation of light hydrocarbon gases as the source of carbon.

The intermediate ^{13}C values of highly cemented sands reflect a combination of the two end-members within the sample. Similar analytical results and interpretations for a Catahoula deposit were reported by Goldhaber and others (1979b).

(4) All sand samples contained a few percent of clay-sized material. Petrographic examination indicates a greater abundance (6 percent versus 2 percent) of redistributed colloidal or precipitated clay as well as total matrix within the altered zone. X-ray analysis of the less than $2\text{-}\mu$ fraction shows that montmorillonite is the dominant clay mineral. However, two trends are apparent. First, montmorillonite becomes increasingly sodium-rich toward the fault in unaltered sand (fig. 30E). It is not apparent whether this variation is a product of mineralization epigenesis, or is related to later discharge of sodium-bearing waters along the fault zone. Second, a pronounced enrichment in kaolinite

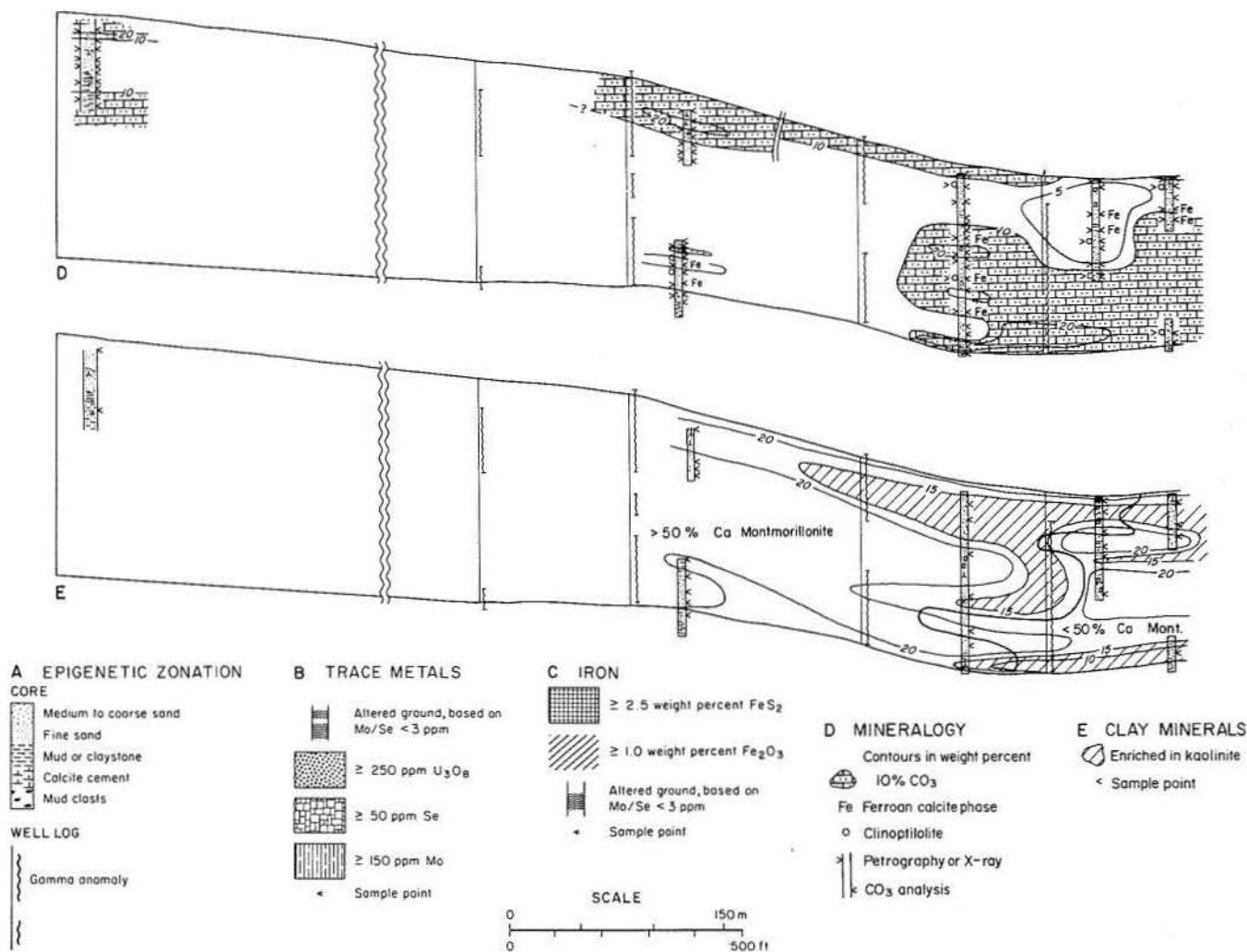


Figure 30 (continued)

characterizes the mineralized sulfidic zone (fig. 30E). Analogous enrichment in kaolinite across other uranium mineralization fronts has been noted by several authors.

(5) There is no evidence of significant enrichment of several other trace metals, including beryllium, copper, nickel, lead, and zinc (table 4). Average concentration of each is commonly highest in argillaceous zones and is near or below the world average for shales (Krauskopf, 1967).

(6) Sulfate content is low, but is slightly greater in mineralized samples (table 4).

(7) Total organic carbon content is extremely low (less than .01 percent) in nearly all samples with a slightly higher average in the mineralized zone.

(8) The zeolite clinoptilolite occurs in trace amounts (tenths of a percent) randomly through the host sand body (appendix B, table B-1).

In summary, uranium ore deposits at Ray Point exhibit a variety of compositional features that are

typical of many alteration front deposits and that reveal primary mineralization to be a product of ground-water flow across an Eh/pH-defined geochemical barrier separating reduced, sulfidic, and oxidized, altered parts of an aquifer.

Ore Paragenesis

Diagenetic features record the evolution of ground-water chemistry and flux through the mineralized aquifer. Interpretation of the paragenetic history is important in determining the timing and mechanisms of mineralization. Paragenesis of the primary Ray Point mineralized front is summarized in figure 31. Ubiquitous limonite and hematite in the Oakville, combined with depositional and paleoclimatological interpretations, indicate widespread oxidation of Oakville sediments during and after deposition. Subsequent intrusion of

Table 4. Compositional summary of Zamzow core cross section sample suite.²

Constituent	Altered (percent)	Average (ppm)	Mineralized (percent)	Range	No. of Analyses
U ₃ O ₈		235		2 - 2,500	60
Mo		65		1 - 629	60
Se		28		1 - 384	60
As		29		2 - 129	60
Be		0.3		0.2 - 1.5	18
Cu		8		2 - 15	18
Ni		11		1 - 25	18
Pb		9		1 - 68	18
Zn		58		11 - 157	18
FeS ₂	0.9		2.5	0.4 - 5.7	60
Fe ₂ O ₃	1.3		1.2	0.5 - 3.8	60
SO ₄	0.03		0.09	0.01 - 1.0	60
CO ₃	8		10	3 - 25	60
Organic C	0.01		0.03	0 - 0.06	14
Clay/Mud Matrix	11		7	—	31

Table 5. Carbon isotope composition of selected Oakville samples (PDB standard).

		¹³ C (per mil)	Wt% CO ₃
Ray Point District			
F-1	Cemented sand	-14.2	—
M-1	Cemented sand	-14.9	—
M-2	Massive vein fill	-33.3*	60
Z-3-157.5	Cemented sand	-22.3	25
George West District			
GW-1-275	Cemented sand	-19.8	27
GW-1-300	Friable sand	-9.9†	12
GW-3-290	Cemented sand	-21.0	23
GW-3-295	Cemented sand	-16.0	23

*Pure late stage CO₃

†Dominantly detrital and early diagenetic CO₃

parts of the aquifer by sulfidizing connate waters discharged from depth introduced the first generation of isotopically heavy pyrite (Goldhaber and others, 1978, 1979a). Renewal of meteoric ground-water flux developed the geochemically active alteration tongue and established the primary zonation of metals, calcite, and clay minerals that is, for the most part, still preserved. Subsequent intrusions of sulfide-rich connate waters ultimately superimposed and maintained reducing, sulfidic conditions in the shallow Oakville aquifer. Consistent uranium-lead age dates of 5.1 m.y. indicate final sulfidization by early Pliocene (Reynolds and others, 1980). With continued deposition, burial, and increasing confinement, flux of meteoric waters was restricted and little-changed until Pleistocene erosion rejuvenated shallow parts of the aquifer, and near-surface oxidation began to impinge on primary mineralization. By this time, the Wilcox fault zone was also acting as a discharge boundary for the deep aquifers of northern Live Oak County, channeling reduced chemically evolved meteoric waters into the shallow Oakville. Local remobilization of uranium and trace metals under the modern hydrologic regime is producing divergent styles of mineralization, such as the redistributed uranium-molybdenum ores concentrated in veinlike bodies along the fault zone (Galloway and others, 1979a, p. 75-77). Occurrence of isotopically light sulfur in the vein deposits (Austin, 1970) confirms a geologically young supergene origin from modern ground-water sulfide.

GEORGE WEST DISTRICT

The George West district lies along the southern margin of the George West fluvial axis (fig. 8). Mining is and has been restricted to in situ methods and currently includes an area of nearly 50 km² (20 mi²). Ore-grade mineralization is concentrated in basal sand units of the Oakville, which contain vertically stacked, coalescent alteration tongues that encompass as many as four individual sand bodies (fig. 32). Two separate alteration fronts are evident (fig. 33). The northern front trends slightly oblique to isolith contours bounding the host sand complex and coincides with a major strike-parallel bend in the paleochannel belt. The southerly oxidation tongue, which is bounded by the Clay West-Moser-Burns front, has been traced for more than 7 km (4.5 mi) and mirrors the isolith trends generated by two intersecting fluvial belts (fig. 33). The altered zone lies along the thick core of the channel complex, downdip of unaltered parts of the aquifer. Host sand bodies are interpreted to be sheet splay and sandy bed-load channel-fill complexes. Deposits are deep, ranging from 60 to 200 m (200 to 700 ft), and are well below the water table in confined parts of the Oakville aquifer. Some continuing remobilization of uranium is indicated by reported radiometric disequilibrium between uranium and its daughter isotopes.

Alteration and mineralization patterns also reflect local structure as well as facies patterns. A northeast-trending graben, created by the shallow extension of

DEPOSITION ↓ BURIAL ↓ EROSION ↓ MINING	HYDROLOGIC EVENTS	GEOCHEMICAL EVENTS	Clay coats	Silicate leach	Iron oxidation	Calcite	Pyrite	Calcite leach	Marcasite	Kaolinite	EXPLANATION
	Vadose leaching	Syndepositional oxidation of aquifer	—	—	—	—	—	—	—	—	
Initial meteoric flux	↓	—	—	—	—	—	—	—	—	—	***** Mineralized zone
Connate flux ↻ Renewed meteoric flux	Sulfidization ↓ Alteration and metallogenesis	+++++	— ? —	+++++	*** **	* * *	+++++	*****	*****		
Connate flux	Sulfidization ↓	—	—	—	—	—	—	—	—	—	++++ Altered zone
Limited meteoric flux	—	—	—	— ? —	—	—	—	—	—	—	
Rejuvenated meteoric flux	Near-surface oxidation and remobilization	—	—	—	—	—	—	—	—	—	

Figure 31. Paragenesis of the Zamzow mineralization front and associated geochemical zones. Vertical bars indicate periods of active precipitation or dissolution. Stars and bars indicate processes restricted to the zones of uranium mineralization and oxidative alteration, respectively.

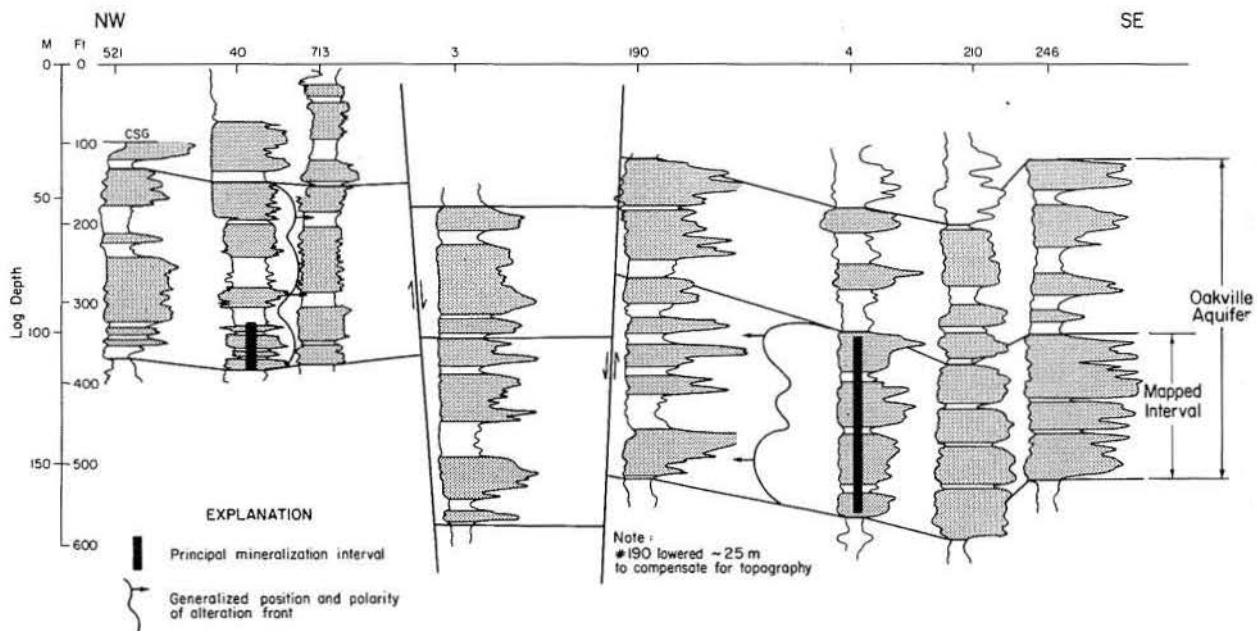


Figure 32. Cross section through the George West district. Mineralization fronts converge on the major down-to-the-coast fault and its associated antithetic fault. For location, see figure 33.

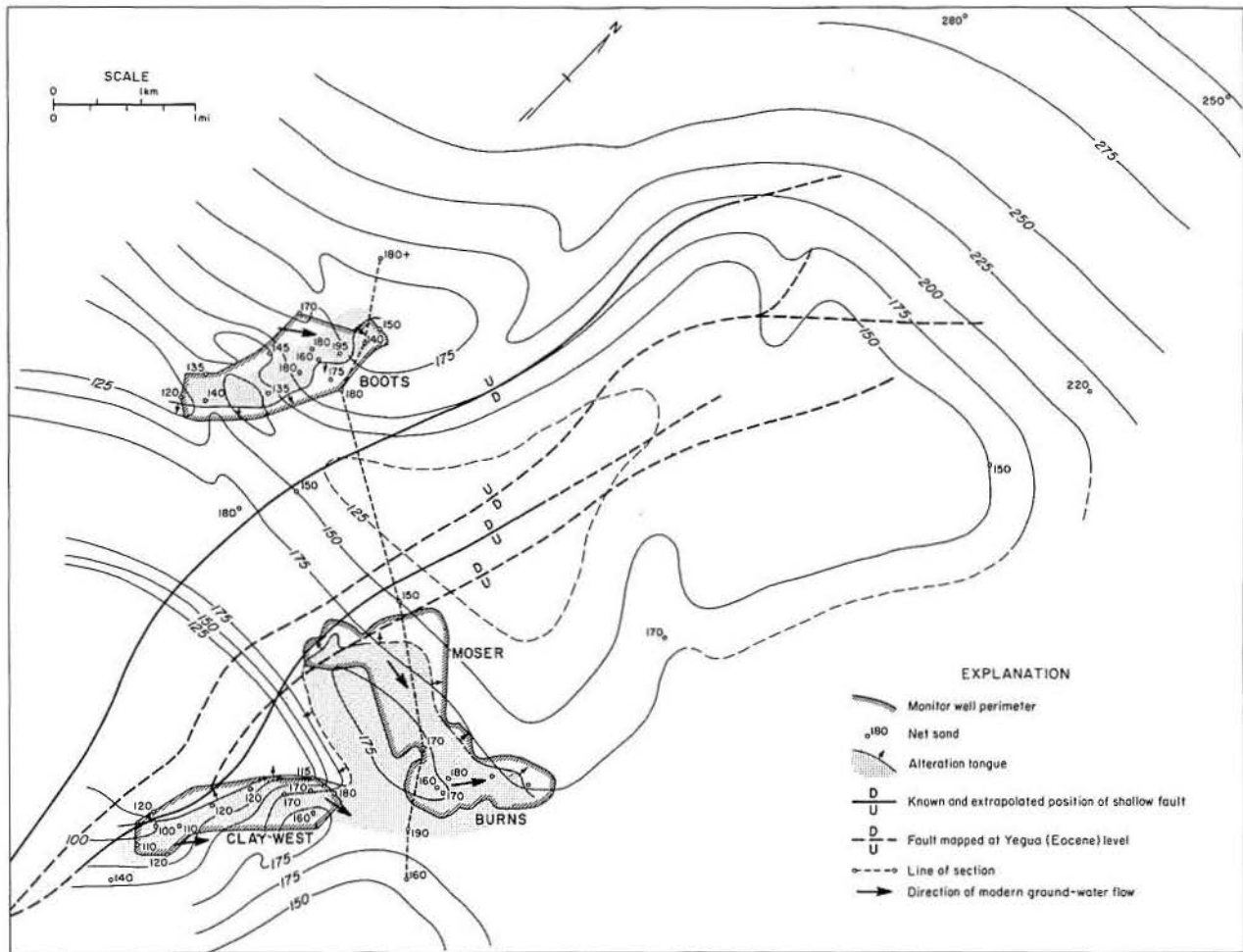


Figure 33. Geographic and geologic setting of the George West district, Live Oak County. Parallelism of structural, stratigraphic, and alteration trends is particularly striking. Oakville ground water moves generally along strike, nearly parallel or slightly oblique to the mineralization fronts. Isolith values are for the mineralized lower Oakville interval (see figure 32).

a Wilcox growth fault and a related antithetic fault (figs. 32 and 33), physically separates individual sand bodies and appears to form a focus toward which both alteration fronts converge. Parallelism between the fault zone and the lower Oakville facies trends indicates early expression of the fault; however, major displacement obviously postdates Oakville deposition.

Regional hydraulic head for the Oakville slopes to the northeast in the district. Hydrologic data collected by mine operators provide specific information about ground-water flux within the host sands. Local flow directions range from east to southeast and are typically somewhat oblique to nearly parallel to the mineralization front trend (Clay West, Burns, Boots leases; fig. 33). In the Moser lease, flow crosses the alteration front from the unaltered side. Thus, modern flux is not everywhere analogous to that of the primary mineralizing solutions.

Hydraulic head is slightly greater in upper Oakville sands, confirming that the district lies within a topographically high regional recharge zone for the Oakville aquifer.

Geochemical and Mineralogical Zonation

The lower Oakville sand sequence displays four geochemical zones: (1) the oxidized altered zone, (2) the resulfidized altered zone, (3) the mineralized sulfidic zone, and (4) the barren sulfidic zone. Geochemical and mineralogical analysis of 92 samples of 12 representative cores from 2 different deposits provides a description of 3 of the zones in and near mineralization fronts (table 6; appendix B, table B-2). Geographic distribution of cores precludes presentation of data in cross-section format;

Table 6. Compositional summary of George West district core sample suite.

Constituent	Deposit A (GW 1-6)			No. of Analyses	Deposit B (GW 7-12)			No. of Analyses
	Altered	Average Mineralized (ppm)	Range (ppm)		Altered	Average Mineralized (ppm)	Range (ppm)	
U ₃ O ₈		727	2 - 10,300	42		625	3 - 10,800	50
Mo		83	1 - 1,370	42		14	1.4 - 310	50
Se		97	0.5 - 1,638	42		22	0.4 - 152	50
As		6.6	1.2 - 14.0	22		—	—	—
Be		2.5	2.5	21		2.5	2.5	15
Cu		7	0.5 - 27	21		5	0.5 - 10	15
Ni		13	4 - 37	21		10	3 - 23	15
Pb		5	5 - 24	21		6	5 - 42	15
Zn		38	12 - 96	21		27	11 - 111	15
FeS ₂	0.3	1.1	0.01 - 2.65	42	1.4	1.8	0.41 - 4.82	50
Fe ₂ O ₃	1.5	1.0	0.25 - 4.92	42	0.7	1.0	0.25 - 2.83	50
SO ₄	0.04	0.06	0.01 - 0.16	42	0.03	0.07	0.005 - 0.20	50
CO ₃	6	15	1 - 36	42	11	10	1 - 25	50
Organic C Clay/mud matrix	0.01	0.012	0.01 - 0.030	15	—	—	—	—
	18	8	—	44	—	—	—	—

however, vertical variability of constituents and comparison of cores from different positions relative to the alteration front show that the Zamzow deposit is a reasonable model for George West deposits. Conclusions are

1. Uranium, molybdenum, and selenium are concentrated in the mineralized sulfidic zone. In deposit A, which preserves a well-developed pyrite-free alteration zone, selenium is most abundant in the distal fringe of the alteration tongue (sample mean of 249 ppm), but remains anomalous in the mineralized sulfidic zone (mean of 97 ppm). Both uranium, which occurs in part as the mineral coffinite, and molybdenum lie dominantly within sulfidic sediment. The alteration boundary is typically marked by the distinct sequence Se → U → Mo concentration peaks. Proportionally, uranium is the dominant metal; molybdenum and selenium occur in subequal amounts, and are particularly depleted in samples from deposit B. Arsenic is also concentrated in the mineralized zone.

2. Iron oxides are present in both the altered and the mineralized zones, averaging about 1 percent. Iron sulfide is nearly absent in altered samples from deposit A; however, it is abundant in many samples from deposit B that otherwise display features typical of the altered zone. Its presence suggests a phase of postmetallogenic resulfidization of altered ground that is under attack by more recent oxidation. As at Zamzow, total iron and FeS₂ contents are greatest in the mineralized sulfidic zone.

3. Carbonate distribution is a product of several generations of calcium carbonate precipitation, including an isotopically light, late-stage, pore-filling cement (table 5). Leaching of carbonate from the oxidized altered zone of deposit A is particularly pronounced. Several samples contained less than 3 percent CO₃. However, no pattern is apparent in deposit B. A minor but distinct ferroan calcite phase was observed in a few samples.

4. Clay minerals are dominantly calcium montmorillonite, although sodium montmorillonite has been reported. Kaolinite is present in trace amounts, but no zonation is evident. Clay occurs as detrital matrix, pedogenic and early diagenetic clay coats and segregations, and discrete sand- to pebble-sized fragments. Altered samples contain more total clay-sized matrix (table 6).

5. Beryllium, copper, nickel, lead, and zinc contents are low in and around the mineralization front.

6. Sulfate content is uniformly low.

7. Organic carbon content is extremely low, but is slightly higher in mineralized samples.

8. Clinoptilolite occurs rarely in trace amounts, primarily in the lowest sand unit.

Ore Paragenesis

Paragenesis of the George West uranium deposits is directly analogous to that of Ray Point. The sequence is shown in figure 34. Principal differences are

DEPOSITION ↓ BURIAL ↓ EROSION ↓ MINING	HYDROLOGIC EVENTS	GEOCHEMICAL EVENTS	Clay coats	Silicate leach	Iron oxidation	Calcite	Pyrite	Calcite leach	Marcosite	Kaolinite	EXPLANATION
	Vadose leaching	Sydepositional oxidation of aquifer	—	—	—	—	—	—	—	—	
Initial meteoric flux	↓		—	—	—	—	—	—	—	—	
Connate flux	Sulfidization										
Renewed meteoric flux	Alteration and metallogenesis		+	?	+++++	*	*	+++++	*	?	Mineralized sulfidic
Connate flux (local) sulfidization			+	?	+++++	*	*	+++++	*	?	
Limited meteoric flux				—				?			Altered zone
Rejuvenated meteoric flux	Aggressive oxidation and remobilization										

Figure 34. Paragenesis of mineralization and associated zones along the southern alteration front, George West district, based on examination of core samples from two deposits.

(1) absence of contemporary exposure of primary mineralization to near-surface oxidation at or near the water table, and (2) widespread preservation or reimposition of oxidizing conditions within the

altered zone along parts of the fronts. As a consequence of the latter, sulfide oxidation and redistribution of metals is locally active where ground-water flow traverses the mineralization front.

Conclusions

The physical geology, hydrostratigraphy, and ore-deposit geology provide the framework for regional and local hydrologic and hydrochemical analyses, which were additional parts of the overall Oakville aquifer study (Henry and others, 1980; Smith and others, 1980). Specific conclusions about the Oakville and its relationship to the uranium-bearing and ground-water-bearing Tertiary succession of the South Texas Uranium Province include the following:

1. Oakville deposition records the continued evolution toward arid climatic conditions begun in Oligocene time and apparent in the underlying Catahoula Formation. Both major and minor basin fringe rivers assumed increasing importance in aggrading the coastal plain, modifying the picture

of a single large paleo-Rio Grande alluvial apron that dominated Catahoula deposition (Galloway, 1977).

2. The Oakville Sandstone corresponds closely to a well-defined hydrostratigraphic unit that is both overlain and underlain by less permeable confining units. Consequently, at shallow to intermediate depths it is relatively homogeneous in terms of regional flux patterns and hydrochemical evolution of contained ground waters.

3. In situ permeability of Oakville sands correlates with interpreted depositional facies. Thus, facies maps can be used to construct an interpretive, derivative map of total aquifer transmissivity.

4. Size and extent of uranium mineralization fronts are spatially and stratigraphically correlated with

aquifer transmissivity. Largest uranium deposits occur within or along the margins of the most transmissive trends defined by bed-load fluvial axes. Smaller uranium deposits occur in less transmissive areas.

5. Oakville uranium deposits resemble those of the underlying Catahoula Formation in both geologic setting and paragenesis. However, Oakville deposits in Live Oak and adjacent counties are closer to fault zones and have increasingly complex geochemical

histories terminated by large-scale resulfidization.

6. Areas inferred to have greatest potential for additional significant uranium reserves (fig. 1) lie along highly transmissive major bed-load fluvial belts of the Hebbroville, George West, and New Davy axes. Smaller deposits, localized primarily by intrinsic carbonaceous or other reductants, may occur within mixed-load channel deposits of the Burton/Penn axes and the Moulton streamplain.

Acknowledgments

This study was funded by the U.S. Environmental Protection Agency, Grant Nos. R805357010 and R805357020. J. G. Price, D. Mathew, W. R. Kaiser, and L. F. Brown, Jr., reviewed the manuscript. Drafting was supervised by James W. Macon and Dan F. Scranton. Lucille C. Harrell directed manuscript typing, and Amanda R. Masterson was principal editor. Clara L. Ho, Chemist-in-charge of the Mineral Studies Laboratory, directed analytical work. Photographic

printing was by Jim Morgan. The report was designed by Judy P. Culwell and assembled by Jamie S. Haynes and Micheline R. Davis.

Particular appreciation is expressed to the staff of several companies, including Intercontinental Energy Corporation, United States Steel Corporation, and Exxon Minerals Corporation, for access to data and samples. Without industry cooperation, this study would have been impossible.

References

- Adams, J. A. S., and Maeck, W. G., 1954, Fluorometric and colorimetric microdetermination of U in rocks and minerals: *Analytical Chemistry*, v. 26, p. 1635-1639.
- Austin, S. R., 1970, Some patterns of sulfur isotope distribution in uranium deposits: *Wyoming Geological Association Earth Science Bulletin*, v. 3, p. 5-20.
- Baker, E. T., Jr., 1978, Stratigraphic and hydrogeologic framework of part of the coastal plain of Texas: U.S. Geological Survey Open-File Report 77-712, 32 p.
- Bardsley, C. E., and Lancaster, J. D., 1965, Sulfur, *in* Black, C. A., ed., *Methods of soil analysis, Part 2: American Society of Agronomy*, p. 1102-1116.
- Barnes, V. E., project director, 1974a, *Geologic atlas of Texas — Austin sheet: The University of Texas at Austin, Bureau of Economic Geology*, scale 1:250,000.
- 1974b, *Geologic atlas of Texas — Seguin sheet: The University of Texas at Austin, Bureau of Economic Geology*, scale 1:250,000.
- 1975, *Geologic atlas of Texas — Beeville - Bay City sheet: The University of Texas at Austin, Bureau of Economic Geology*, scale 1:250,000.
- 1976, *Geologic atlas of Texas — Crystal City - Eagle Pass sheet: The University of Texas at Austin, Bureau of Economic Geology*, scale 1:250,000.
- Brewer, R., 1964, *Fabric and mineral analysis of soils: New York, John Wiley*, 470 p.
- Bruce, C. H., 1972, Pressured shale and related sediment deformation: a mechanism for development of regional contemporaneous faults: *Gulf Coast Association of Geological Societies Transactions*, v. 22, p. 23-31.
- Chorley, R. J., and Kennedy, B. A., 1971, *Physical geography, a systems approach: London, Prentice-Hall International*, 370 p.
- Doyle, J. D., 1979, *Depositional patterns of Miocene facies, Middle Texas Coastal Plain: The University of Texas at Austin, Bureau of Economic Geology Report of Investigations No. 99*, 28 p.
- Eargle, D. H., Dickinson, K. A., and Davis, B. O., 1975, *South Texas uranium deposits: American Association of Petroleum Geologists Bulletin*, v. 59, no. 5, p. 766-779.
- Ece, O. I., 1978, *Uranium mineralization in northwest Bee County, Oakville Formation, Texas Coastal region: The University of Texas at Austin, Master's thesis*, 116 p.
- Ely, L. M., 1957, *Microfauna of the Oakville Formation, LaGrange area, Fayette County, Texas: University of Texas, Austin, Master's thesis*, 118 p.
- Fine, L. O., 1965, *Selenium, in* Black, C. A., ed., *Methods of soil analysis, Part 2: American Society of Agronomy*, p. 1118.

- Folk, R. L., 1974, *Petrology of sedimentary rocks*: Austin, Hemphill Publishing Co., 182 p.
- Galloway, W. E., 1977, *Catahoula Formation of the Texas Coastal Plain: depositional systems, composition, structural development, ground-water flow history, and uranium distribution*: The University of Texas at Austin, Bureau of Economic Geology Report of Investigations No. 87, 59 p.
- _____, 1978, *Uranium mineralization in a coastal-plain fluvial aquifer system: Catahoula Formation, Texas*: *Economic Geology*, v. 73, p. 1655-1676.
- Galloway, W. E., Finley, R. J., and Henry, C. D., 1979a, *South Texas Uranium Province — geologic perspective*: The University of Texas at Austin, Bureau of Economic Geology Guidebook 18, 81 p.
- Galloway, W. E., and Kaiser, W. R., 1980, *Catahoula Formation of the Texas Coastal Plain: origin, geochemical evolution, and characteristics of uranium deposits*: The University of Texas at Austin, Bureau of Economic Geology Report of Investigations No. 100, 81 p.
- Galloway, W. E., Kreitler, C. W., and McGowen, J. H., 1979b, *Depositional and ground-water flow systems in the exploration for uranium — a research colloquium*: The University of Texas at Austin, Bureau of Economic Geology, 267 p.
- Goldhaber, M. B., Reynolds, R. L., and Rye, R. O., 1978, *Origin of a South Texas roll-type uranium deposit: II. Sulfide petrology and sulfur isotope studies*: *Economic Geology*, v. 73, p. 1690-1705.
- _____, 1979a, *Formation and resulfidization of a South Texas roll-type uranium deposit*: U.S. Geological Survey Open-File Report 79-1651, 41 p.
- Goldhaber, M. B., Reynolds, R. L., Rye, R. O., and Grauch, R. I., 1979b, *Petrology and isotope geochemistry of calcite in a South Texas roll-type uranium deposit*: U.S. Geological Survey Open-File Report 79-828, 21 p.
- Hardie, L. A., Smoot, J. P., and Eugster, H. P., 1978, *Saline lakes and their deposits: a sedimentological approach*, in Matter, A., and Tucker, M. E., eds., *Modern and ancient lake sediments*: International Association of Sedimentologists Special Publication No. 2, p. 7-42.
- Harshman, E. N., 1974, *Distribution of elements in some roll-type uranium deposits*, in *Formation of uranium ore deposits*: Vienna, International Atomic Energy Agency, p. 169-183.
- Henry, C. D., Smith, G. E., and Galloway, W. E., 1980, *Uranium and molybdenum in ground water of the Oakville Sandstone, South Texas: implications for restoration of uranium mines*: South Texas Minerals Section, Society of Mining Engineers of American Institute of Mining and Metallurgical Engineering, Proceedings of Fourth Annual Uranium Seminar, p. 19-34.
- Ho, C. L., and Dupre, B., 1980, *A rapid method for U₃O₈ measurement using fluorometric method*: Pittsburgh Conference on Analytical Chemistry and Applied Spectroscopy.
- Ho, C. L., and Tweedy, S. W., 1980, *Analysis of As by distillation and graphite furnace on atomic absorption spectrophotometer*: Pittsburgh Conference on Analytical Chemistry and Applied Spectroscopy.
- Huang, W. H., 1977, *Stability relations of uraninite and coffinite in sedimentary environments*: *Geological Society of America Abstracts with Programs*, v. 9, no. 7, p. 1029.
- Jeffery, P. G., 1970, *Arsenic*, in *Chemical methods of rock analysis*: New York, Pergamon Press, p. 112-122.
- Jonas, E. C., and Brown, T. E., 1959, *Analysis of interlayer mixtures of three clay mineral types by x-ray diffraction*: *Journal of Sedimentary Petrology*, v. 29, p. 77-86.
- Klohn, M. L., and Pickins, W. R., 1970, *Geology of the Felder uranium deposits, Live Oak County, Texas*: American Institute of Mining and Metallurgical Engineers, Mining Engineers Society Reprint No. 70-1-138, 19 p.
- Krauskopf, K. B., 1967, *Introduction to geochemistry*: New York, McGraw-Hill, 721 p.
- Kreitler, C. W., 1976, *Lineations and faults in the Texas Coastal Zone*: The University of Texas at Austin, Bureau of Economic Geology Report of Investigations No. 85, 32 p.
- McGowen, J. H., and Garner, L. E., 1970, *Physiographic features and stratification types of coarse-grained point bars: modern and ancient examples*: *Sedimentology*, v. 14, p. 77-111. *Reprinted as The University of Texas at Austin, Bureau of Economic Geology Geological Circular 75-9, 27 p.*
- McKee, E. D., Crosby, E. J., and Berryhill, H. L., Jr., 1967, *Flood deposits, Bijou Creek, Colorado, June 1965*: *Journal of Sedimentary Petrology*, v. 37, no. 3, p. 829-851.
- Miall, A. D., 1977, *A review of the braided-river depositional environment*: *Earth-Science Reviews*, v. 13, p. 1-62.
- _____, 1978, *Lithofacies types and vertical profile models in braided river deposits: a summary*, in *Fluvial sedimentology*: Calgary, Canadian Society of Petroleum Geologists Memoir 5, 859 p.
- Michael, S., and White, C. L., 1976, *Fluorometric determination of submicrogram concentration of Se in sulfide samples*: *Analytical Chemistry*, v. 48, p. 1484-1486.
- Perel'man, A. I., 1972, *Geochemistry of elements in the supergene zone*: Jerusalem, Keterpress Enterprises, 266 p.
- Quin, B. F., and Brooks, R. R., 1975, *The rapid colorimetric determination of molybdenum with dithiol in biological, geological, and steel samples*: *Analytica Chimica Acta*, v. 74, p. 75-84.
- Ragsdale, J. A., 1960, *Petrology of Miocene Oakville Formation, Texas Coastal Plain*: University of Texas at Austin, Master's thesis, 196 p.
- Renick, B. C., 1936, *The Jackson, Catahoula, and Oakville Formations in a part of the Texas Gulf Coastal Plain*: University of Texas, Austin, Bureau of Economic Geology, Bulletin 3619, 104 p.

- Reynolds, R. L., and Goldhaber, M. B., 1978, Origin of a South Texas roll-type uranium deposit: 1. Alteration of iron-titanium oxide minerals: *Economic Geology*, v. 73, p. 1677-1689.
- _____, 1979, Marcasite in roll-type uranium deposits: *American Association of Petroleum Geologists Bulletin*, v. 63, no. 3, p. 514-515.
- Reynolds, R. L., Goldhaber, M. B., and Ludwig, K. R., 1980, History of sulfidization of South Texas roll-type uranium deposit (abs.): *American Association of Petroleum Geologists Bulletin*, v. 64, no. 5, p. 772.
- Rust, B. R., 1978, Depositional models for braided alluvium, in *Fluvial sedimentology*: Calgary, Canadian Society of Petroleum Geologists Memoir 5, 859 p.
- Schumm, S. A., 1977, *The fluvial system*: New York, John Wiley, 338 p.
- Sellards, E. H., Adkins, W. S., and Plummer, F. B., 1932, *The geology of Texas*, vol. 1, stratigraphy: University of Texas, Austin, *University of Texas Bulletin* 3232, 1007 p.
- Shell Oil Company, 1975, *Stratigraphic atlas — North and Central America*: Houston, Texas, Shell Oil Company, unpaginated.
- Shelton, J. W., and Noble, R. L., 1974, Depositional features of braided-meandering stream: *American Association of Petroleum Geologists Bulletin*, v. 58, no. 4, p. 742-752.
- Shmariovich, Ye. M., 1973, Identification of epigenetic oxidation and reduction as impositions on sedimentary rocks: *International Geology Review*, v. 15, no. 11, p. 1333-1340.
- Smith, G. E., Galloway, W. E., and Henry, C. D., 1980, Effects of climatic, structural, and lithologic variables on regional hydrology within the Oakville aquifer of South Texas: South Texas Minerals Section, Society of Mining Engineers of American Institute of Mining and Metallurgical Engineers, *Proceedings of Fourth Annual Uranium Seminar*, p. 3-18.
- Spradlin, S. D., 1980, *Miocene fluvial systems: southeast Texas*: The University of Texas at Austin, Master's thesis, 139 p.
- Thomas, G. L., 1960, *Petrography of the Catahoula Formation in Texas*: University of Texas, Austin, Master's thesis, 88 p.
- Toth, J., 1978, Gravity-induced cross-formational flow of fluids, Red Earth Region, Alberta, Canada: analysis, patterns, and evolution: *Water Resources Research*, v. 14, p. 805-843.
- Tucker, D. R., 1967, *Faults of South and Central Texas*: Gulf Coast Association of Geological Societies Transactions, v. 17, p. 144-147.
- Vasil'eva, E. G., 1972, Simulation of depositional processes of uranium, selenium, and molybdenum during the interaction between metal-bearing oxygenated waters and a counterflow of gaseous reducing agents: *Lithology and Mineral Resources*, v. 7, no. 6, p. 703-713.
- Walker, T. R., Waugh, B., and Grone, A. J., 1978, Diagenesis in first-cycle desert alluvium of Cenozoic age, southwestern United States and northwestern Mexico: *Geological Society of America Bulletin*, v. 89, no. 1, p. 19-32.
- Weeks, A. M. D., 1945, *Oakville, Cuero, and Goliad Formations of Texas Coastal Plain between Brazos River and Rio Grande*: American Association of Petroleum Geologists Bulletin, v. 29, no. 11, p. 1721-1732.

Appendix A

Sample Localities for Regional Mineralogical Analysis

Duval County

- 4/4-1 Road cut, State Highway 16, 13.5 mi S. of Freer
4/4-4 Road cut, State Highway 16, 14 mi S. of Freer
4/4-6 Road cut, U.S. 59, 9 mi NE of Freer
4/5-11 Road cut, U.S. 59, 18.5 mi NE of Freer at county line

McMullen County

- 4/5-8 Hillslope exposure, 11 mi E. of junction of State Highway 16 and R.M. 1962, on a county road
4/5-9 Gravel quarry, county road 3 mi N. and E. of Loma Alta Community and R.M. 624
4/5-10 Road cut, R.M. 624, 8 mi E. of Loma Alta Community

Live Oak County

- 3/22-3 Smith uranium pit, off R.M. 1358, 1.6 mi W. of junction of R.M. 1358 and R.M. 623
P-1 Core, uranium prospect
Feld-2 Open pit, Felder uranium mine, Ray Point district
Z-3 Core, Zamzow in situ mine, Ray Point district
Lam-3 Core, Lamprecht in situ mine, Ray Point district
GW-6, 7 Cores, in situ mine, George West district
3/31-1 Creekbed, S. of R.M. 1358, 1.5 mi E. of Oakville
4/5-1 Sand pit (near), county road 4 mi E. and S. of Clayton
4/5-3 Creekbed, county road 2.5 mi S. of junction of R.M. 1873 and R.M. 889
4/5-4 Creekbed, county road 3.5 mi S. of junction of R.M. 1873 and R.M. 889
4/5-7 Caliche pit, county road 1.2 mi ESE. of Lane
4/6-1 Road cut, U.S. 281, 3.5 mi S. of George West

Bee County

- Paw-1 Core, Pawnee leach mine, Pawnee area

Karnes County

- 3/21-7 Sand pit, R.M. 627, 0.6 mi S. of Ruckman
3/22-1 Creekbed, R.M. 627, 0.1 mi N. of junction of R.M. 81 and R.M. 627
4/6-4 Sand pit, county road, 3.6 mi SW of Kenedy
4/6-5 Caliche pit, R.M. 2102, 0.3 mi W. of junction of R.M. 1353 and R.M. 2102
4/6-7 Sand pit, State Highway 239, 0.8 mi SW of junction of State Highway 72 and State Highway 239
4/6-9 Dump dugout, State Highway 123, in Karnes County 0.6 mi N. of junction of State Highway 123 and State Highway 80
Tms-1 Open pit, Thomas mine, Nopal area

De Witt County

- 3/21-2 Sand pit, county road, 2.7 mi SW of Nopal Community
3/21-3 Caliche pit, F.M. 108, 2 mi S. of Nopal Community
3/21-4 Sand pit, county road, 2 mi NW of Little Chicago Community
3/21-5 Sand pit, State Highway 119, 0.3 mi SE of New Davy
3/21-6 Caliche/sand pit, county road, 3.5 mi S. of Garfield
4/10-4 Road cut, county road, 0.5 mi W. of Bellevue
4/10-6 Road cut, county road, 0.8 mi N. of Nopal Community
4/10-7 Creek bank, county road, 2.5 mi W. of junction of F.M. 240 and F.M. 2542
4/10-8 Sand pit, F.M. 240, 0.1 mi S. of junction F.M. 240 and F.M. 2542
4/10-9 Sand pit, county road, 0.5 mi S. of F.M. 238, 2.7 mi SW of Westhoff
4/10-11 Creekbed, F.M. 766, 5 mi N. of Valley View
4/11-1 Road cut, U.S. 183 in Hochheim, 0.3 mi W. of junction of U.S. 183 and State Highway 111
4/11-2 Creekbed, F.M. 443, 2.5 mi N. of Hochheim

Gonzales County

- 3/21-1 New stock tank, county road, 3 mi N. of Davy Community
4/10-1 Gullies, county road, 4.5 mi S. of junction of U.S. 181 and F.M. 2067
4/10-2 Borrow ditch, county road, 1 mi E. of Cheapside

Lavaca County

- 4/11-3 Sand pit, F.M. 966, 0.5 mi S. of junction of F.M. 966 and F.M. 958
4/11-5 Landfill pit, county road, 4.5 mi NW of Shiner
4/11-6 Creekbed, county road, 1.5 mi N. of Shiner

Lavaca County (cont.)

5/15-1 Sand pit, F.M. 532, 5.3 mi E. of junction R.M. 795 and F.M. 532
5/15-2 Creekbed, State Highway 95, 1 mi S. of Moulton
5/15-3 Sand pit, county road, 2.2 mi S. of Moulton
5/15-5 Creek bank, county road, 4.3 mi SE of Moulton
5/15-6 Creekbed, county road, 2.4 mi SE of Moulton

Fayette County

5/15-7 Sand pit, State Highway 95, 1.5 mi SW of Flatonia
5/16-1 Bluff, county road, 1.5 mi NW of junction of U.S. 77 and F.M. 155
5/16-2 Stream gully, county road, 2 mi W of junction of F.M. 3233 and F.M. 155
5/16-3 Sand pit, county road, 1 mi SE of O'Quinn
5/16-7 Creekbed, State Highway 71, 3 mi SE of LaGrange
5/16-9 Creekbed, county road, 1.4 mi NE of Halstead Community
5/17-1 Hill slope, county road, 2.5 mi S. of triple junction of State Highway 159, State Highway 237, and F.M. 2981
5/17-2 Sand pit, F.M. 1291, 4 mi SE of Warrenton
5/17-4 Tank, F.M. 1457, 0.4 mi SE of Becker
5/17-5 Creek bank, State Highway 237, 2.5 mi N. of Round Top

Washington County

5/17-6 Road metal pit, county road, 1.8 mi SE of La Bahia
5/17-8 Gravel pit, county road, 2.4 mi NW of junction of U.S. 290 and State Highway 237
5/17-9 Creek bank, county road, 2.5 mi SE of Burton
5/17-12 Flooded pit, county road, 1.2 mi S. of junction of F.M. 390 and F.M. 1948
5/18-3 Sand pit, county road, 0.5 mi W. of Stults Ranch Airfield
5/18-4 Sand pit, F.M. 912, 0.4 mi E. of junction of State Highway 105 and F.M. 912
5/18-6 Sand pit, county road, 1 mi N. of Winkelmann

Grimes County

5/18-1 Road cut, State Highway 90, 3.5 mi SW of Anderson

Appendix B

Geochemical and Mineralogical Analysis of Core Samples, George West and Ray Point Districts

Methodologies of analyses were as follows:

Total U₃O₈:

Sample is fused with Li-tetraborate followed by dissolving the flux in diluted nitric acid. U₃O₈ in solution is complexed with trioctylphosphine oxide and is extracted into cyclohexane (Adams and Maeck, 1954). An aliquot of U₃O₈ in cyclohexane is fused in a sodium fluoride - lithium fluoride matrix and analyzed fluorometrically (Ho and Dupre, 1980).

Mo:

The method used is slightly modified from that of Quin and Brooks (1975). Sample is fused with potassium hydrogen sulfate, followed by sample dissolution in distilled 6N HCl. Mo in solution is complexed with dithiol and extracted into amyl acetate. The green-colored Mo-dithiol complex is measured spectrophotometrically at 682 nm on a Pye-Unicam SP8-100 spectrophotometer.

Se:

A procedure modified from those of Fine (1965) and Michael and White (1976) was used. Sample is digested with a mixture of sulfuric acid and nitric acid at 150°C until free of excess HNO₃. Se in solution is complexed with 2, 3-naphthalene diamine and extracted into cyclohexane. Se-organic complex in cyclohexane is measured spectrofluorometrically at an excitation wavelength of 374 nm and emission wavelength of 517 nm using the differential control of a Farran Mark I spectrofluorometer.

As:

The method used was modified from that of Jeffery (1970) by Ho and Tweedy (1980). Sample is fused with a mixture of MgO and K₂CO₃ in graphite crucible at 900°C followed by dissolving the flux in distilled HCl. Arsenic in HCl solution is distilled in presence of hydrazine sulfate and HBr. AsCl₃ in distillate is collected in HNO₃ and analyzed on graphite furnace on IL651 atomic absorption spectrophotometer.

Zn, Pb, Cu, Ni, and Be:

Sample is digested in a mixture of distilled HCl and HNO₃ (1:1 by volume) for two hours at 150°C on a Technicon Digestion block. Metals in clear filtrate are analyzed by IL651 atomic absorption spectrophotometer. Beryllium is measured in the same manner as other metals except 8-hydroxyquinoline is added to suppress Al interference.

Fe:

Fe₂O₃ - Fe: Sample is repeatedly extracted with hot distilled 6N HCl until free of Fe in subsequent acid extract. Fe in combined HCl extracts is determined by atomic absorption.

FeS₂ - Fe: Residue after the HCl extraction for Fe₂O₃ - Fe is then treated with hot distilled HNO₃ to dissolve pyrite. Fe in HNO₃ extract is measured by atomic absorption. Sulfate-S oxidized from pyrite is measured by a turbidimetric method; FeS₂ is calculated from Fe and SO₄-S in HNO₃ extract.

SO₄-S:

Sample is leached with 1N HCl. SO₄ in HCl extract is measured turbidimetrically at 420 nm using the secondary light path on a Pye-Unicam SP8-100 spectrophotometer (Bardsley and Lancaster, 1965).

CO₃:

Sample is ignited at 650°C to a constant weight to remove organic C. The residue is further ignited at 1050°C to a constant weight to decompose carbonate. The weight loss as result of evolution of CO₂ between 650°C and 1050°C is multiplied by a factor of 1.364 to give the weight of CO₃.

Total Organic Carbon:

Contracted analysis utilizing a Leco automatic carbon determinator.

Clay Minerals:

Volumetric estimation is based on 200 counts of standard petrographic thin sections. Semiquantitative mineralogical analysis utilized conventional x-ray diffractograms of oriented, less than 2 meter-size fractions. Separate slides are glycolated, heated to 550°C, and equilibrated with a KNO₂ saturated solution. Na and Ca montmorillonite are distinguished using the method of Jonas and Brown (1959). Based on relative abundance, clay minerals and zeolites were classified as dominant (D), present (P), trace (tr), questionably present (?), and absent or below level of detection (—) (see tables B-1 through B-3).

Table B-1. Analytical data for core samples, Zamzow mine site.

Core Depth	Lithology	U ₃ O ₈	Mo	Trace metals (ppm)							Major constituents (weight percent)						Fine fraction					
				Se	As	Cu	Be	Zn	Pb	Ni	Fe ₂ O ₃	FeS ₂	CO ₃	SO ₄	TOC	% Clay matrix / particles	Na Mont	Ca Mont	Kaol	Other	Climopt	
Z-1	100.0	Silt	17	9	<1	5	10	1	52	10	8	0.8	1.7	23	0.01	0.004	3/0	—	—	—	—	—
	102.5	Silt	73	26	<1	—	—	—	—	—	—	0.7	1.6	9	0.05	—	—	—	—	—	—	—
	105.0	Md.Sd.	240	33	1	—	—	—	—	—	—	0.7	2.7	8	0.05	—	1/65	—	—	—	—	—
	107.5	Md.Sd.	1300	103	1	22	8	<1	72	10	18	0.8	5.7	8	0.13	—	0.5/0	—	—	—	—	—
	109.5	Md.Sd.	540	34	<1	—	—	—	—	—	—	—	2.5	9	0.05	—	0/0.5	—	—	—	—	—
	110.5	Md.Sd./Cly.	340	111	1	—	—	—	—	—	—	2.0	2.5	8	0.30	—	—	P	D	P	—	—
	113.0	Clay	4	20	<1	—	—	—	—	—	—	1.6	1.9	5	0.03	—	41/9.5	P	D	P	—	—
	115.0	Silt	34	23	1	107	5	<1	157	10	15	1.2	1.1	7	0.03	0.018	—	—	—	—	—	—
	117.0	Md.F.Sd.	6	1	2	—	—	—	—	—	—	0.7	0.5	13	0.01	—	9/45	P	P	P	tr il	—
	119.0	Silt	4	3	1	—	—	—	—	—	—	1.3	0.6	10	0.01	—	—	—	—	—	—	—
Z-2	156.0	Md.Sd.	18	4	15	2	10	<1	16	2	8	0.5	0.5	6	0.02	0.020	7.5/4.5	P	D	P	—	—
	157.0	Md.Sd.	18	4	20	—	—	—	—	—	—	0.7	0.5	5	0.02	—	—	—	—	—	—	—
	159.0	Crs.Sd.	25	6	11	—	—	—	—	—	—	0.8	0.4	10	0.01	—	—	—	—	—	—	—
	161.0	M.Sd.	740	19	2	—	—	—	—	—	—	0.8	0.5	6	0.02	—	7.5/4.5	P	D	P	? il	P
	163.0	Crs.Sd.	43	15	9	—	—	—	—	—	—	0.6	0.5	4	0.02	—	—	—	—	—	—	—
	165.0	Crs.Sd.	130	82	25	—	—	—	—	—	—	0.6	0.6	9	0.02	—	5.5/1	P	D	—	tr il	P
	168.0	Silt	45	50	8	16	15	2	148	7	25	3.2	4.2	5	0.04	—	—	—	—	—	—	—
	171.0	Clay	4	4	<1	—	—	—	—	—	—	3.2	1.7	5	0.02	—	—	P	D	tr	? il	—
	173.0	Clay	4	3	<1	—	—	—	—	—	—	3.4	1.8	5	0.02	—	—	—	—	—	—	—
Z-3	137.0	Crs.Sd.	34	34	1	—	—	—	—	—	—	0.6	1.4	12	0.06	—	—	—	—	—	—	—
	140.0	Md.Sd.	120	150	4	12	8	<1	16	7	8	1.0	3.5	8	0.24	0.012	4.5/1	P	D	P	? il	P
	144.0	Md.Sd.	170	147	6	—	—	—	—	—	—	1.1	3.5	9	0.07	—	—	P	D	P	? il	?
	148.0	Md.Sd.	96	89	1	—	—	—	—	—	—	1.0	3.4	8	1.0	—	—	—	—	—	—	—
	150.0	Md.Sd.	110	172	1	—	—	—	—	—	—	0.8	2.8	9	0.08	—	—	—	—	—	—	—
	151.5	Md.Sd.	550	117	24	—	—	—	—	—	—	1.1	4.0	12	0.06	—	—	—	—	—	—	—
	153.0	Md.Sd.	31	11	20	—	—	—	—	—	—	0.9	2.7	12	0.04	0.010	9.5/7	P	D	P	—	—
	155.0	Md.Sd.	43	2	28	15	8	1	130	2	20	1.6	1.2	10	0.05	—	—	—	—	—	—	—
	157.0	F.Sd.	17	2	14	—	—	—	—	—	—	0.7	1.1	25	0.03	—	—	—	—	—	—	—
	159.0	Md.Sd.	39	2	1	—	—	—	—	—	—	0.7	0.5	4	0.02	—	—	—	—	—	—	—
	161.0	Md.Sd.	28	2	>1	—	—	—	—	—	—	0.9	0.7	12	0.02	—	—	—	—	—	—	—
	164.0	F.Sd.	38	4	2	12	8	<1	23	7	12	1.0	1.4	12	0.04	0.016	6.5/1.5	P	D	P	? il	P
	167.0	F.Sd.	880	25	21	—	—	—	—	—	—	0.5	3.3	10	0.02	—	—	—	—	—	—	—
	173.0	Crs.Sd.	15	38	6	—	—	—	—	—	—	0.7	0.6	12	0.01	<0.01	5/5	D	P	tr	? il	—
	177.0	Md.Sd.	20	25	55	—	—	—	—	—	—	0.9	0.9	8	0.02	<0.01	—	P	D	tr	? il	—
	179.0	Md.Sd.	680	39	385	45	5	<1	19	68	18	0.9	2.4	8	0.05	—	—	—	—	—	—	—
	182.5	Md.Sd.	19	7	2	—	—	—	—	—	—	0.4	0.6	23	0.01	—	—	—	—	—	—	—
	183.5	Clay	7	2	1	16	4	<1	13	<1	<1	2.7	2.5	4	0.01	—	—	—	—	—	—	—
Z-4	138.0	Crs.Sd.	35	2	94	—	—	—	—	—	—	0.8	0.3	6	0.01	—	7/3	P	D	P	? il	—
	140.0	Clay	18	2	57	—	—	—	—	—	—	2.7	1.5	3	0.03	—	—	—	—	P	—	—
	142.0	Clay	—	—	—	—	—	—	—	—	—	—	—	—	—	—	—	P	P	P	—	—
	144.0	Crs.Sd. - Clay	21	1	40	12	5	1	90	7	10	3.8	1.8	4	0.04	—	—	—	—	—	—	—
	147.5	Crs.Sd. - Clay	49	3	65	—	—	—	—	—	—	2.6	1.8	5	0.02	—	21/2	P	P	P	—	—
	151.5	Md.Sd.	30	25	380	—	—	—	—	—	—	—	0.44	3	0.02	—	4/10.5	D	P	P	—	—
	155.0	Md.Sd.	250	598	8	56	2	<1	11	4	15	0.8	4.0	3	0.08	0.014	4.5/8	P	P	P	tr il	P
	157.0	Md.Sd.	19	500	10	—	—	—	—	—	—	1.4	3.5	4	0.08	—	—	—	—	—	—	—
	161.0	Md.Sd.	110	225	4	—	—	—	—	—	—	1.8	3.8	5	0.07	—	24/2	P	P	P	—	—
	164.0	Md.Sd.	5	228	6	18	8	<1	52	4	<1	0.6	1.7	13	0.02	0.028	2/1	P	P	?	? il	P
Z-5	170.0	F.Sd.	5	44	1	18	8	<1	50	12	6	1.2	4.6	12	0.05	0.062	9/5	—	—	—	—	—
	173.0	Md.Sd.	2	17	1	—	—	—	—	—	—	0.7	1.8	17	0.01	—	—	—	—	—	—	—
	175.0	Md.Sd.	3	29	<1	—	—	—	—	—	—	0.7	1.7	22	0.02	—	2.5/0	—	—	—	—	—
	177.0	Silt	87	192	2	—	—	—	—	—	—	1.4	3.8	12	0.09	—	—	—	—	—	—	—
	179.0	Md.Sd.	400	6	25	10	8	<1	18	1	2	0.9	1.0	10	0.01	0.012	3/1	P	D	tr	il	?
	181.0	Md.Sd.	71	3	55	—	—	—	—	—	—	1.0	1.1	6	0.03	—	11/8.5	P	D	tr	tr il	—
	182.0	Md.-F.Sd.	—	—	—	—	—	—	—	—	—	—	—	—	—	—	8/11.5	P	D	tr	—	—
	183.5	F.Sd.	22	4	4	—	—	—	—	—	—	1.4	1.6	8	0.04	—	—	—	—	—	—	—
Z-6	137.5	Md.Sd.	14	26	1	14	10	<1	49	<1	2.5	0.8	2.1	23	0.02	0.018	0/1	—	—	—	—	—
	140.0	Md.Sd.	910	40	7	—	—	—	—	—	—	0.9	2.4	8	0.11	—	1/1.5	P	P	P	tr il	P
	143.0	Md.Sd.	2500	53	21	—	—	—	—	—	—	0.8	2.6	7	0.10	—	—	—	—	—	—	—
	146.0	Md.Sd.	2400	108	100	18	5	<1	19	2	20	1.2	3.9	9	0.69	0.062	5.5/5.5	D	P	P	—	?
	149.0	Crs.Sd.	425	88	34	—	—	—	—	—	—	0.9	1.9	12	0.12	—	3.5/1	P	P	—	tr il	—
	179.5	F.Sd.	225	629	7	129	8	<1	105	4	8	1.2	2.7	17	0.09	0.062	15.5/0	D	P	tr	tr il	—
	181.5	Clay	10	37	1	—	—	—	—	—	—	2.2	1.8	10	0.04	—	—	—	—	—	—	—

D Dominant P Present tr Trace ? Questionably present — Absent or below level of detection il Illite

Table B-2. Analytical data for core samples, George West deposit A.

Core	Depth	Lithology	Trace metals (ppm)											Major constituents (weight percent)					Fine fraction				
			U ₃ O ₈	Mo	Se	As	Cu	Be	Zn	Pb	Ni	Fe ₂ O ₃	FeS ₂	CO ₃	SO ₄	TOC	% Clay matrix/ particles	Na Mont	Ca Mont	Kaol	Other	Clinopt	
GW-1	275.0	Md.Sd.	2	4	2	4	3	<2.5	12	5	4	0.4	0.5	27	0.01	—	0/2	—	—	—	—	—	
	280.0	Md.Sd.	79	560	1	—	—	—	—	—	—	0.4	0.8	23	0.03	—	—	—	—	—	—		
	285.0	Md.Sd.	204	101	4	3	3	<2.5	15	5	8	0.3	0.5	26	0.02	0.024	0.5/1	—	D	—	—		
	290.0	Md.Sd.	363	85	11	—	—	—	—	—	—	0.5	0.8	18	0.03	—	0.5/2	—	—	—	—		
	295.0	Crs.Sd.	70	27	15	3	5	<2.5	19	5	7	0.3	0.1	19	0.01	—	1/1	—	D	—	—		
	300.0	Crs.Sd.	275	186	53	—	—	—	—	—	—	0.4	0.4	12	0.02	—	1/2	—	—	—	—		
	305.0	Crs.Sd.	2080	1370	114	13	7	<2.5	59	8	37	0.6	0.9	6	0.06	0.016	0/6.5	—	—	—	—		
	307.0	Crs.Sd.	—	—	—	—	—	—	—	—	—	—	—	—	—	—	—	D	—	tr il	—		
	310.0	Md.Sd.	80	55	1250	—	—	—	—	—	—	0.9	2.7	3	0.03	—	7/6	—	—	—	—		
	315.0	Md.Sd.	29	4	20	4	3	<2.5	22	5	11	0.4	0.6	15	0.01	—	2.5/2	—	D	tr	? il	—	
GW-3	290.0	Clay	51	53	11	2	4	—	15	8	8	0.3	0.6	23	0.03	0.014	0/0	P	D	?	? il	—	
	295.0	Md.Sd.	70	16	9	—	—	—	—	—	—	0.3	0.5	23	0.02	—	0/0	—	—	—	—	—	
	300.0	Md.Sd.	110	89	6	1	<2.5	<2.5	<2.5	<5	8	0.3	0.4	24	0.03	0.012	0/0	—	—	—	—	—	
	305.0	Md.Sd.	90	79	4	—	—	—	—	—	—	0.6	0.6	24	0.03	—	6.5/1.5	—	—	—	—	—	
	315.0	Md.Sd.	66	18	25	4	4	<2.5	21	<5	9	0.6	1.0	22	0.02	—	1/4.5	P	D	tr	? il	—	
GW-4	501.0	Md.Sd.	3150	37	8	7	3	<2.5	52	10	9	1.8	1.5	15	0.11	0.004	51/1	P	D	tr	tr il	—	
	503.0	F.Sd.	—	—	—	—	—	—	—	—	—	—	—	—	—	—	—	P	D	—	tr il	—	
	505.0	Clay	40	2	420	—	—	—	—	—	—	2.1	0.1	4	0.07	—	5/10.5	—	—	—	—	—	
	511.0	F.Sd.	18	5	302	7	27	<2.5	24	<5	5	1.2	0.1	4	0.04	0.000	8/4.5	—	—	—	—	—	
	514.0	Md.Sd.	33	4	1638	—	—	—	—	—	—	2.6	0.1	6	0.07	—	—	D	tr	il	—		
	521.0	Crs.Sd.	24	2	85	11	5	<2.5	35	<5	13	2.2	0.1	4	0.06	0.006	3/9	—	—	—	—	—	
	526.0	Md.Sd.	7750	98	4	—	—	—	—	—	—	0.7	1.7	5	0.05	—	14.5/4.5	—	—	—	—	—	
	529.0	Md.Sd.	10,300	59	10	13	<.5	<2.5	30	24	5	0.8	1.5	5	0.10	0.030	9/7	P	D	—	il	—	
	533.0	Md.Sd.	4000	81	16	—	—	—	—	—	—	0.9	1.7	2	0.10	—	4.5/2.5	—	—	—	—	—	
	538.5	F.Sd.	23	3	2	2	15	<2.5	35	<5	9	0.9	0.7	16	0.04	0.008	10.5/1	—	D	—	il	P	
GW-5	441.0	Clay	6	4	5	4	18	<2.5	75	<5	21	2.9	1.6	11	0.13	0.012	—	—	—	—	—		
	447.0	Md.Sd.	28	11	3	—	—	—	—	—	—	0.6	1.0	3	0.03	0.028	13/5	—	D	tr	tr il		
	449.0	Clay	23	34	44	10	9	<2.5	96	<5	23	3.3	1.6	4	0.13	—	1.5/2	—	—	—	—		
	456.0	Md.Sd.	144	37	3	—	—	—	—	—	—	0.4	1.1	36	0.04	—	1/0	—	—	—	—		
	460.0	Md.Sd.	538	55	4	11	5	<2.5	42	5	6	0.8	1.0	5	0.09	0.024	—	—	D	tr	tr il		
	463.0	Clay	8	4	<1	—	—	—	—	—	—	3.9	0.3	17	0.16	—	—	—	—	—	—		
	466.0	Md.Sd.	7	17	4	3	11	<2.5	60	<5	15	2.4	1.3	18	0.08	—	—	—	—	—	—		
GW-6	281.0	F.Sd.	713	300	5	7	5	<2.5	53	—	27	1.0	1.2	20	0.06	—	—	—	—	—	—		
	285.0	Md.Sd.	14	2	1	—	—	—	—	—	—	0.8	<0.1	6	0.02	0.008	5/7.5	P	D	?	tr il		
	288.0	Md.Sd.	16	2	1	—	—	—	—	—	—	1.0	<0.1	11	0.02	—	1.5/1	P	D	—	tr il		
	292.0	Md.Sd.	6	3	1	7	10	<2.5	67	<5	35	1.8	<0.1	1	0.05	0.010	21.5/7.5	—	—	—	—		
	296.0	Md.Sd.	20	1	1	—	—	—	—	—	—	1.7	<0.1	1	0.03	—	7.5/3.5	—	—	—	—		
	300.0	Md.Sd.	15	1	2	—	—	—	—	—	—	0.8	<0.1	1	0.04	—	25/5.5	P	D	?	? il		
	304.0	Md.Sd.	14	3	2	8	4	<2.5	30	<5	14	1.2	<0.1	1	0.02	—	8.5/6.5	—	—	—	—		
	305.5	Md.Sd.	10	2	7	—	—	—	—	—	—	4.9	<0.1	2	0.11	—	22/4.5	—	—	—	—		
	312.0	F.Sd.	6	2	10	6.0	3	<2.5	29	<5	9	1.0	<0.1	1	0.02	0.004	8.5/7	—	D	tr	tr il	?	
	318.0	Md.Sd.	56	58	4	—	—	—	—	—	—	0.6	0.9	16	0.02	—	6.5/4.5	—	—	—	—		
	322.0	Md.Sd.	14	10	1	14	—	—	—	—	—	1.3	1.4	7	0.04	—	36/6	—	—	—	—		
	324.0	Md.Sd.	9	2	1	—	—	—	—	—	—	1.2	1.5	3	0.03	—	12.5/12	—	D	—	—		

D Dominant
P Present
tr Trace
? Questionably present
— Absent or below level of detection
il Illite

Table B-3. Analytical data for core samples, George West deposit B.

Core	Depth	Lithology	Trace metals (ppm)										Major constituents (weight percent)					Fine fraction				
			U ₃ O ₈	Mo	Se	As	Cu	Be	Zn	Pb	Ni	Fe ₂ O ₃	FeS ₂	CO ₂	SO ₄	TOC	% Clay matrix/particles	Na Mont	Ca Mont	Kaol	Other	Clinopt
GW-7	510.0	Md.Sd.	38	14	14	—	—	—	—	—	—	—	0.6	1.0	9	0.05	—	—	—	—	—	—
	520.0	Md.Sd.	81	20	1	—	—	—	—	—	—	—	0.4	1.0	25	0.02	—	—	—	—	—	—
	530.0	Silt	20	3	1	—	—	—	—	—	—	—	1.6	2.0	8	0.04	—	—	—	—	—	—
	535.0	Md.Sd.	2880	5	11	—	—	—	—	—	—	—	1.4	4.8	5	0.06	—	—	—	—	—	—
	540.0	Md.Sd.	11	2	18	—	—	—	—	—	—	—	0.4	0.4	13	0.01	—	—	—	—	—	—
	610.0	F.Sd.	7	2	6	—	—	—	—	—	—	—	0.8	1.4	15	0.02	—	—	P	P	tr	il
	615.0	Md.Sd.	9	3	15	—	—	—	—	—	—	—	0.7	2.8	4	0.04	—	—	—	—	—	—
	620.0	Md.Sd.	23	3	13	—	—	—	—	—	—	—	0.3	0.5	20	0.01	—	—	—	—	—	—
	625.0	F.Sd.	14	18	2	—	—	—	—	—	—	—	0.3	0.7	20	0.02	—	—	—	—	—	—
	633.0	F.Sd.	24	11	<1	—	4	<2.5	22	<5	12	0.5	1.1	4	0.02	—	—	—	—	—	—	—
GW-8	460.0	Md.Sd.	28	9	2	—	—	—	—	—	—	0.5	1.1	5	0.04	—	—	—	—	—	—	
	470.0	Md.Sd.	275	28	4	—	—	—	—	—	—	0.7	1.2	5	0.17	—	—	—	—	—	—	
	480.0	Md.Sd.	246	38	3	—	4	<2.5	26	<5	13	0.7	1.3	6	0.13	—	—	—	—	—	—	
	487.5	Md.Sd.	25	7	2	—	—	—	—	—	—	2.0	1.6	9	0.06	—	—	—	—	—	—	
	492.5	Clay	50	31	5	—	—	—	—	—	—	2.5	2.3	8	0.06	—	—	—	—	—	—	
	500.0	F.Sd.	35	14	3	—	—	—	—	—	—	1.0	1.7	11	0.04	—	—	—	—	—	—	
	509.0	Md.Sd.	6	3	59	—	—	—	—	—	—	0.7	1.3	10	0.02	—	—	—	—	—	—	
	600.0	Md.Sd.	13	3	93	—	2	<2.5	15	<5	4	0.6	3.1	4	0.02	—	—	—	—	—	—	
	605.0	Md.Sd.	30	7	84	—	6	<2.5	11	<5	3	0.5	2.0	6	0.02	—	—	—	—	—	—	
	610.0	F.Sd.	513	5	3	—	—	—	—	—	—	0.4	1.3	20	0.01	—	—	—	—	—	—	
	615.0	Md.Sd.	250	40	2	—	7	<2.5	28	<5	6	0.7	2.4	9	0.12	—	—	—	—	—	—	
	620.0	Md.Sd.	48	12	2	—	—	—	—	—	—	0.5	1.0	5	0.06	—	—	—	—	—	—	
	624.0	Md.Sd.	88	11	3	—	—	—	—	—	—	1.2	1.6	5	0.08	—	—	—	—	—	—	
GW-9	620.0	F.Sd.	6	2	22	—	—	—	—	—	—	0.5	1.5	5	0.02	—	—	—	—	—	—	
	625.0	Md.Sd.	49	7	32	—	—	—	—	—	—	0.5	1.8	3	0.04	—	—	—	—	—	—	
	630.0	F.Sd.	18	2	42	—	—	—	—	—	—	0.6	1.4	20	0.02	—	—	—	—	—	—	
	635.0	Md.Sd.	7	2	152	—	—	—	—	—	—	0.6	1.0	4	0.03	—	—	—	—	—	—	
	640.0	Md.Sd.	28	10	6	—	—	—	—	—	—	0.8	2.5	4	0.10	—	—	—	—	—	—	
	645.0	Md.Sd.	15	5	3	—	3	<2.5	15	<5	4	0.6	1.0	3	0.07	—	—	—	—	—	—	
	650.0	F.Sd.	19	5	1	—	—	—	—	—	—	0.9	2.1	10	0.03	—	—	—	—	—	—	
	656.5	Md.Sd.	4750	8	19	—	<5	<2.5	18	13	7	0.8	1.5	5	0.07	—	—	—	—	—	—	
	GW-10	585.0	F.Sd.	20	2	26	—	—	—	—	—	—	0.4	0.5	22	0.02	—	—	—	—	—	—
590.0		F.Sd.	10	1	7	—	—	—	—	—	—	0.6	0.8	15	0.03	—	—	—	—	—	—	
595.0		Md.Sd.	10	2	50	—	—	—	—	—	—	0.9	1.4	19	0.05	—	—	—	—	—	—	
600.0		Md.Sd.	8	2	105	—	4	<2.5	15	<5	10	1.2	2.0	17	0.02	—	—	—	—	—	—	
604.0		Md.Sd.	10,800	10	30	—	2	<2.5	20	42	20	0.7	3.6	1	0.12	—	—	—	—	—	—	
607.5		F.Sd.	1340	4	1	—	—	—	—	—	—	0.4	0.9	19	0.02	—	—	—	—	—	—	
615.0		Md.Sd.	5250	13	15	—	—	—	—	—	—	2.1	2.8	4	0.09	—	—	—	—	—	—	
620.0		Md.Sd.	1890	49	8	—	—	—	—	—	—	0.8	1.8	9	0.20	—	—	—	—	—	—	
625.0		Md.Sd.	1860	310	3	—	5	<2.5	25	<5	7	0.8	2.6	13	0.16	—	—	—	—	—	—	
GW-11	375.0	Silt	74	2	<1	—	—	—	—	—	—	2.2	3.6	7	0.09	—	—	—	—	—	—	
	385.0	F.Sd.	7	5	4	—	—	—	—	—	—	1.2	1.9	8	0.05	—	—	—	—	—	—	
	392.5	Md.Sd.	54	6	13	—	—	—	—	—	—	0.8	1.2	9	0.09	—	—	—	—	—	—	
	397.5	Md.Sd.	750	3	10	—	—	—	—	—	—	0.9	1.5	15	0.02	—	—	—	—	—	—	
	402.5	Md.Sd.	850	6	4	—	5	<2.5	26	<5	11	0.6	0.9	14	0.06	—	—	—	—	—	—	
	412.5	Md.Sd.	625	12	2	—	—	—	—	—	—	2.3	1.9	5	0.13	—	—	—	—	—	—	
	417.5	F.Sd.	22	3	1	—	—	—	—	—	—	0.8	1.3	12	0.07	—	—	—	—	—	—	
	545.0	Clay	3	1	20	—	—	—	—	—	—	1.5	1.1	21	0.06	—	—	—	—	—	—	
	552.5	Md.Sd.	7	3	69	—	—	—	—	—	—	2.8	1.5	4	0.10	—	—	—	—	—	—	
	557.5	Md.Sd.	8	2	41	—	—	—	—	—	—	0.6	0.5	12	0.02	—	—	—	—	—	—	
	562.5	Md.Sd.	7	2	73	—	4	<2.5	16	<5	7	0.6	1.1	7	0.03	—	—	—	—	—	—	
	570.0	Md.Sd.	7	2	58	—	—	—	—	—	—	0.7	1.0	8	0.04	—	—	—	—	—	—	
	577.5	Clay	1690	11	21	—	9	<2.5	111	35	23	1.9	1.6	9	0.07	—	—	—	—	—	—	
	581.5	Clay	300	9	30	—	—	—	—	—	—	1.4	2.1	15	0.06	—	—	—	—	—	—	
586.5	Md.Sd.	238	5	21	—	—	—	—	—	—	0.4	1.4	20	0.03	—	—	—	—	—	—		
591.5	F.Sd.	463	11	4	—	—	—	—	—	—	0.7	1.1	7	0.04	—	—	—	—	—	—		
GW-12	250.0	Md.Sd.	45	4	2	—	—	—	—	—	—	0.5	1.2	11	0.03	—	—	—	—	—	—	
	257.5	Md.Sd.	325	6	9	—	—	—	—	—	—	0.3	0.6	16	0.02	—	—	—	—	—	—	
	265.0	Md.Sd.	1190	23	55	—	—	—	—	—	—	0.7	3.6	8	0.03	—	—	—	—	—	—	
	272.5	Md.Sd.	23	5	10	—	—	—	—	—	—	0.6	1.7	8	0.05	—	—	—	—	—	—	

D Dominant tr Trace — Absent or below level of detection
P Present ? Questionably present il Illite

